ABSTRACT

Title of Dissertation:	TAILORING GUANOSINE HYDROGELS FOR VARIOUS APPLICATIONS
	Taylor N. Plank, Doctor of Philosophy, 2018
Dissertation Directed By:	Professor Jeffery T. Davis, Department of Chemistry and Biochemistry

Supramolecular hydrogels are of current interest for their ease of use, potential biocompatibility, and reactivity to stimuli. These gel materials have found use in a number of fields ranging from drug delivery and tissue engineering to sensing and environmental remediation. For over a century, guanosine (G **1**) and its derivatives have been known to form hydrogels based on self-assembled G_4-quartet structures. Recent research has focused on extending the lifetime stability of these hydrogels and modifying their properties to better suit the gels for applications in multiple fields. One such method involves the mixing of G **1** (or G-derivatives) with 0.5 eq of $KB(OH)_4$, which results in the formation of guanosine-borate (GB) diesters. The GB-diesters self-assemble into G_4-quartets stabilized by K^+, the G_4-quartets then stack to form wires that entangle to make a fibrous hydrogel network. This thesis details modifications of this GB-hydrogel system and explores applications of the resulting hydrogels.

Modification of the 5′-OH group of G **1** to form 5′-deoxy-5′-iodoguanosine (5′-IG **2**) results in a hydrogel that self-destructs via intramolecular cyclization to 5′-deoxy-N3,5′-cycloguanosine (5′-*c*G **3**). Guanine analog drugs can be incorporated into this hydrogel network and then released upon self-destruction of the gel.

Substitution of boric acid with benzene-1,4-diboronic acid (BDBA **4**) to form hydrogels with G **1** and K^+ results in hydrogels that can be crosslinked with Mg^{2+}. These G-BDBA-Mg hydrogels have a lower critical gelator concentration (cgc) than their non-crosslinked counterparts and can be used for cell growth applications.

Utilizing binary mixtures of 8-aminoguanosine (8AmG **5**) with G **1** allows for the formation of hydrogels with various salts. Hydrogels made of different salts preferentially absorb either cationic or anionic dyes from water, making them candidates for use in environmental remediation.

Other 8-substituted G-analogs, including, 8-bromoguanosine (8BrG **6**), 8-iodoguanosine (8IG **7**), and 8-morpholinoguanosine (8morphG **8**) can be used in binary mixtures with G **1** to form gels at room temperature upon mixing with $KB(OH)_4$. Room temperature hydrogels have potential applications in enzyme immobilization, drug encapsulation, and environmental cleanup.

TAILORING GUANOSINE HYDROGELS FOR VARIOUS FUNCTIONS

By

Taylor N. Plank

Thesis submitted to the Faculty of the Graduate School of the
University of Maryland, College Park, in partial fulfillment
of the requirements for the degree of
Doctor of Philosophy
2018

Advisory Committee:
Professor Jeffery T. Davis, Chair
Professor Daniel E. Falvey
Assistant Professor Osvaldo Gutierrez
Associate Professor Paul Paukstelis
Professor Gregory F. Payne

ACKNOWLEDGEMNTS

Thank you to all of my lab mates, past and present, who have made my time in the Davis group enjoyable. To Gretchen, thank you for being all around amazing as both a lab-mate and a friend. You helped keep me sane through the madness of grad school with coffee runs, happy hours, baseball games, and girls' nights. Thank you for always understanding my complaints and emoji filled texts even after you graduated. To Soumya, Keith, and Songjun, thank you for all of your insight and for making the lab a fun place. To Luke, Brooke, Sabrina, Deiaa, Mitchell, and Sindy, thank you for your work in lab and for challenging me to be a better mentor. Lastly, thank you Will, for coming back to lab and telling us great stories, and most importantly, thank you for your encouragement, job advice, and for encouraging me to apply at Stevenson.

Thank you to Dr. Lee Friedman for everything I learned from you about teaching when I served as your TA and GAANN fellow, and thank you for your career

advice and letters of recommendation. Thank you also to Dr. Monique Koppel, for giving me the opportunity to teach your class, and for your letters of recommendation.

To my graduate school friends, Marla, Carmen, and Siobhan, thank you for your understanding and for the Wednesday night dinners (and wine).

To my parents, John and Necia Plank, my grandparents, and the rest of my family, thank you for loving me and providing support and encouragement even when you had no idea what I was doing in graduate school. I feel so lucky to have such an amazing, caring family who unconditionally loves me, thank you.

To my future in-laws, Bill and Kim, thank you for welcoming me into your family and always being interested in what I am doing.

Last, but most definitely not least, Luke, thank you for everything. Thank you for believing in me, even when I don't believe in myself and for supporting me in everything I want to do. Thank you for driving 11 hours both ways to see me when we were both poor graduate students and for taking a job in DC so we could be together while I finished graduate school. Thank you for enthusiastically listening to every practice talk, reading every paper draft, and offering your fake-chemist advice. You truly make my world a happier place, I love you.

TABLE OF CONTENTS

LIST OF FIGURES

Chapter 1: Introduction

1.1 Introduction

Inspired by nature, the self-assembly of molecules is a powerful tool in creating functional materials.[1] One such example are supramolecular guanosine (G **1**) hydrogels,[2,3] formed via the self-assembly of the naturally occurring nucleoside (or its derivatives) into G_4-quartets (**Figure 1.1**).[4] While G **1** hydrogels have been known for over a century,[5] there has been a recent increase in their use for a variety of applications as these gels are easily synthesized and are potentially bio-compatible.[6–8]
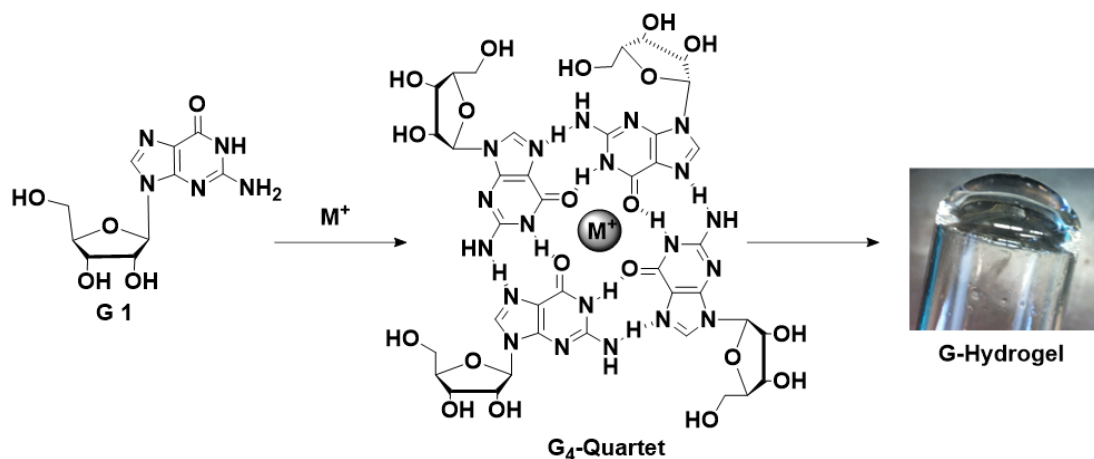
Figure 1.1: When added to aqueous solution of monovalent cation, G **1** self-assembles into cation stabilized G_4-quartets. This protocol leads to formation of a G-hydrogel.

In the past 10 years research on G-hydrogels has focused on enhancing the stability of these systems.[9–11] Previous research in our group focused on utilizing boric acid to crosslink the gel network via borate-ester formation. We were able to form robust guanosine-borate (GB) hydrogels. The anionic GB-esters play a pivotal role in solubilizing G **1** and extending the gel's long-term stability.[12] The strength of these gels

can be modulated by the cation identity, and both guanine analogs, and diols can be incorporated into the gel network.[13] In addition, due to their negative charge, they are able to absorb cationic dyes from water.[14] This thesis, "Tailoring Guanosine Hydrogels for Various Functions" details further experiments modifying different components of the GB-hydrogel system in order to better suit the hydrogels for applications. Modifications of (a) the sugar's 5′-OH position, (b) the 2′,3′-diol *via* altering the borate-ester species, and (c) the H8 position of the nucleobase are discussed.

1.2   Thesis Organization

This thesis is organized into seven chapters. **Chapter 1** introduces hydrogels with a general background on gelation and information on utilizing boron cross-linking in supramolecular hydrogels. This chapter concludes with a brief history of G-hydrogels, including recent work on boron containing G-hydrogels. **Chapter 2** describes a 5′-deoxy-5′-iodoguanosine (5′-IG **2**) hydrogel formed with potassium borate that self-destructs via intramolecular cyclization to form 5′-deoxy-N3,5′-cycloguanosine (5′-*c*G **3**), which breaks down the gel network. This self-destruction is used to release G-analog drugs that were incorporated into the hydrogel network.[15] **Chapter 3** focuses on hydrogels made of G **1** with K⁺ and benzene-1,4-diboronic acid (BDBA **4**), which can be used for cell growth.[16] **Chapter 4** discusses binary hydrogels of 8-aminoguanosine (8AmG **5**)/G **1** in environmental remediation. These gels can be formed with various salts allowing them to uptake either cationic or anionic dyes from water.[17] **Chapter 5** explores the gelation of other 8-substituted-guanosine analogs, such as 8-bromoguanosine (8BrG **6**), 8-iodoguanosine (8IG **7**), and 8-mopholinoguanosine

(8morphG **8**). When any of these derivatives are combined in binary mixtures with G **1** and KB(OH)$_4$ hydrogels form quickly at room temperature. **Chapter 6** details potential future directions for research on GB-hydrogels. Finally, **Chapter 7** contains supporting information, including experimental procedures, synthetic methods, and supplemental figures. A bibliography of all literature cited herein concludes the thesis.

1.3   Introduction to Gels

Gels are common materials. From toothpaste and hair gel, to jello, we encounter many gels on a daily basis. Despite the numerous gels in our lives, explaining what a gel is has historically been a difficult task.[18] Perhaps best described by Dr. Dorothy Lloyd, a gel is "easier to recognize than define," as there are multiple types of gels all with different characteristics.[19] In general, gels are substances that, despite being mostly solvent (90% or more by weight), do not flow and have solid-like rheologies. These features arise from the formation of two phases within the material, the 3D solid-like gel network (the gel phase) that entraps the solvent (the sol phase) thus preventing the liquid from flowing (**Figure 1.2**). Gels made with organic solvents are known as organogels, while those made with water are referred to as hydrogels.[20–22]
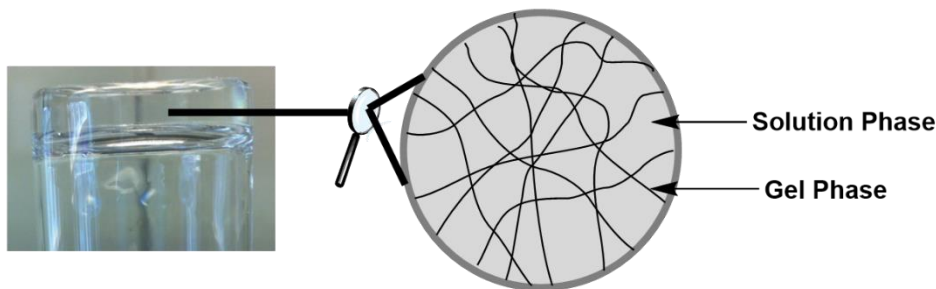
Figure 1.2: A depiction of the two phases contained within a gel.

Gels can also be classified as either chemical gels or physical gels. Chemical gels contain covalently crosslinked gel networks, meaning the network can only be disrupted if covalent bonds are broken. Due to the covalent crosslinks, chemical gels normally shrink or swell in the presence of external stimuli rather than breaking apart. On the other hand, physical gels are held together via non-covalent interactions that are reversible and therefore can disassemble upon interactions with stimuli (**Figure 1.3**).[2,21]
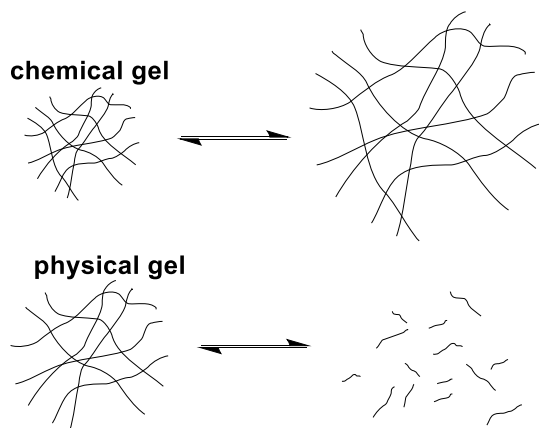
Figure 1.3: Chemical gel (top) networks form via covalent bonds, therefore the gels swell or shrink in the presence of external stimuli. In contrast, physical gels (bottom) form from non-covalent interactions and can dissociate when exposed to stimuli.

Supramolecular gels (also known as molecular gels), are a subset of physical gels that generally refers to the gelation of low molecular weight gelators (LMWG) (technically some polymer gels could be classified as supramolecular gels, however they are not the focus of this thesis) via noncovalent interactions, including H-bonding, π-π stacking, van der Waals forces, Coulombic attractions, etc. The LMWGs self-assemble into 1D structures that further aggregate to form a 3D network of entangled fibers, referred to as a self-assembled fibrillar network (SAFiN) (**Figure 1.4**).[2,6]
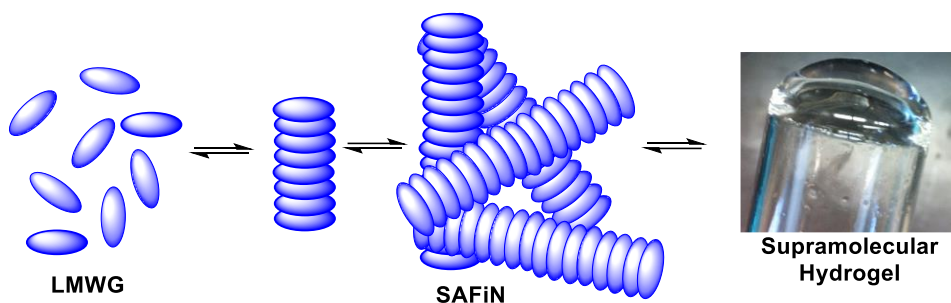
Figure 1.4: Supramolecular gels form via self-assembly of LMWGs 1D structures with subsequent aggregation into 3D networks.

There are some examples of gelation occurring at room temperature (one of which will be discussed in **Chapter 5** of this thesis), but these are not the norm as the gelation process usually involves heating the LMWG and solvent until the gelator dissolves (or adding the LMWG to hot solvent), the solution is then allowed to cool at room temperature and upon cooling a gel forms.[2,6,22]

The multi-step self-assembly process required to form the SAFiN makes supramolecular gels particularly sensitive to stimuli such as temperature, acids/bases, light, redox, mechanical forces, and more. This stimuli responsiveness can be harnessed to utilize supramolecular gels for a variety of applications including, sensing, drug release, environmental remediation, and more.[23,24]

1.4 Boron-Species as Cross-Linkers

Having three valence electrons and an empty, Lewis acidic p-orbital, boron plays a critical role in many areas of science. Boron has been recognized for its role in synthesis as many boron-containing species act as key reagents in many important reactions. As an element naturally occurring in many minerals it plays an important

role in prebiotic chemistry. In addition, with a Lewis acidic, empty p-orbital, boron-containing species have found use in supramolecular and polymer chemistry for their ability to form dynamic covalent bonds with oxygen.[25]

Boric acid, B(OH)$_3$ is well known to form borate esters with 1,2- and 1,3-diols, resulting in negatively charged, tetravalent, tetrahedral boron. These borate ester bonds are dynamic and reversible with acid and base (**Figure 1.5**).[26]
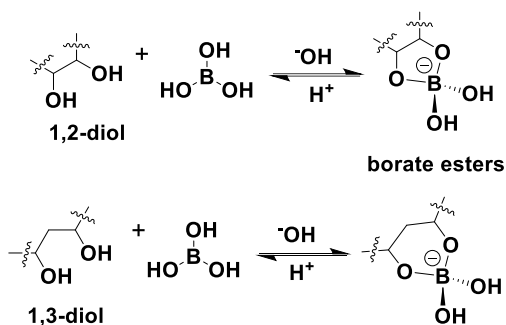
Figure 1.5: Borate esters form between boric acid and a 1,2- (top) or 1,3-diol (bottom) in the presence of base. These dynamic bonds can be reversed with acid.

Borate ester species are commonly used to crosslink polymers to create hydrogels. Perhaps most commonly known with polyvinyl alcohol (PVA **9**), which is a common household adhesive (**Figure 1.6**). This interaction is the basis of many at home science projects to create "slime" by mixing borax soap with school glue.[27]
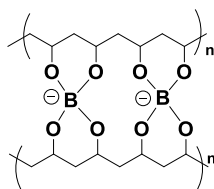
Figure 1.6: Borate ester cross-linking between two chains of PVA **9**.

In addition to PVA **9**, boric acid is known to cross-link many other diol-containing polymers. This boron cross-linking has been utilized in numerous polymer hydrogels. Boronic acids (R-B(OH)$_2$, where R is any carbon containing group) have also been used to the same effect in organogels. These materials have found many uses, one of the most prominent being in glucose sensing.[28,29] For more information on the applications of boron, including uses in polymer gels and organogels, see several recent review articles and books on these topics.[25,30–32] The remainder of this chapter will focus on the use of borate esters in supramolecular hydrogels made from LMWGs including peptides, triazine analogs, and G-derivatives.

1.4.1 Supramolecular Hydrogels with Boron

Sankar and Dastidar reported a triazine based triboronic acid hydrogelator (tHG **10**) that forms hydrogels based on both hydrophobic stacking interactions and, interestingly, H-bonding based boronic acid dimers (**Figure 1.7**) when mixed in water and a small amount of DMSO. These gels could be loaded with the anticancer drug, doxorubicinHCl (DOX **11**) without disrupting the gel network (since DOX **11** has no 1,2- or 1,3-diols, it does not disrupt the boronic acid dimers). The drug could then be slowly released from the gel with a decrease in pH to break up the gel network. Similarly insulin could be loaded into the gel network and released when triggered by glucose. Hydrogels of tHG **10** show promise for targeted drug release applications.[33]

7
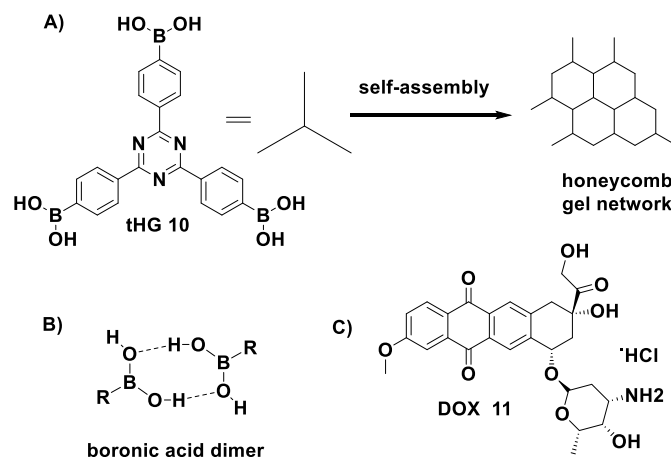
Figure 1.7: A) The formation of a honeycomb gel network by tHG **10**. B) H-bonded boronic acid dimer that is part of the gel network C) Structure of DOX **11**.

A supramolecular hydrogel containing a boronic acid-substituted fluorescence resonance energy transfer (FRET) acceptor that can be used as a sensor for polyols was reported by the Hamachi group. This gel forms when the phosphate containing gelator PO_4g **12**, is mixed with Ca^{2+} ions (**Figure 1.8**).[34]
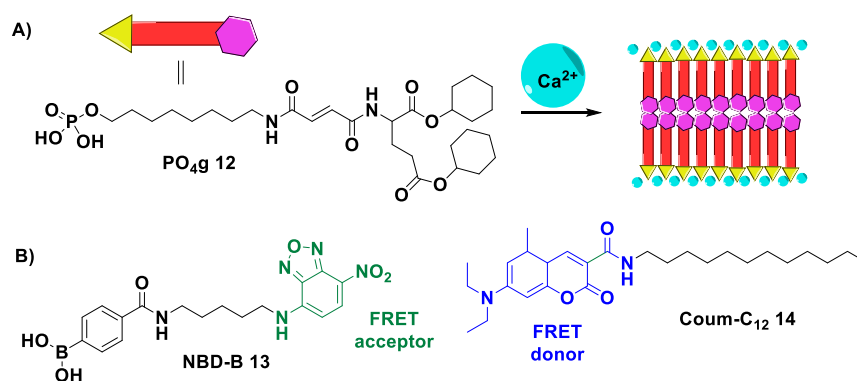
Figure 1.8: A) The formation of a gel network by PO_4g **12** with Ca^{2+}. B) The FRET donor and acceptor pair.

A FRET acceptor, the boron-appended NBD-B **13**, and donor, coumarin dye (Coum-C$_{12}$ **14**), can be incorporated into the hydrogel network. NBD-B **13** has a boronic acid group that is capable of binding polyols. When bound with a polyol FRET is turned off. Without any polyols the system emits green. In the presence of polyols, there is blue emission, indicating FRET has been turned off by the polyol-boronic acid binding. In addition to sensing in the gel state the authors spotted a mixture of PO$_4$g **12**, NBD-B **13**, and Coum-C$_{12}$ **14** onto a piece of cellulose-based filter paper pre-saturated with CaCl$_2$. Even after 1 week the paper system worked as a polyol sensor, with a color change in the presence of polyols, making this hydrogel-paper sensor an affordable and portable diagnostic tool.[34]

1.4.2 Peptide-Based Supramolecular Hydrogels with Boron

Hamachi and coworkers also explored the gelation of different peptide derivatives, finding that BPmoc-F$_3$ **15** forms a gel network that be disrupted due to degradation of the gelator upon reaction with H$_2$O$_2$ (**Figure 1.9**).[35]
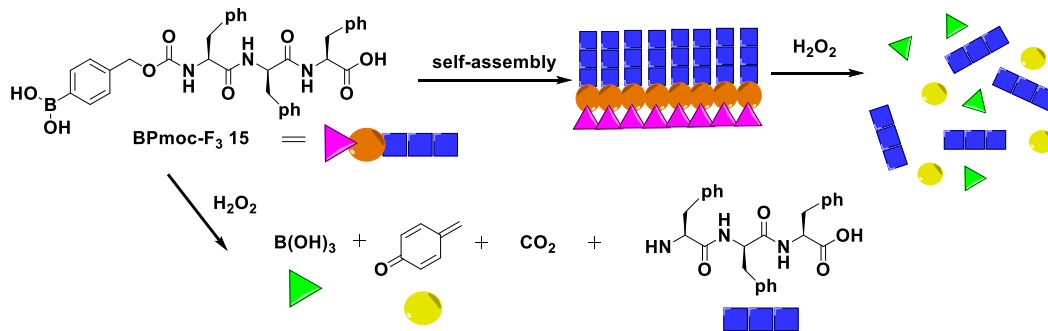
Figure 1.9: The self-assembly of BPmoc-F$_3$ **15** to form a gel network is shown. This gel can be destroyed by H$_2$O$_2$, which causes the degradation of the gelator.

In order to transform the gel system into a practical sensor for biomolecules the authors incorporated various oxidase enzymes into the gel network. These oxidase enzymes generate H_2O_2 *in situ* upon reaction with their substrates (**Figure 1.10A**). In turn, this H_2O_2 generation causes gel breakdown, indicating the presence of the target biomolecule (**Figure 1.10B**).[36,37]
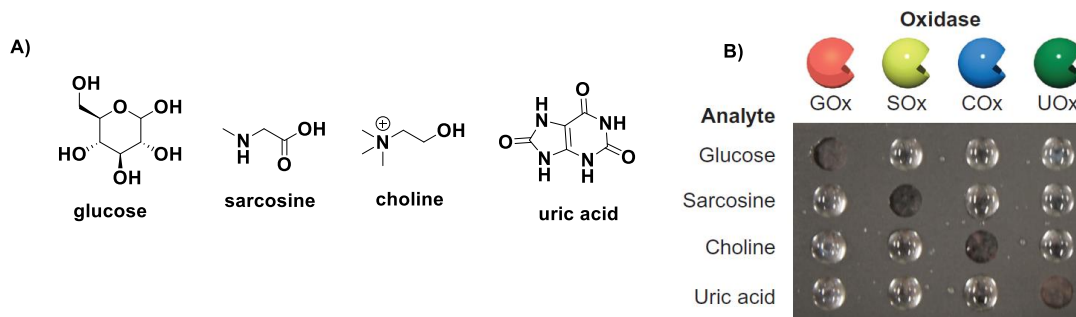
Figure 1.10: A) The biomolecules tested. B) A grid showing the gels or solutions resulting from the biomolecules present with different oxidase enzymes. Only the gels with the oxidase enzyme corresponding to the correct molecules produced H_2O_2 resulting in the gel-solution transition. The mismatched systems remained gels. Part B of this figure is reproduced with permission from Springer.[36]

Cameron and coworkers reported a hydrogel composed of the dipeptide derivative BrNap-AV-OH **16** (**Figure 1.11A**). At a pH below the pK_a of the carboxylic acid the gelator aggregates to form a hydrogel network, when the pH is higher, the carboxylate anion solubilizes the gelator, resulting in a solution. By adding phenylboronic acid (phB(OH)$_2$ **17**) to hydrogel system the authors were able to use gelation as a saccharide sensor. When phB(OH)$_2$ **17** reacts with a diol (like those present in sugars) to form a boronate ester species (**Figure 1.11B**) the pH of the solution is lowered. This decrease in pH results in gelation by BrNap-AV-OH **16**. The authors envision a potential application for this system as a smart-bandage in which saccharide

coated bacteria would trigger gelation upon reaction with phB(OH)$_2$ **17**, thus trapping bacteria in a gel matrix.[38]
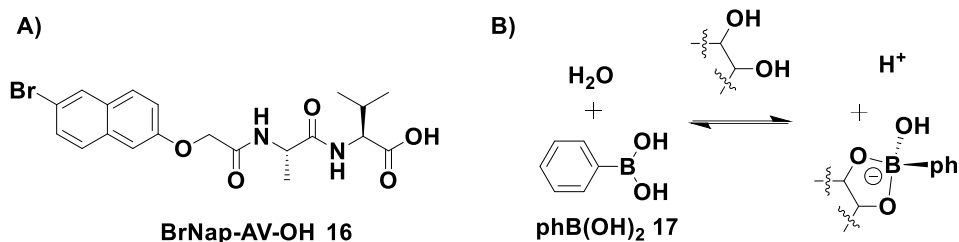
Figure 1.11: A) The gelating species - a dipeptide derivative. B) The formation of boronate esters is accompanied by an acidification of the solution.

The Spoerke group combined the gelating ability of a phenylalanine dipeptide with the diol sensing abilities of boronic acid into the hydrogelator BFF **18** (**Figure 1.12**). Similar to BrNap-AV-OH **16**, BFF **18** is charged, and therefore soluble at higher pH values, but will form a hydrogel at low pH values. This system can be tuned not only by pH, but also by addition of a diol-containing species. Diol species react with the boronic acid moiety to form an anionic boronate ester, thus solubilizing the gelator.[39]
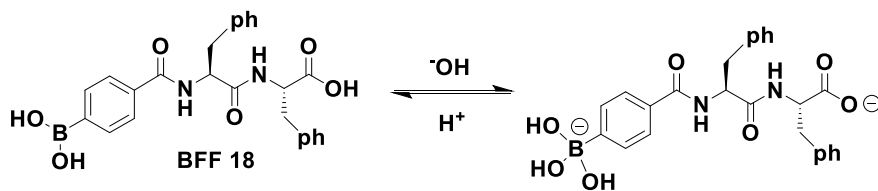
Figure 1.12: Hydrogelator BFF **18** is charged at high pH values, resulting in solubilization and destruction of hydrogels.

11

1.4.3 Summary of Non-Guanosine Supramolecular Hydrogels with Boron

This section has explored recent developments in low molecular weight supramolecular hydrogels that utilize boron species. The examples discussed showcase the versatility of boronic acids as both parts of hydrogelators and in sensors for polyols. The remainder of this chapter will focus on the use of boric acid and boronic acids in guanosine-analog hydrogels.

1.5 A Brief History of Guanosine Hydrogels

Gelation of a G **1** derivative was first reported by Bang in 1910,[5] however it wasn't until 1962 that Gellert and coworkers proposed G_4-quartet based structures as the foundation for the gelation of 5′-guanosine monophosphate (5′-GMP 1**9**).[40] Further exploration of a variety of G **1** analogs by Guschlbauer and colleagues in the 1970s solidified the importance of the G_4-quartet in gel formation.[41–43] The G_4-quartet is an H-bonded macrocycle composed of four guanine-containing units stabilized by a cation in the central cavity. These planar structures can further assemble via π-π stacking into columnar aggregates.[4] In the last 20 years there have been several examples of G_4-quartet hydrogels with a wide range of potential applications including drug incorporation and delivery, sensing, tissue engineering, and more.[44–49]

One major issue with supramolecular G **1** hydrogels is their tendency to crystallize over time. In the presence of excess KCl, G **1** will initially form a transparent hydrogel, but over time hydrophobic G **1** crystallizes in the sol phase of the gel and eventually leads to a complete breakdown of the gel network (**Figure 1.13**). This instability is a major setback for long-term storage and applications of G **1** hydrogels.
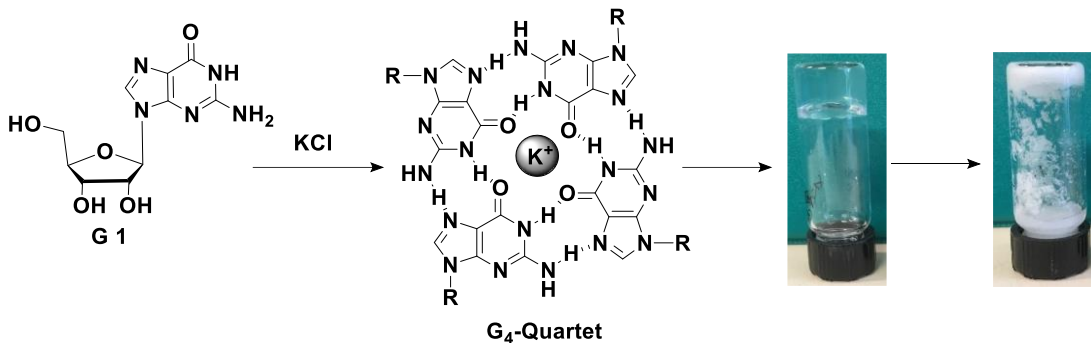
Figure 1.13: G **1** forms transparent hydrogels in the presence of KCl, however, over time the nucleoside crystallizes, destroying the gel network.

1.5.1 Binary Guanosine Hydrogels

One method developed to prevent crystallization is the creation of binary hydrogels made with two G-derivatives. The use of two nucleosides adds a level of disorder to the hydrogel system and prevents crystallization. In 2008, the McGown group reported the formation of a binary hydrogel made from G **1** and 5′-GMP **19** (**Figure 1.14**), with increased lifetime and stability. Readily soluble 5′-GMP **19** helps to solubilize hydrophobic G **1** to form more stable hydrogels. Using different ratios of G **1**:5′-GMP **19** the authors are able to tune the temperature response of the hydrogels to either thermoassociate or thermodissociate.[9] Since this initial report several other binary gel systems with G **1** have been reported.
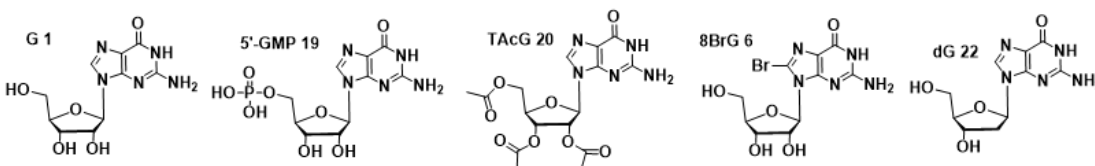
Figure 1.14: G **1** and G-derivatives used to form binary hydrogels with G **1**.

Mariani and colleagues also explored hydrogels of G **1** and 5′-GMP **19**, finding that tuning the ratio of G **1**:5′-GMP **19** alters the amount of water the gel network is capable of supporting. They envision using these gels for entrapping target molecules.[50]

Rowan and coworkers utilized binary mixtures of 2′,3′,5′-tri-O-acetylguanosine (TAcG **20**) with G **1** that form transparent, stable hydrogels when mixed in 60:40-40:60 ratios. Varying the ratio within this range results in hydrogels with different mechanical strengths and thermal stabilities. With too much G **1** the gels would precipitate, and with too much TAcG **20** no gels would form (**Figure 1.15**).[10,51]
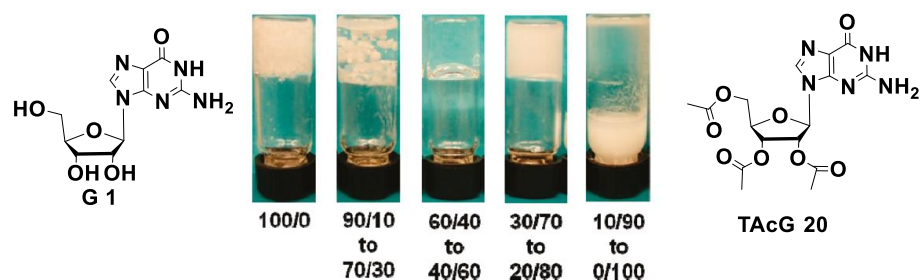
Figure 1.15: Hydrogels or solutions formed with different ratios of G **1**: TAcG **20**. Images of gels reprinted with permission from the American Chemical Society.[10]

The Dash group formed stable and transparent hydrogels from binary mixtures of 8BrG **6** and G **1**, which could be used in varying ratios. Organic dyes were able to diffuse through and subsequently be released from these hydrogels (**Figure 1.16**), implying that the gels could be used for the uptake and release of target compounds.[11]
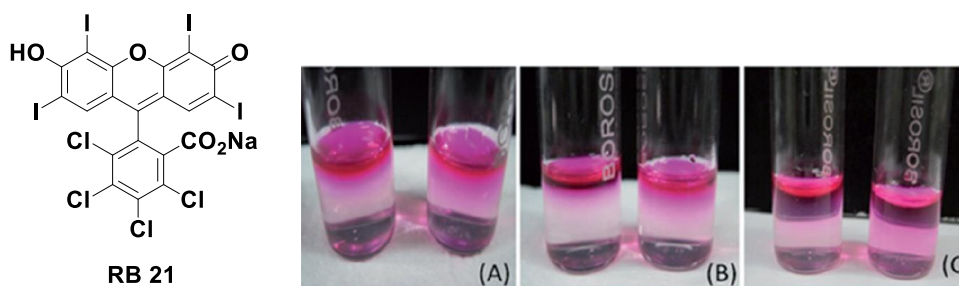
Figure 1.16: Images of the RB **21** (structure, top) diffusing through two G **1**/BrG **6** (left 1:1, right 1:2) hydrogels after A) 1 hr, B) 24 hrs, and C) 72 hrs. Pictures reprinted with permission from Wiley.[11]

Adhikari, Kraatz, and coworkers made hydrogels of G **1** with 2′-deoxy-guanosine (dG **22**). They found they could alter the gel strength and stability by varying the cation used to template G_4-quartet formation.[52]

Enhancing the lifetime of G **1** hydrogels through the use of binary mixtures with other G-derivatives has greatly improved the applicability of these hydrogels for practical applications. However, some of these systems still require high salt concentrations in order to form, making them problematic for biological applications. A different approach to stabilize G **1** hydrogels utilizes a stabilizing borate anion.

1.5.2 Stabilizing Guanosine Hydrogels with an Anion

In 2014 our group described the formation of a transparent and indefinitely stable hydrogel made by heating G **1** with 0.5 eq of aqueous KOH and $B(OH)_3$, the gel forms upon cooling. In the gelation mechanism (**Figure 1.17**) G **1** and $KB(OH)_4$ react to form dynamic guanosine-borate (GB) esters; GB-monoester (**23**) and two species of GB-diesters (**24** and **25**). These GB-esters then self-assemble into G_4-quartets that further stack to form G_4-wires, which entangle to make the hydrogel network.[12]
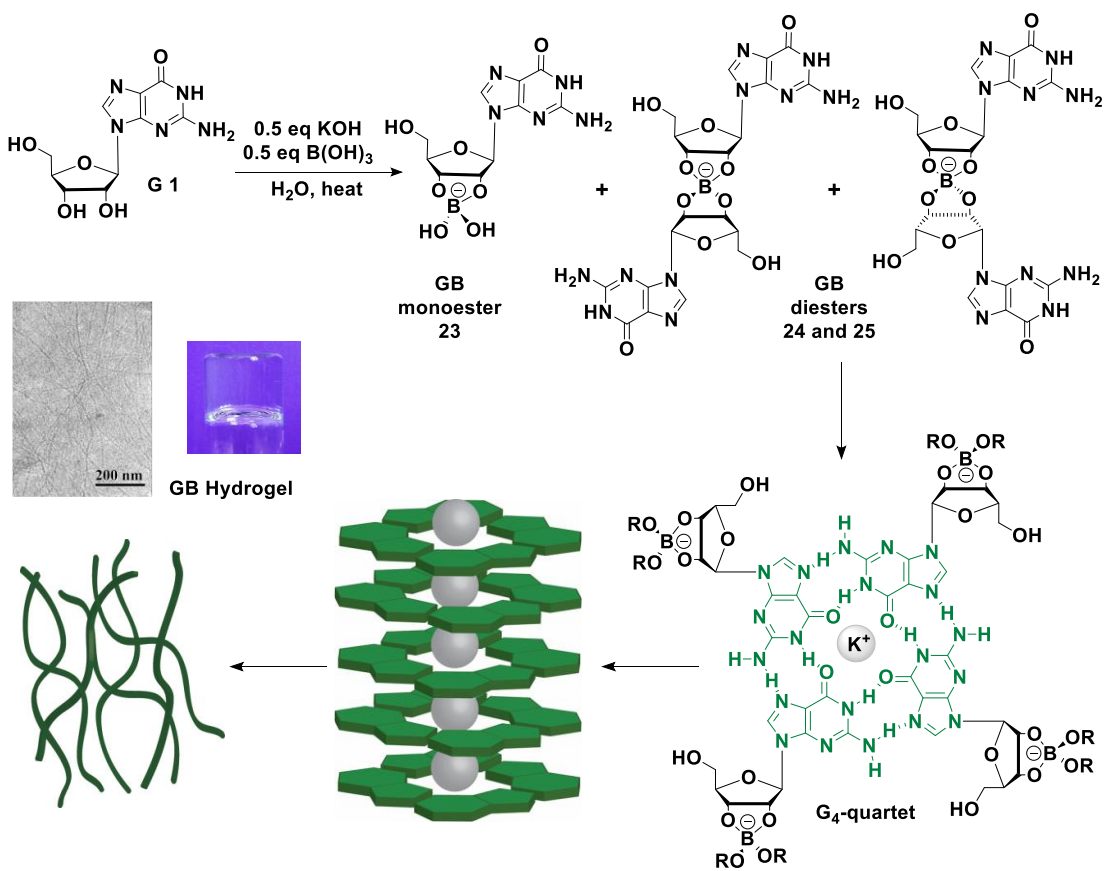
Figure 1.17: The gelation mechanism for the formation of GB-hydrogels of G **1** with KB(OH)$_4$.[12,13]

We found that the gel's strengths and physical properties could be controlled by the identity of the stabilizing cation (Li$^+$, Na$^+$, K$^+$, Rb$^+$, Cs$^+$), with K$^+$ giving the most robust hydrogels and Li$^+$ forming weaker gels. These gels were also capable of incorporating diol-containing molecules (through borate-ester linkages) and guanine-derivatives (via G$_4$-quartet H-bonding). We also found that these gels were stable in 155 mM K$^+$ solutions. Due to the anionic borate esters in the gel network, the hydrogels would selectively incorporate and hold cationic dyes (such as methylene blue, MB **26**), over anionic dyes (such as rose bengal, RB **21**) (**Figure 1.18**).[12,13]
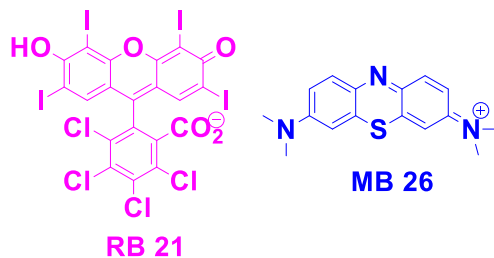
Figure 1.18: The anionic GB hydrogel selectively absorbs cationic MB **26** from an aqueous solution of MB **26** and anionic RB **21**.[12]

We further explored these charge based interactions using the known G-quadruplex ligand, thioflavin T (ThT **27**). Substoichiometric amounts of ThT **27** (and other cationic, aromatic dyes) strengthened the weaker Li^+ hydrogels and acted as molecular chaperones for gelation by templating the formation of G_4-quartets. The dye was able to repair a hydrogel that had been liquefied via sonication (**Figure 1.19**).[14]
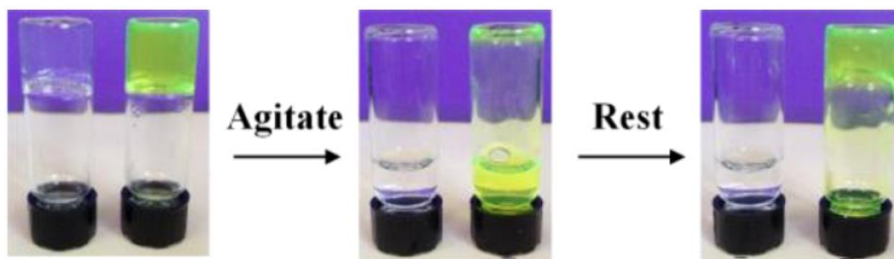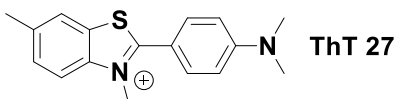
Figure 1.19: Substoichiometric amounts of ThT **27** helps to repair a GB-Li^+ hydrogel.[14]

Additional work from our group focuses on modifying components of the GB hydrogel system (including substitutions on the G **1** monomer, and the boron species) and is presented in **Chapters 2 – 6** of this thesis.

Since our group introduced borate containing G **1** hydrogels in 2014 there has been an explosion of GB hydrogels in the chemical literature reported from several different groups. These new reports utilize GB hydrogels or GB-derivative hydrogels in a variety of fields ranging from sensing to drug release and bioinks for 3D printing.

1.5.3 Guanosine-Boron Hydrogels with Hemin

There are several examples of G **1** hydrogels that incorporate hemin **28** into the gel network, which endows the gels with catalytic activity (**Figure 1.20**). This activity can be harnessed in redox reactions and for sensing applications.
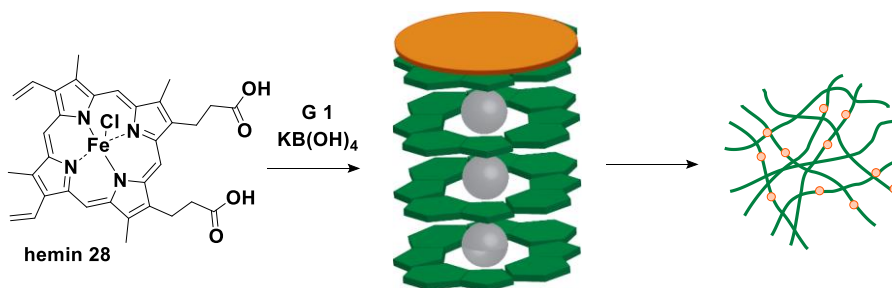
Figure 1.20: Hemin **28** binds to G_4-quartets to be incorporated into a hydrogel network.

Using G **1**, phB(OH)$_2$ **17**, and hemin **28** the Dash group detailed a system that forms hydrogels in the presence of K$^+$ (**Figure 1.21**). The hemin **28** containing gels are able to oxidize 3,3′,5,5′-tetramethylbenzidine (TMB **29**), which undergoes a color change with oxidation. In the presence of Pb^{2+} the oxidation activity is turned off due to the preference of the G_4-quartets for Pb^{2+} over K$^+$. The cation change results in a

change in the G_4-quartet structure that disrupts hemin binding.[53] Li, Zhu, and coworkers explored a similar system utilizing the GB-hydrogel with G **1** and KB(OH)$_4$ and hemin. They also found that in the presence of Pb^{2+} no oxidation of TMB **29** occurred.[54] These hydrogel systems can be used as sensors for detecting Pb^{2+}.
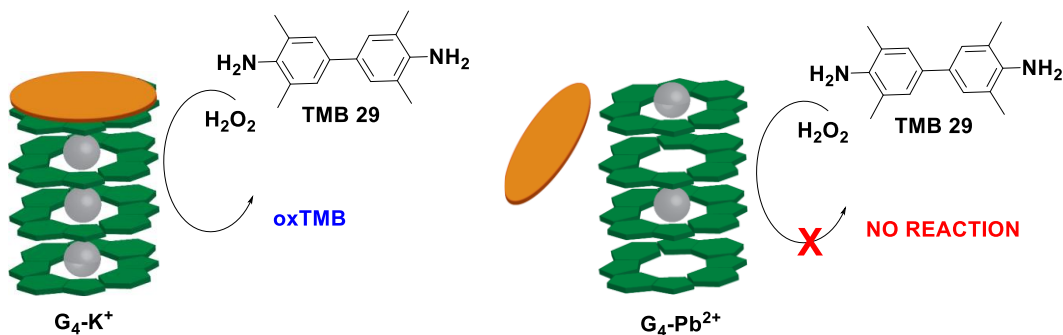
Figure 1.21: In the presence of H_2O_2 TMB **29** is oxidized in GB-K$^+$ hydrogels with hemin **28**, however with GB-Pb^{2+} hydrogels no reaction occurs

Zhang, Pei, and coworkers used G **1** with KB(OH)$_4$ and hemin **28** to create a printable hydrogel. This gel can be printed onto an electrochemical electrode, which can be incorporated into flexible bioelectronic devices, such as glucose sensors.[54]

1.5.4 Guanosine-Boron Hydrogels for Biological Applications

The Sadler group utilized the GB-hydrogel to incorporate a photoactivatable dopamine-conjugated platinum (IV) anticancer drug (Pt-DA **30**) (**Figure 1.22**). The gel showed cytotoxicity against cisplatin-resistant A2780Cis human ovarian cancer cells. This cytotoxicity was selective for cancer cells over normal non-cancerous cells.[55]
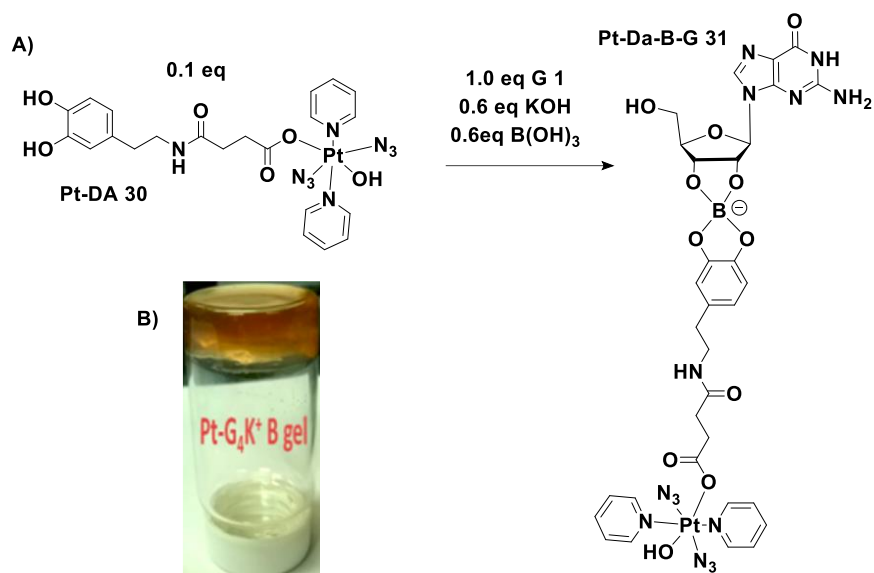
Figure 1.22: A) The anti-cancer drug derivative Pt-DA **30** forms a boronate ester (Pt-Da-B-G **31**) with G **1** that can be incorporated into a hydrogel network via G_4-quartet H-bonding. B) The Pt-G_4-K^+ B hydrogel is a brownish color. Photo reprinted with permission from the American Chemical Society.[55]

Utilizing G **1** with 2-formylboronic acid (2-FBA **32**) and tris(2-aminoethyl)amine (TAEA **33**) the Shi and Ma groups formed hydrogels based on G_4-quarets and cooperative boronate-ester, iminoboronate linkages. These dynamic linkages are sensitive to pH and diol functional groups and can therefore be controlled via addition of acid and/or glucose. When model compounds were loaded into the hydrogel, they could be released following zero-order kinetics upon addition of H^+ or glucose (**Figure 1.23**). With their pH and glucose responses, these hydrogels have potential for use in targeted and controlled drug delivery.[56]
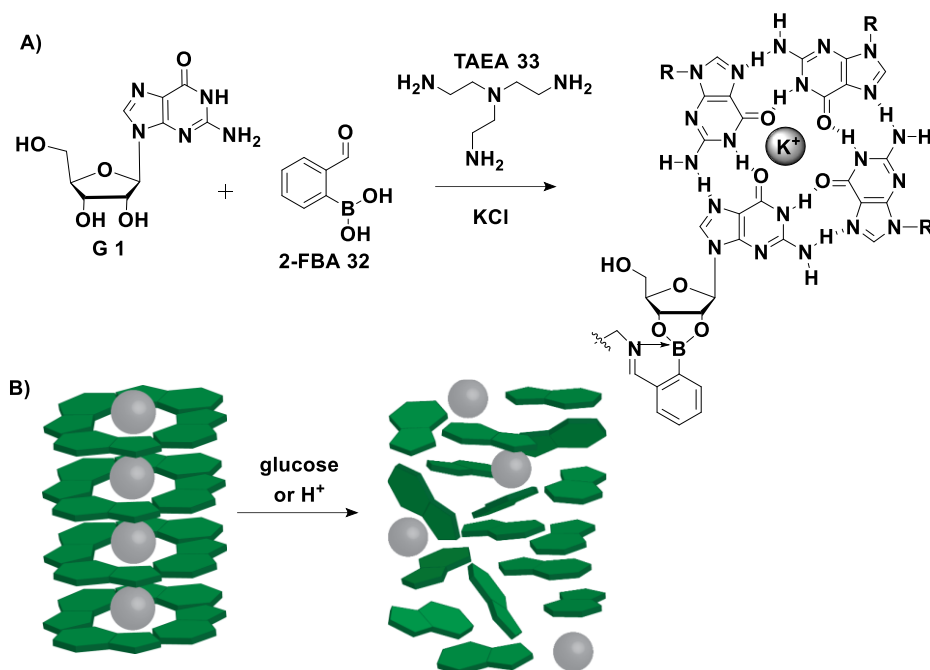
Figure 1.23: A) G **1** forms hydrogels with 2-FBA **32** and TAEA **33**. B) The hydrogels break down in the presence of glucose or acid, and will release any cargo they hold following zero-order kinetics.

Lastly, Kalaskar, Das and coworkers, reported hydrogels formulated with G **1**, phB(OH)$_2$ **17** and K$^+$. These hydrogels are thixotropic and self-healing, making them ideal candidates for 3D printable bioink. In addition the gels were shown to be non-toxic to human dermal fibroblast (HDF) cells and the authors utilized cell-loaded gels as bioink without damage to the cells nor the hydrogels (**Figure 1.24**).[57]
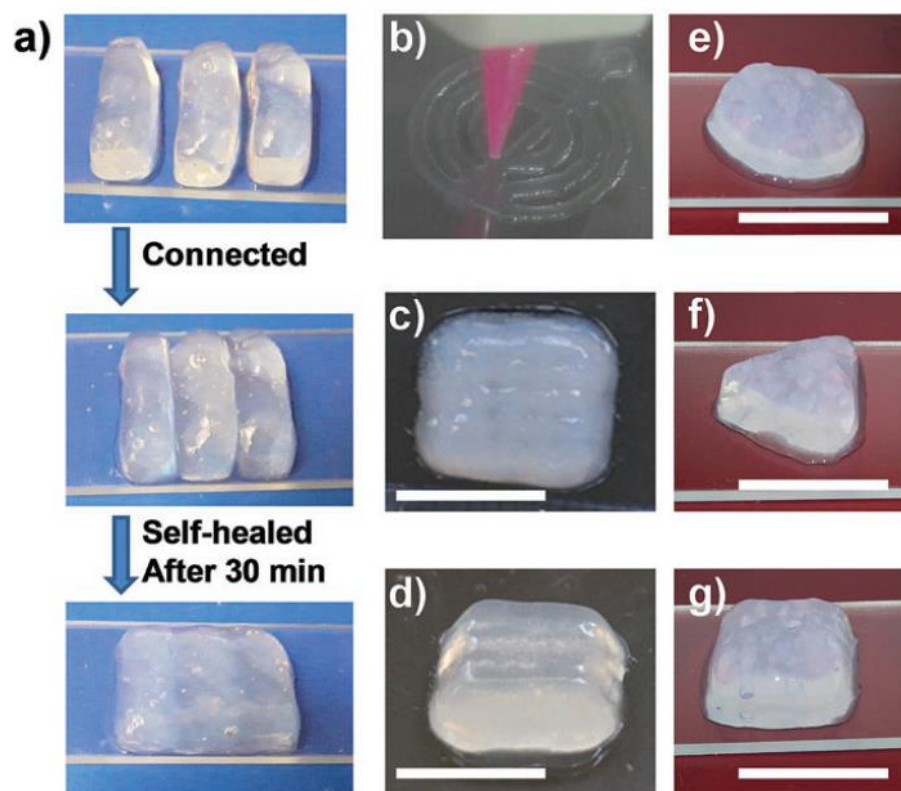
Figure 1.24: a) Shows the self-healing properties of the G **1**, phB(OH)$_2$ **17** hydrogels. b) The gel is used as a bioink for 3D printing c-g) Different shapes printed by the hydrogel (scale bar = 10 mm). Reprinted with permission from the Royal Society of Chemistry.[57]

1.6   Conclusions

Supramolecular hydrogels, including boron-crosslinked and G **1** gels, are a rapidly growing field of research. As explored in this chapter the dynamic and stimuli responsive nature of these gels makes them great candidates for use in various applications in a number of fields. The subsequent chapters of this thesis explore my work from the last five years on guanosine-analog hydrogels for drug delivery, cell growth, environmental remediation, and room temperature gelation.

Chapter 2: Hydrogels from 5′-Iodo-5′-Deoxyguanosine – Self Destruction for Drug Delivery

2.1 Summary

The research in this chapter focuses on utilizing guanosine-borate (GB) hydrogels for drug release. Since previous research in our lab showed that guanosine (G **1**) analog drugs could be incorporated into the GB gel network,[12] we aimed to create a functionalized GB hydrogel that could self-destruct to release the drug.

We found that 5′-deoxy-5′-iodoguanosine (5′-IG **2**) forms gels with $KB(OH)_4$. These G_4-quartet based gels break down over time as (5′-IG **2**) decomposes via intramolecular cyclization to form 5′-deoxy-N3,5′-cycloguanosine (5′-*c*G **3**), which is missing a H-bond donor necessary for G_4-quartet formation. Hydrogel breakdown can be modulated via temperature. G-analog drugs (acyclovir and ganciclovir) can be incorporated into the gel network and released over time as the gel degrades.

2.2 Introduction

Supramolecular hydrogels,[8,21] formed by low-molecular weight compounds, are being investigated for use in chemical sensing, organic electronics, tissue engineering, and drug delivery.[6,58,59] While derivatives of G **1** have been known to gel water since the early 1900's,[5] there has been renewed interest in G **1** gels for their ease of preparation, unique properties, and potential biocompatibility.[9–11,49,52] As described in the introduction to this thesis, our group had previously described a supramolecular

hydrogel made by mixing G **1** and 0.5 eq of KB(OH)$_4$ in H$_2$O.[12–14] The nucleoside's

2′,3′-diol reacts with borate to form anionic GB diesters that self-assemble into H-

bonded G$_4$-quartets.[4,60]

Having identified the key components for the formation of robust hydrogels in

the GB gel system previously developed in our lab we set out to alter gel properties by

altering the 5′-OH group. We reasoned that unlike the 2′,3′-diol (required for borate

ester formation), and the G nucleobase (required for G$_4$-quartet formation), the 5′-

position was not directly involved in the gelation mechanism and was therefore not

critical for gelation (**Figure 2.1**). The ability to functionalize the 5′-OH group is further

supported by the existence of hydrogels made from 5′-substituted guanosines;

including 5′-GMP,[5,61,62] 5′-hydrazides,[44] 5′-OAc,[10,51] 5′-sulfate,[42] and 5′-Cl analogs.[43]
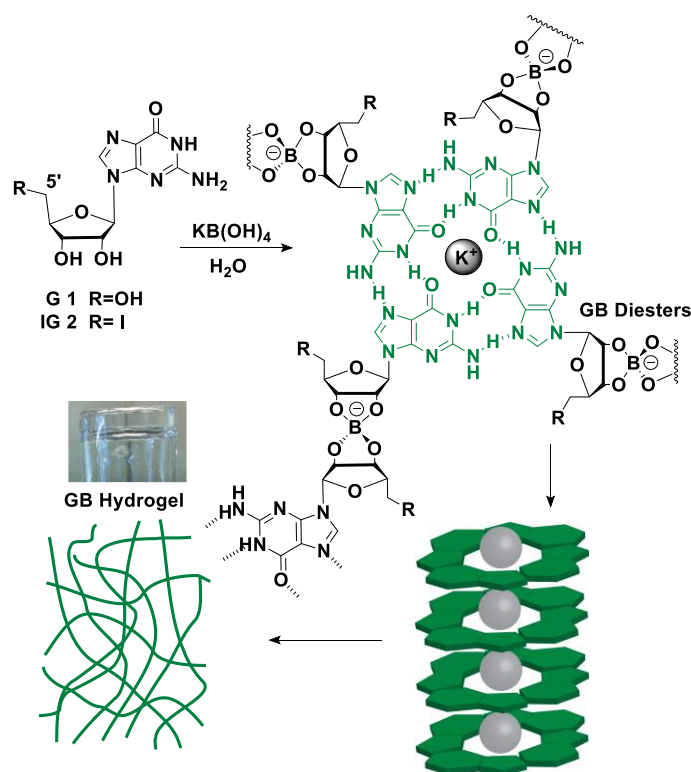
Figure 2.1: A hydrogel is made when G **1** or 5′-IG **2** reacts with KB(OH)$_4$ to form GB esters that self-assemble into G$_4$-wires stabilized by K$^+$. These wires entangle to give a fibrous network.[15]

We reasoned that incorporating a good leaving group at C5′, such as an iodo group to form 5′-deoxy-5′-iodoguanosine (5′-IG **2**),[63] would facilitate intramolecular cyclization by N3 to form 5′-deoxy-N3,5′-cycloguanosine (5′-*c*G **3**) when the nucleoside was in the *syn* conformation (**Figure 2.2**) This N3, C5′ cyclization is known for other guanosine analogs with good 5′-leaving groups.[64–66] Formation of 5′-*c*G **3** should disrupt the G$_4$-quartet based gel network, as 5′-*c*G **3** is missing an H-bond donor (**Figure 2.2**) necessary for the formation of G$_4$-quartets. Our goal in creating such a "self-destroying" hydrogel was to use the system for controlled release of compounds (such as guanine containing drugs) that had been pre-incorporated into the hydrogel.

With this objective in mind, we began our investigation on 5′-modifications by studying hydrogelation of 5′-IG **2** with KB(OH)$_4$.
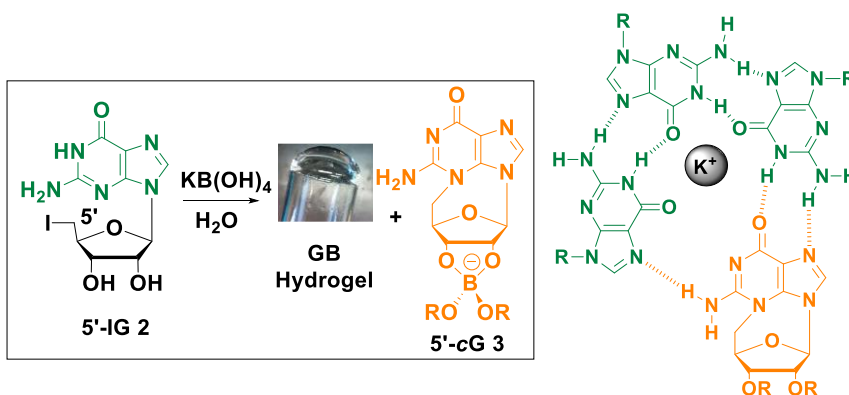
Figure 2.2: Left: 5′-IG **2** and aqueous KB(OH)$_4$ give a supramolecular hydrogel with in situ formation of 5′-cG **3**. Right: Lacking a N1 H-bond donor 5′-cG **3** cannot form stable G$_4$-quartets, its *in situ* formation destroys the hydrogel network.[15]

2.3 Hydrogels Made of 5′-IG 2 with KB(OH)$_4$

We found that GB gels can be made by heating aqueous suspensions of poorly soluble 5′-IG **2** with 2 eq of KB(OH)$_4$ to 90 °C, removing the sample immediately from the heat bath and then allowing that clear solution to cool at RT. While these hydrogels made from 5′-IG **2** were weaker than GB gels from G **1** (storage modulus, G′, was ~10,000 Pa for 72 mM G **1** gels;[13] whereas G′ was ~700 Pa for 72 mM 5′-IG **2** gels), the 5′-IG **2** hydrogels were transparent and appeared stable for weeks at RT. Importantly, gels did not form upon cooling if the sample was kept at 90 °C for > 10 min before being removed from the heat bath; instead viscous solutions were obtained. This suggested that 5′-IG **2** had cyclized to give 5′-cG **3**, preventing hydrogelation.

2.4 Formation of 5′-cG 3

Two pieces of information supported the proposal that 5′-IG **2** would significantly populate a *syn* conformation, enabling the intramolecular cyclization to 5′-cG **3** upon deprotonation of N1H (pK_a ~9; gel pH ~8.6)[67] (**Figure 2.2**). First, using an empirical NMR analysis that compares the chemical shift of H2′ to those of conformationally-locked analogs,[68] we found that 5′-IG **2** has a ~67% preference for the *syn* conformation in DMSO-d$_6$. Second, like GB hydrogels made from G **1**,[12,13] B-11 NMR indicates that 5′-IG **2** hydrogels contain borate diesters (**Figure 2.3**) and 2′,3′-borate esters of nucleosides are known to favor the *syn* conformation.[69–72]
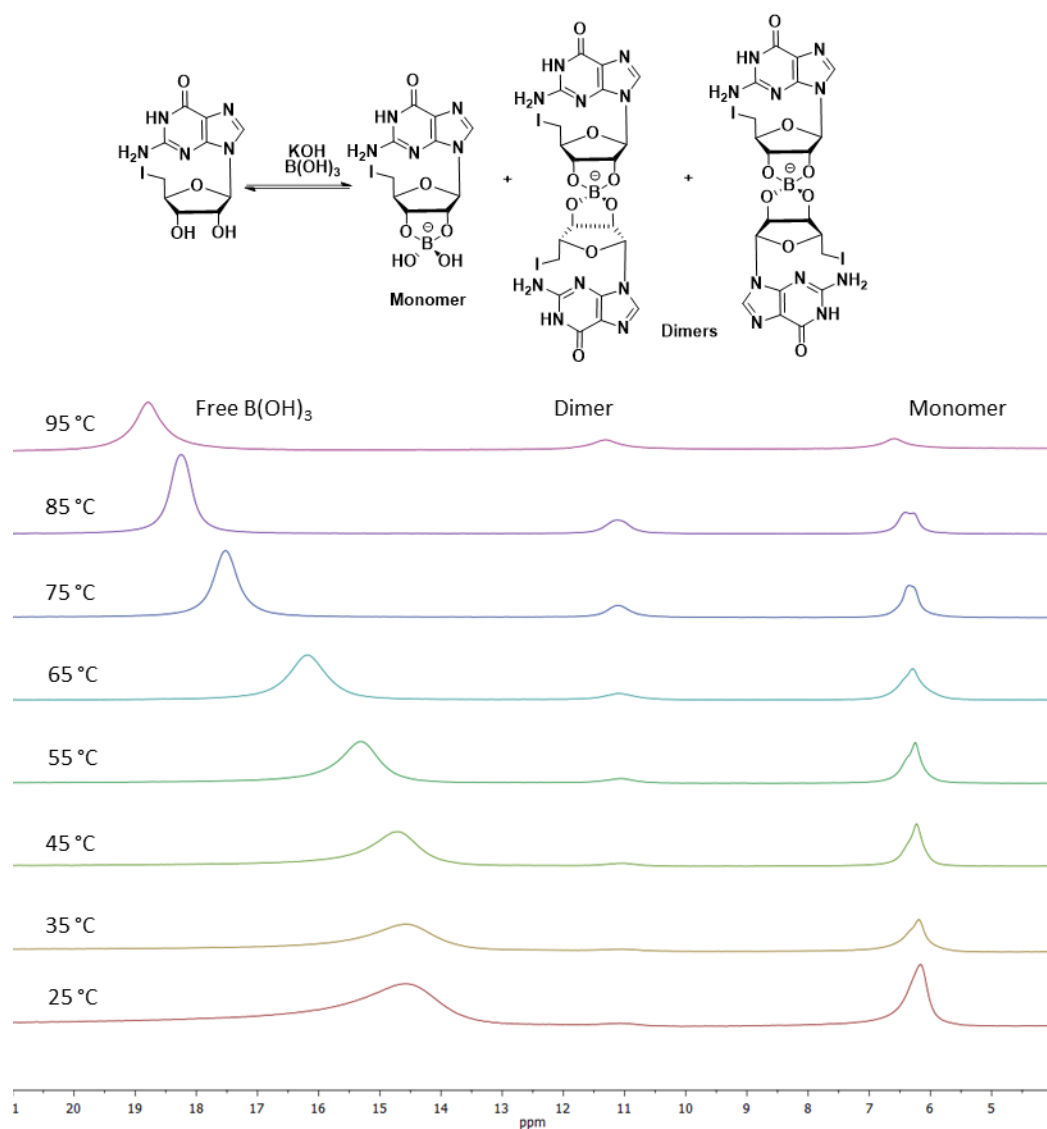
Figure 2.3: Top: The possible borate ester species present in the 5′-IG **2** gel system. Bottom: Variable temperature ^{11}B NMR spectra; experiments were performed on 50 mM 5′-IG **2** gels.[15] Peaks are assigned based on literature precedent.[12]

Both mass spectrometry and NMR spectroscopy confirmed that 5′-*c*G **3** was formed *in situ* when samples were heated to 90 °C. ESI-MS analysis (**Figure 2.4**) of a GB-K$^+$ hydrogel made from 5′-IG **2** showed significant signals for 5′-*c*G **3** + H$^+$ (m/z=266 amu) and for 5′-*c*G **3** + K$^+$ (m/z=304 amu).
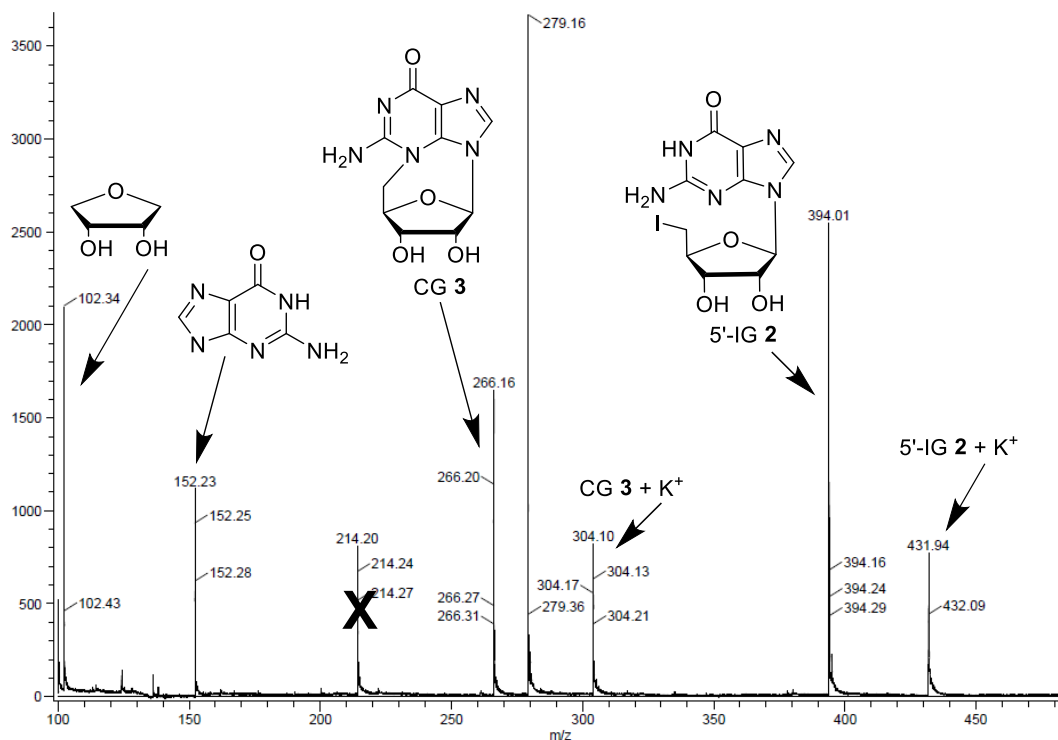
Figure 2.4: Mass spectrum of a 50 mM 5′-IG **2** gel. Peaks are labeled with their corresponding species. The peak at 214 m/z is a contaminant in the mass spectrometer.[15]

A ^{1}H-^{1}H COSY NMR spectrum of the same hydrogel showed separate sets of signals for the borate esters of both 5′-IG **2** and 5′-cG **3** (**Figure 2.5b**). The N3, C5′ cyclization was apparent from the significant deshielding and separation of the H5′,5″ signals for 5′-cG **3** (δ 4.40 and 3.97 ppm) relative to those for 5′-IG **2** (a complex ABX pattern centered at δ 3.35 ppm). These ^{1}H chemical shifts for H5′,5″ of 5′-cG **3**, confirmed by a 2D ^{1}H-^{13}C HSQC experiment (**Figure 2.5a**), matched literature values.[65]
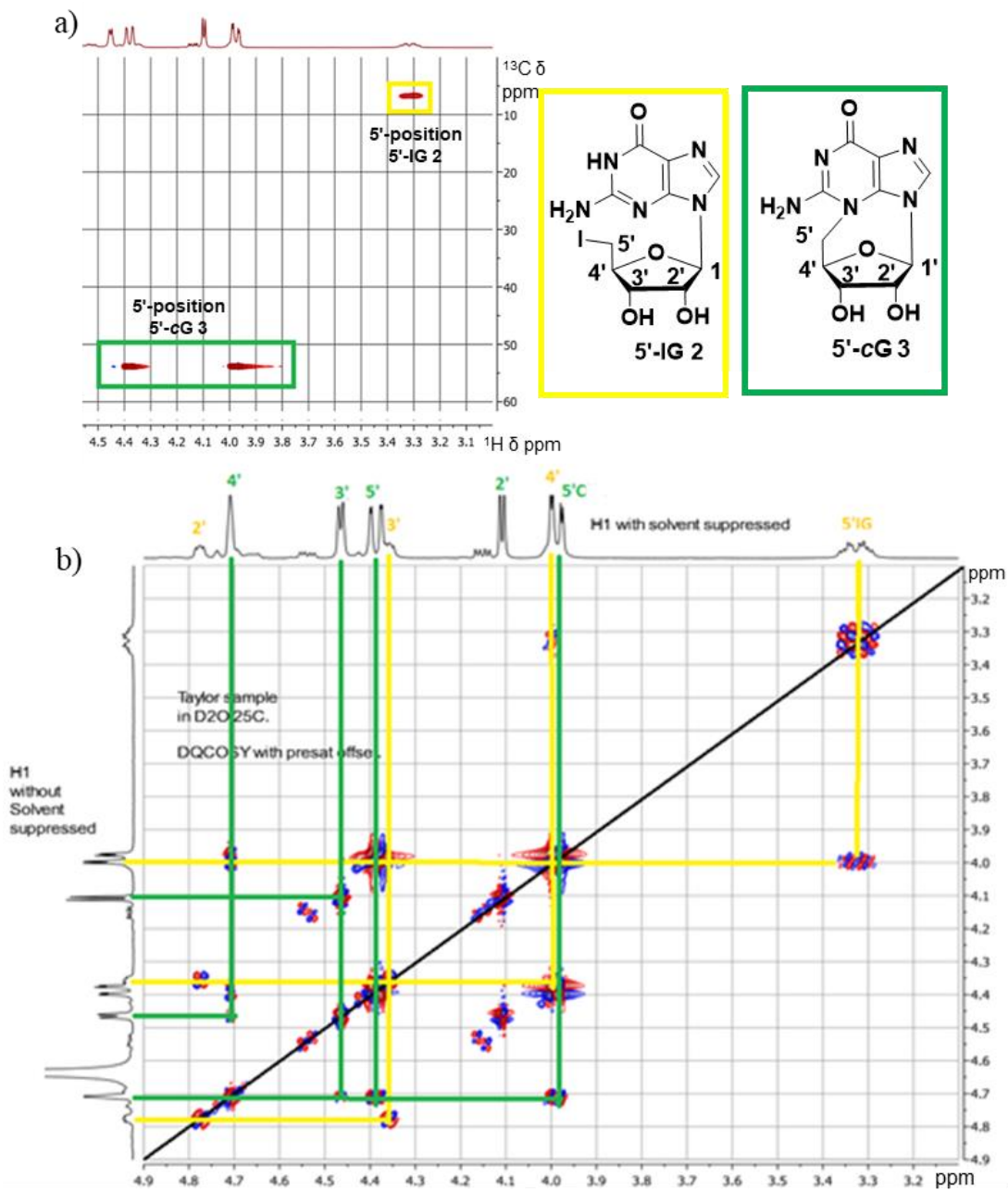
Figure 2.5: a) The HSQC spectrum indicates two different species from the 5′-signals (yellow and green boxes). b) COSY was used to assign the peaks to 5′-IG **2** (yellow labels) and 5′-cG **3** (green labels).[15]

2.5 Control of 5′-*c*G 3 Formation and Influence on Gel Properties

To confirm that 5′-*c*G **3** is responsible for destroying the gel's integrity we compared two different samples made from 5′-IG **2** and KB(OH)$_4$. The first sample, a transparent and stable hydrogel, was made by mixing 5′-IG **2** with 2 eq of KB(OH)$_4$, heating the solution to 90 °C at a rate of 5 °/min, removing the sample from the 90 °C bath, and allowing it to cool at RT. The second sample, which gave a viscous solution, was formed by mixing 5′-IG **2** with 2 eq of KB(OH)$_4$ in water and heating to 90 °C. But, rather than remove sample 2 from the heat bath immediately it was kept at 90 °C for an additional 15 min before cooling at RT. We used ^{1}H NMR to determine the ratios of 5′-IG **2** and 5′-*c*G **3** in each sample (we added acid to ensure that all species were in their monomeric forms, and thus visible in solution NMR, rather than in supramolecular assemblies too large to be seen). The ratio of 5′-IG **2**/5′-*c*G **3** in sample 1 was 65:35 based on integration of the H1′ signals. Sample 2 had a 5′-IG **2**/5′-*c*G **3** ratio of 25:75 confirming that a) 5′-IG **2** is the gelator and b) 5′-*c*G **3** inhibits gelation by 5′-IG **2** (**Figure 2.6**).
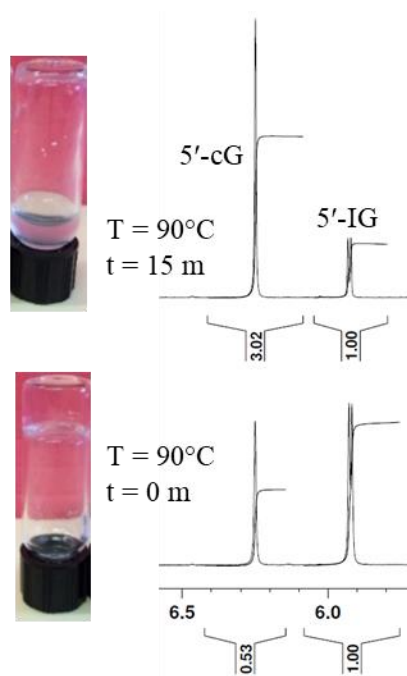
Figure 2.6: ^{1}H NMR experiments on the dissociated gel systems formed with different heating times show that 5′-IG **2** is the gelator. Spectra show the H1′ region. The gel (bottom) is roughly 65% 5′-IG **2** and 35% 5′-cG **3**. The viscous solution (top) contains far more 5′-cG **3** (75%) than 5′-IG **2** (25%).[15]

2.5.1 ^{1}H NMR Shows Higher Temperature Increases 5′-*c*G 3 Formation

Since heating temperature plays a critical role in formation of 5′-*c*G **3** we tested how lowering the heating temperature would affect gelation. We observed that the final temperature to which the gelator solution was heated influenced the appearance, composition, and rheology of the hydrogels. Gels made from 5′-IG **2** (50 mM) ranged from opaque to transparent depending on the temperature to which samples were heated. NMR (**Figure 2.7**) confirmed that the amount of 5′-*c*G **3** varied considerably in these samples, with little cyclization occurring in gels formed at or below 70 °C.
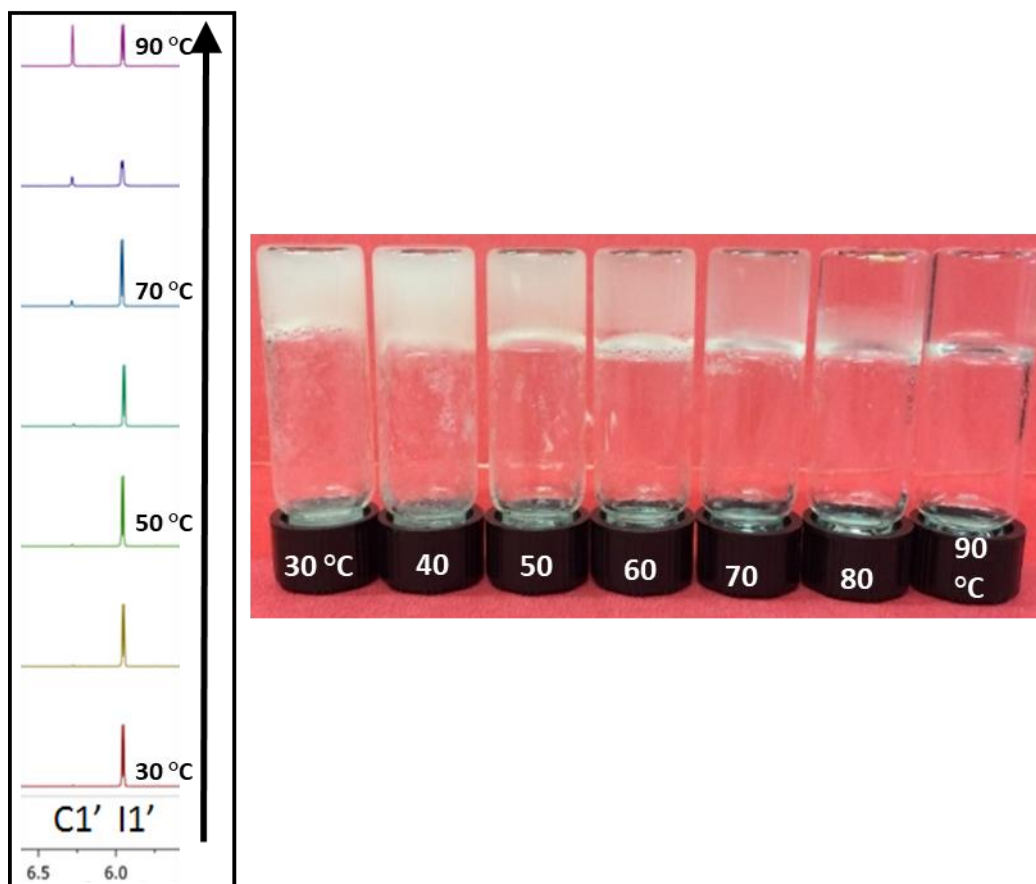
Figure 2.7: Changing the temperature to which gels are heated during formation results in visibly different gels. At 50 mM 5′-IG **2** and 100 mM KB(OH)$_4$, gels range from an opaque white gel when heated to 30 °C to a transparent gel when heated to 90 °C. ^{1}H NMR studies of the dissociated gel networks (the H1′ region is depicted in the spectra) show that these visual changes correspond to varying quantities of 5′-cG **3**, with almost none present in the gels heated to low temperatures (<1% of the total G species in the gel heated to 30 °C), and increasing with heating temperature (~40% of total G species in the gel heated to 90 °C).[15]

2.5.2 Increased 5′-cG **3** Decreases Gel Strength

Rheology showed that the stiffness of 5′-IG **2** GB gels (72 mM) also depended on the preparation conditions. Thus, gels formed after heating to 70 °C were stiffest,

with storage modulus G′ of ~1000 Pa, whereas gels formed after heating to 50 °C and

90 °C had G′ values of ~700 Pa (**Figure 2.8**).
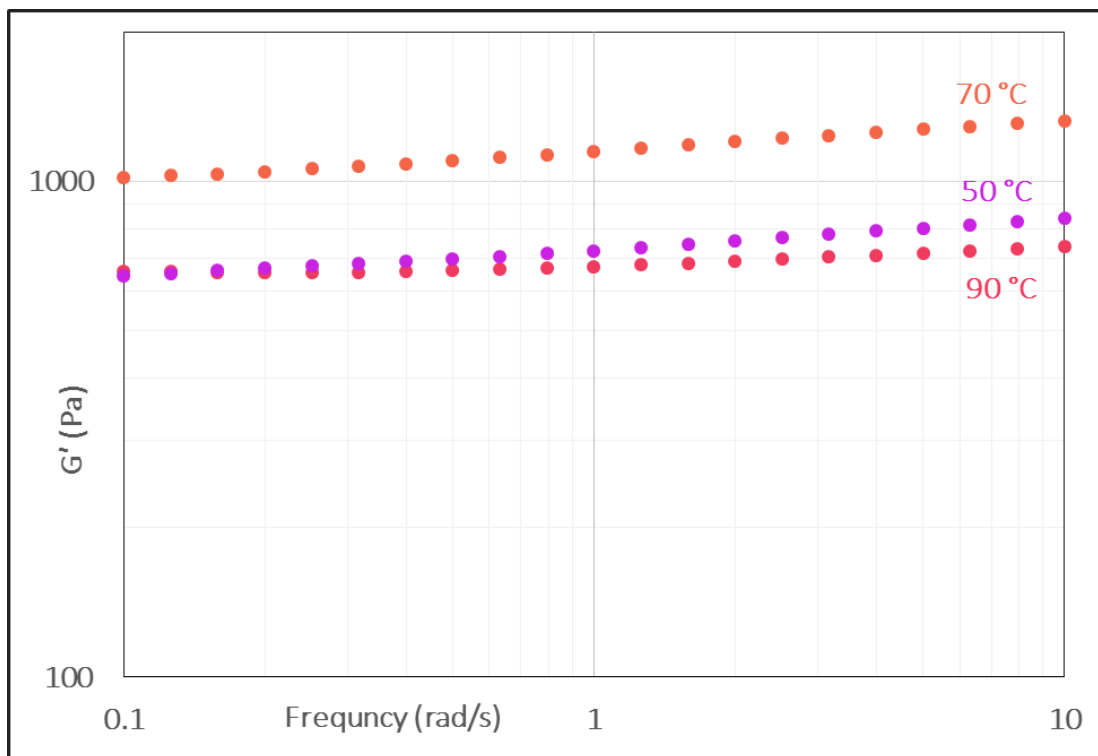
Figure 2.8: Frequency sweeps of 5′-IG **2** gels formed at different temperatures show the gel formed at 70 °C is much stronger than the gels formed at 50 and 90 °C. The G′ value for the gel formed at 70 °C is ~1000 Pa, whereas the values for the gels formed at 50 and 90 °C are around ~700 Pa.[15]

2.5.3 CD Shows Decreased G$_4$-Quartet Signals with More 5′-cG 3

To probe the cause of these rheological differences, we used circular dichroism

(CD) spectroscopy to examine how hydrogelation conditions influenced G$_4$-quartet

formation in different hydrogel samples (**Figure 2.9**). The 5′-IG **2** hydrogel (50 mM)

formed after heating to 70 °C gave a CD spectrum (red trace) similar to that for gels

made from G **1** (blue dotted trace),[12,13] with characteristic G$_4$-quartet peaks at ~290 and

250 nm and troughs at ~270 and 220 nm. This spectrum indicates that this 5′-IG **2** hydrogel contained stacked G_4-quartets.[73,74] Signature CD bands for G_4-quartets were significantly weaker in the hydrogels formed at 50 °C (yellow) and 90 °C (green and purple traces). Overall, these combined observations suggest that the hydrogel's properties depend on a balance between dissolving the poorly soluble hydrogelator 5′-IG **2** and the subsequent cyclization of 5′-IG **2** to 5′-cG **3**. Solubilizing 5′-IG **2** so that it can self-assemble into a G_4-hydrogel is obviously easier at higher temperatures; but, the formation of 5′-cG **3** also increases with temperature.
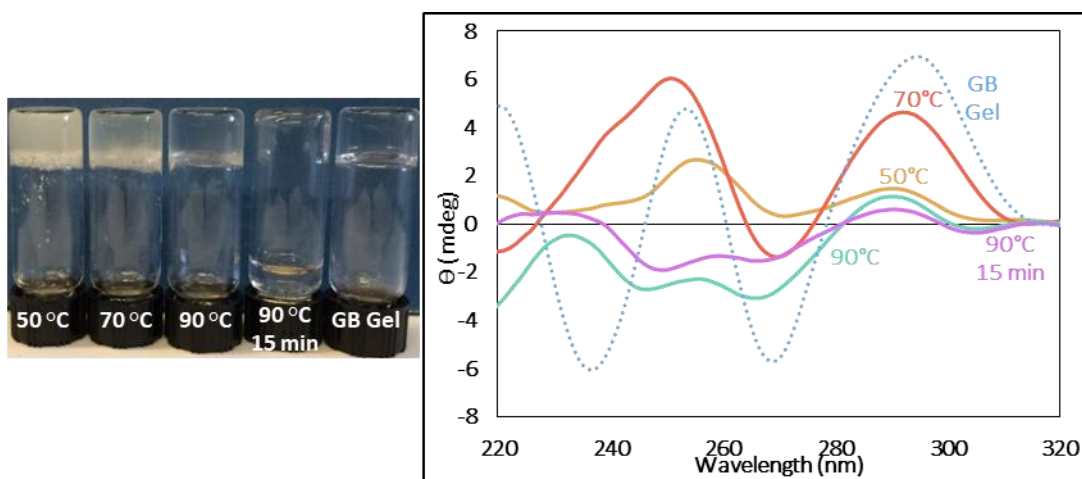
Figure 2.9: 50 mM 5′-IG **2** gels prepared at different heating temperatures give rise to different CD spectra. The gel formed at 70 °C (orange) most closely resembles the GB system (blue), indicating the presence of stacked G_4-quartets. Gels formed at 50 and 90 °C (yellow and green) show a much weaker G_4-quartet signature.[15]

2.6 Utilizing Gel Self-Destruction for Drug Release

Gels often respond to external stimuli, such as mechanical stress, ultrasound, temperature, light, redox processes, pH, ions, chemical reactants and enzymes.[23,24,75] The 5′-IG **2** system is a rare example of a gel whose critical components for formation

(5′-IG **2** and hydroxide) later react to break down the gel. Since 5′-*c*G **3** destroys the gel network we sought to utilize this feature for the "catch and release" of guanine analogs, as depicted in **Figure 2.10**. We knew from our previous work that G-analogs, such as acyclovir (blue), can be incorporated into G4-quartets that make up the GB hydrogel.[12] We reasoned that *in situ* cyclization of 5′-IG **2** (green) to give 5′-*c*G **3** (orange) would perturb the G4-quartets, leading to erosion of the gel. This self-destruction of the hydrogel would enable release of pre-incorporated guanine analogs, such as the anti-viral drugs acyclovir and ganciclovir. [76–78]
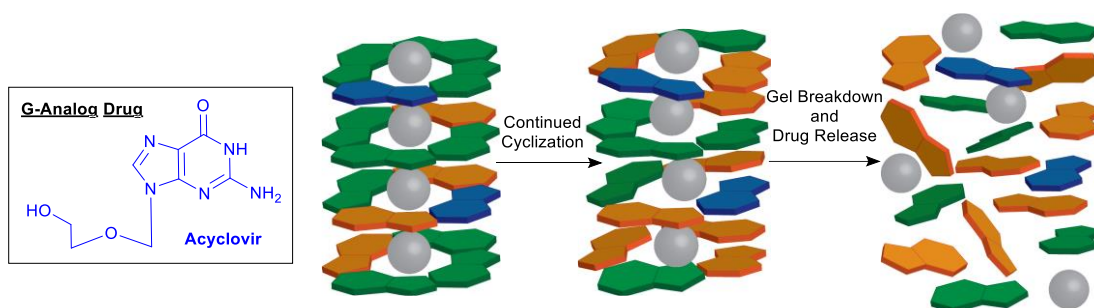
Figure 2.10: Acyclovir (blue) can be incorporated into the 5′-IG **2** (green) gel network. Over time more 5′-*c*G **3** (orange) forms, destroying the gel and releasing the drug.[15]

2.6.1 5′-IG 2 Continues to Cyclize to 5′-*c*G 3 After Gel Formation

Before testing this hypothesis we first explored if cyclization of 5′-IG **2** continued to occur in the gel after its initial formation. We tested gels kept, at both 20 and 37 °C. By using ^{1}H NMR to measure the amounts of 5′-IG **2** and 5′-*c*G **3** in the sol phase, we discovered that cyclization did indeed continue to occur after gelation. NMR data showed that after initial gel formation at 90°C, 56 ± 2 % of the total guanosine species was 5′-IG **2**. After standing for 72 hours at 20 °C, 41 ± 2 % of the G species

was 5′-IG **2** and the gel remained self-supporting. In contrast, after 72 hours at 37 °C only 28 ± 2 % of the sample, a viscous solution, was 5′-IG **2** (**Figure 2.11**).
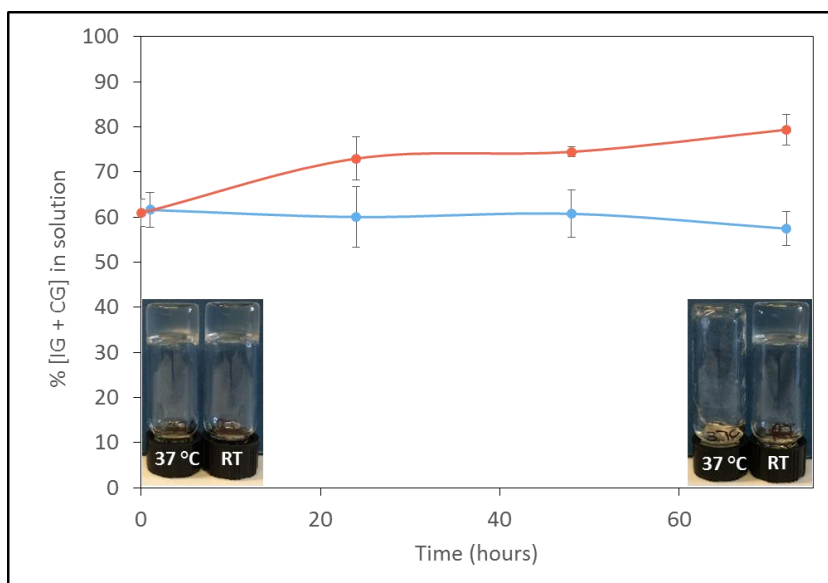
Figure 2.11: Gels at RT (blue) and 37°C (orange) studied over time, after 72 hrs at 37 °C the amount of G-species in solution increased and the system was not a gel.[15]

2.6.2 Drug Incorporation

We were encouraged that the 5′-IG **2** GB hydrogel would show enhanced release of pre-incorporated nucleoside analogs at 37 °C. We monitored the release of two pre-incorporated guanine analogs (the anti-viral drugs acyclovir and ganciclovir)[76–78] from the gel phase into the sol phase at 20 °C and at 37 °C. We pre-incorporated the drugs into the GB gels by adding aqueous $KB(OH)_4$ to a mixture of solid 5′-IG **2** and the drug and then heated and cooled the system as previously described. Using ^{1}H NMR, with an internal standard (d6-DMSO) to measure the H1′ signals for acyclovir and ganciclovir in the sol phase, we found that 1) about 2.5 mM of the G-analogs acyclovir and ganciclovir (out of a total concentration of 5.0 mM) were incorporated into the gel

37

phase of a GB hydrogel made using 5′-IG **2** (50 mM) and 2) both pre-incorporated analogs were then released into the sol phase from the gel over time (**Figure 2.12**).
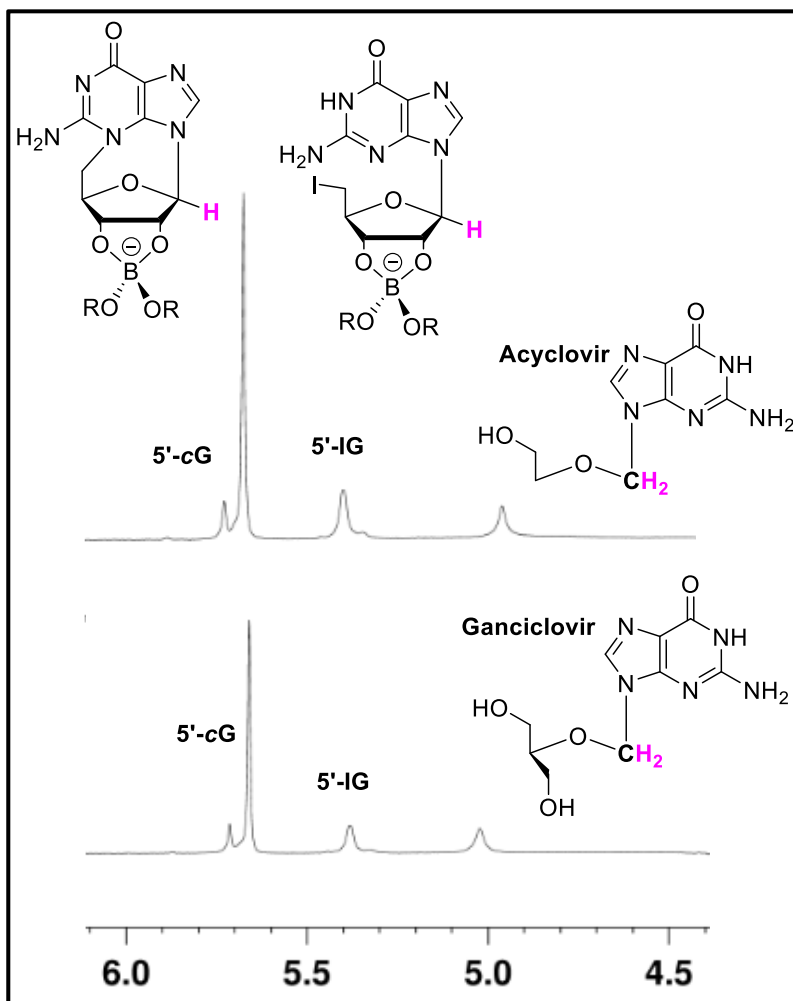
Figure 2.12: The H1′ (pink) region of the spectra shows three peaks representing each species in the sample 5′-*c*G **3**, 5′-IG **2**, and acyclovir (top) or ganciclovir (bottom).[15]

2.6.3 Drug Release

Data in **Figure 2.13** indicates that acyclovir and ganciclovir were both released from the GB gel significantly faster at 37 °C than at 20 °C, which reflects the enhanced rate for N3,C5'-cyclization at body temperature. After 3 days at 37 °C, over 80% of the

pre-incorporated acyclovir had been released into the sol phase, whereas only 13% was released at 20 °C (**Figure 2.13a**). Ganciclovir release at the two temperatures was also quite different. After 3 days at 37 °C, 67% of the ganciclovir was released. In contrast, little, if any, ganciclovir was released from the gel after 3 days at 20 °C (**Figure 2.13b**) the gel network.[12] There is precedent for incorporation and release of acyclovir from another G_4-hydrogel,[46] but this 5′-IG **2** hydrogel shows both higher incorporation and increased release of the drug. Topical applications of a G_4-based hydrogel that slowly decompose and release these pre-incorporated drugs could be beneficial.
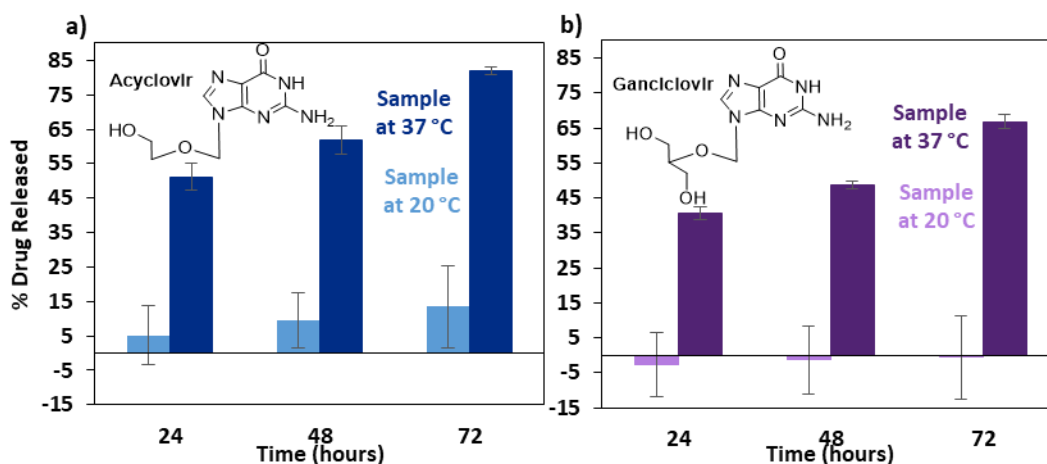
Figure 2.13: Compounds that are pre-incorporated into the gel network can be released over time. a) Acyclovir and b) ganciclovir, can be incorporated into the hydrogel system. Drug release over time increases if the gel is heated. Release data shown is an average of 3 trials. Error bars represent the standard deviation between trials.[15]

2.7 Conclusions

We have shown that 5′-IG **2** forms hydrogels with KB(OH)$_4$ and that **2** also undergoes *in situ* intramolecular cyclization to form non-gelating 5′-*c*G **3**. The temperature-sensitive cyclization continues to occur after gel formation and leads to

self-destruction of the GB hydrogel. The ability to incorporate and release guanosine analogs using such a "self-destroying" gel may find applications for controlled drug release, provided the hydrogelator and 5′-cG **3** are non-toxic.

2.8 Other Results – Solvent Isotope Effect

While performing NMR studies on the 5′-IG **2** gel system using D_2O as the solvent, we discovered a solvent isotope effect. As previously described, transparent gels readily form at 50 mM 5′-IG **2** (with 2 eq of $KB(OH)_4$) in H_2O; however, in D_2O, the result is a translucent viscous solution (**Figure 2.14**).

Figure 2.14: 5′-IG **2** (50 mM) with 2.0 eq of $KB(OH)_4$ gels H_2O but not D_2O. In H_2O clear gels form. Increasing the amount of D_2O in 10% increments yields less viscous, more turbid solutions.

This solvent isotope effect persists over a range of concentrations (**Figure 2.15**) with less viscous, more translucent solutions or gels in D_2O, and stronger, more transparent gels in H_2O.
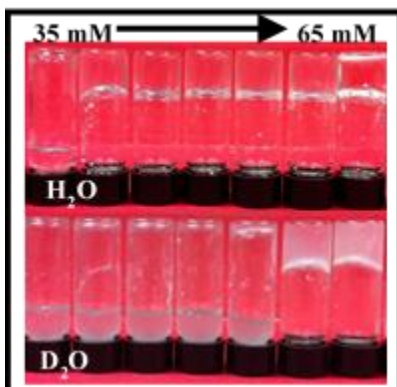
Figure 2.15: The isotope effect persists over a range of 5′-IG **2** concentrations, even when both solvents result in the same phase, either solution (low concentration of 5′-IG **2**) or gel (high 5′-IG **2** concentrations).

There is also a stark rheological difference between gels formed in H_2O and those formed in D_2O. When formed at 90 °C in H_2O, 72 mM 5′-IG **2** gels have a G′ value of ~700 Pa, whereas gels made in D_2O have a lower G′ value of ~300 Pa (**Figure 2.16**).
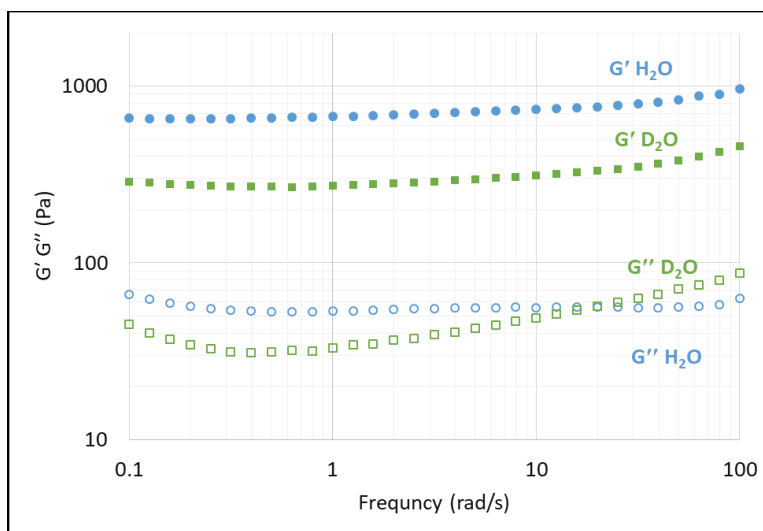
Figure 2.16: The solvent isotope effect of the 5′-IG **2** system is evident in the frequency sweeps of 72 mM gels made with H_2O vs D_2O. With a G′ of ~700 Pa the H_2O system is much stronger than the D_2O system, which has a G′ value of ~300 Pa.

Despite these macroscopic differences, on a microscopic scale ^{1}H NMR spectra of H_2O and D_2O gels are indistinguishable (**Figure 2.17**).
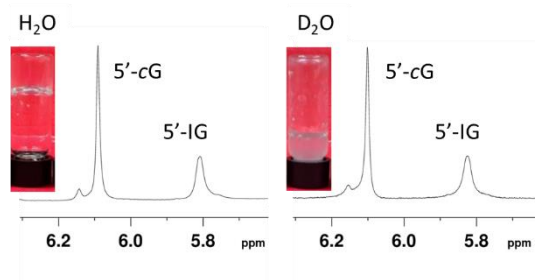
Figure 2.17: Despite the physical differences due to the isotope effect, ^{1}H NMR spectra of the 5′-IG **2** gels in H_2O and D_2O appear the same. The H1′ region is shown.

We believe these findings indicate that the stacking of G_4-quartets somehow differs based on solvent interactions that drive the isotope effect in this system. Previous work on the self-assembly of 5′-GMP indicates that the size and stability of G_4-quartet assemblies differ in H_2O and D_2O. However, no definitive reason for these observed differences is known.[62] While it is well established that the physical properties of H_2O and D_2O are different, there is still much to learn about how and why these differences affect self-assembly.[79] There are many examples in the literature of systems exhibiting isotope effects, but they differ in how changing the solvent alters the system. Some systems seem to be stabilized in D_2O versus H_2O, in others they are destabilized. There are some reports of greater hydrophobic effect in D_2O, and other cases indicating a larger contribution from the hydrophobic effect in H_2O.[80–82] In short, there is no clear consensus on the cause of the solvent isotope effect in self-assembled systems.

While the reasoning behind the H_2O/D_2O difference remains unclear, in the G-based gel systems we have studied, it seems to be present only in the 5′-IG **2**:KB(OH)$_4$

system. This isotope phenomenon does not appear to occur in the GB gel systems,[12–14] or gels made with 5′-IG **2** and excess KCl (**Figure S9**).
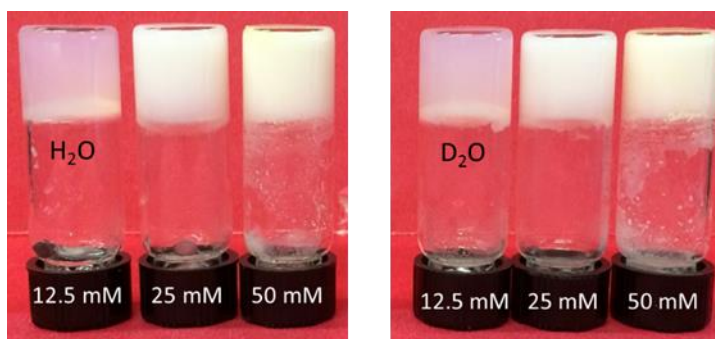
Figure 2.18: Gels made with varying concentrations of 5′-IG **2** and 250mM KCl (H_2O as the solvent on the left and D_2O as the solvent on the right) do not appear to have a noticeable solvent isotope effect.

2.9 Future Directions

To the best of our knowledge this solvent isotope effect in a small molecule hydrogel has never been reported in the literature. It is possible that the H_2O/D_2O effect is so prominent in the 5′-IG **2** system because the gels are not as stable as the G **1** system. Perhaps there is a smaller isotope effect in the G **1** system, but we never noticed it as the system is more stable and H_2O and D_2O gels are visually identical. Future work on this solvent isotope effect could examine a series of known gel systems (such as the GB gels, and other known guanosine analog systems)[9,10,12–14,49,51,52] and test if they exhibit rheological differences, like the 5′-IG **2** system, with changing solvent.

Chapter 3: Guanosine–(Benzene-1,4-Diboronic Acid) Hydrogels for Cell Growth

The majority of this chapter has been published in reference 16:

Rotaru, A.; Pricope, G.; Plank, T.N.; Clima, L.; Ursu, E.L.; Davis, J.T.; Barboiu, M. G-Quartet Hydrogels for Effective Cell Growth Applications *Chem Commun.* **2017**, *53*, 12668-12671.

This work was completed in collaboration with the Rotaru and Barboiu Groups from "Petru Poni" Institute of Macromolecular Chemistry, Centre Advanced Research in Bionanoconjugates and Biopolymers in Romania, and Institut Europeen Membranes, Adaptive Supramolecular Nanosystems Group, Université de Montpellier in France. The Rotaru and Barboiu groups performed the preliminary gel formation experiments, CD spectroscopy, obtained the AFM and SEM images, and carried out the biological experiments (cell growth and cytoxicity). I performed additional gel studies (calculating critical gelation concentration of the different cation gels) and characterized the gels via ^{1}H, and DOSY NMR, PXRD, and rheology.

3.1 Summary

The research in this chapter explores how changing the boron species used to form hydrogels with guanosine (G **1**) can alter gel properties. By using benzene-1,4-diboronic acid (BDBA) in place of $B(OH)_3$ we are able to form guanosine bis-boronate (G-BDBA-G) hydrogels with either K^+ or Ba^{2+}. Moreover, we could add Mg^{2+} to further crosslink the gel network. This significantly decreases the critical gelator concentration (cgc) necessary to form stable hydrogels. These gels are capable of supporting cell growth and showed no visible signs of gel breakdown.

3.2 Introduction

Constitutional self-organization (CSO), self-assembly utilizing both dynamic covalent and supramolecular bonding, provides a unique approach for generating adaptive materials for biomimetic systems.[45,83,84] Hydrogels based on G_4-quartets are a

prime example of these types of materials.[4,85] As described in more detail in the introduction to this thesis, in guanosine based gel systems G **1** self-assembles into H-bonded G_4-quartets that stack to create G_4-wires, forming a gel network. While supramolecular peptide gels have been used in tissue engineering,[1,86,87] the use of nucleoside gels for cell growth has not been well explored.[49,55]

As hydrogels made with various G **1** derivatives are known,[9–11,44,52,53,88–90] we decided to modify our previously reported guanosine-borate (GB) gels by exchanging $B(OH)_3$,[12–15,17] for a boronate species, BDBA **4**.[30,31] We envisioned we would be able to decrease the cgc of the gel due to a) the aforementioned change to ditopic BDBA **4**, which has the more potential for more cross-linking interactions than $B(OH)_3$, and b) adding additional multivalent cations to add another layer of cross-linking between G-BDBA-G moieties (**Figure 3.1**).
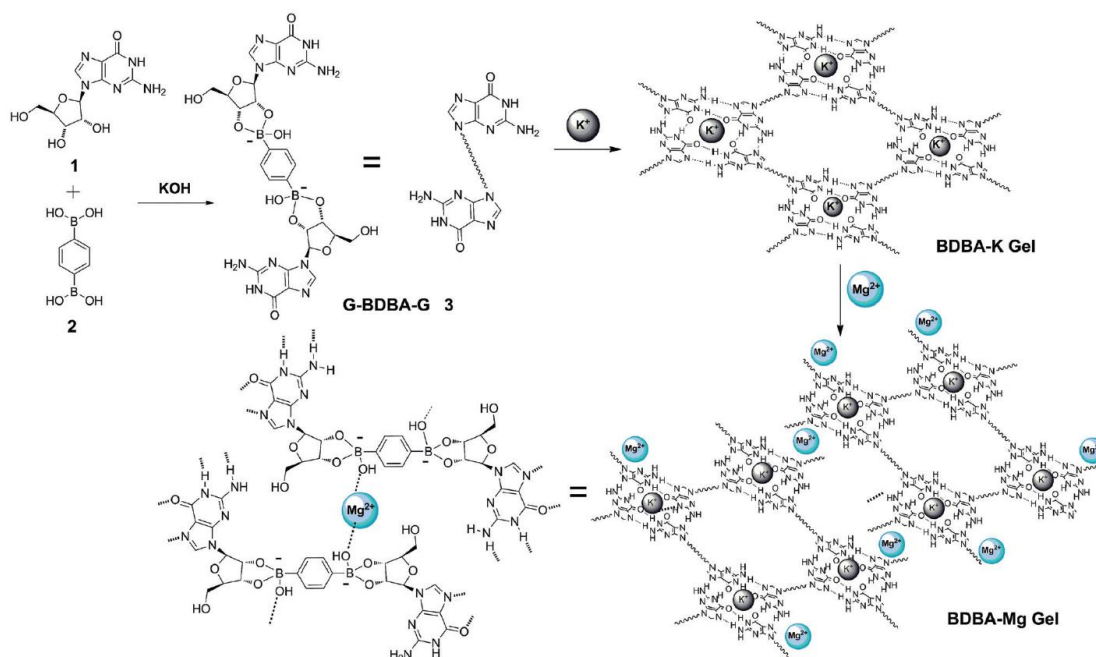
Figure 3.1: The proposed gelation reaction for BDBA-K and BDBA-Mg hydrogels of G **1**.[16]

3.3 Hydrogels from G-BDBA

We found that by using 50.0 mg of G **1** and 0.5 eq of BDBA **4** we were able to form G$_4$-quartet based hydrogels with 1eq K$^+$ or 0.5 eq Ba^{2+}. We found that we could decrease the cgc of the K$^+$ system by adding Mg^{2+} to a preformed BDBA-K gel (**Figure 3.2a**). To compare the cgc of the BDBA-K and BDBA-Mg systems we made a series of gels of varying concentrations and used tip tests, in which a vial containing the hydrogel is inverted to visually see if the gel is self-standing, to determine the cgc for the two systems. We determined that the cgc of G **1** for the BDBA-K gel was ~36 mM (**Figure 3.2b**), while for the BDBA-Mg gel it was significantly lower at <5 mM (**Figure 3.2c**). These results indicate that Mg^{2+} is an effective cross-linker and significantly increases the water content of G$_4$-quartet based hydrogel made from G **1** and BDBA **4**.

Figure 3.2: a) Samples of hydrogels with 50.0 of mg G **1** in various amounts of water (indicated on vials). BDBA-K, 59 mM G **1** (left), BDBA-Ba, 18mM G **1** (middle) and 4mM G **1**, BDBA-Mg (right). b) BDBA-K gels of varying G **1** concentrations (from 88 to 18 mM, as indicated on vials) made with G **1**:BDBA **4**:KOH = 1:0.5:1 c) BDBA-Mg gels of varying concentrations of G **1** (from 88 to 5 mM, as indicated on vials), made by preforming a BDBA-K gel and diluting with H$_2$O, then adding 5 mM Mg^{2+}.[16]

We also attempted to cross-link the BDBA-K gel network using other multivalent cations (**Figure 3.3**); however none of these other cations worked as well as Mg^{2+}. Thus, addition of Li^+, guanidinium, and Fe^{3+} to preformed BDBA-K gel resulted in suspensions or viscous solutions. While Mn^{2+} yielded a brownish-black hydrogel, we determined this color would not be ideal for cell viability studies, so we decided to continue further experiments on only the BDBA-Mg gels.

Figure 3.3: Vials containing G-BDBA and various cations; Li^+, guanidinium (G), and Fe^{3+} result in solutions while Mn^{2+} and Mg^{2+} yield self-standing hydrogels.[16]

3.3.1 NMR Spectroscopy Shows Evidence of G-Boronate Species

To help support the proposed gelation mechanism for the BDBA-K and BDBA-Mg hydrogels made from G **1** (**Figure 3.1**) we utilized NMR spectroscopy. The ^1H NMR spectra in **Figure 3.4** showed evidence of 3 distinct species (namely, G **1** monomer, mono-substituted boronate ester – G-BDBA **34**, and di-substituted boronate ester – G-BDBA-G **35**) in the sol phase of all three gels (BDBA-K, BDBA-Ba and BDBA-Mg). Using diffusion-ordered spectroscopy (DOSY)[91,92] we were able to assign the peaks of the BDBA-Mg gel to each of the three species based on their different

diffusion coefficients. The peak at δ = 5.70 ppm has the largest diffusion coefficient (2.377×10^{-10} m^2 s^{-1}) and therefore belongs to the smallest species, G **1** monomer. The next largest coefficient (1.766×10^{-10} m^2 s^{-1}) corresponds to the monoester G-BDBA **34** at δ = 5.66 ppm. Finally, the peak at δ = 5.91 ppm has the smallest diffusion coefficient (1.698×10^{-10} m^2 s^{-1}), consistent with the largest species, di-substituted G-BDBA-G **35**.
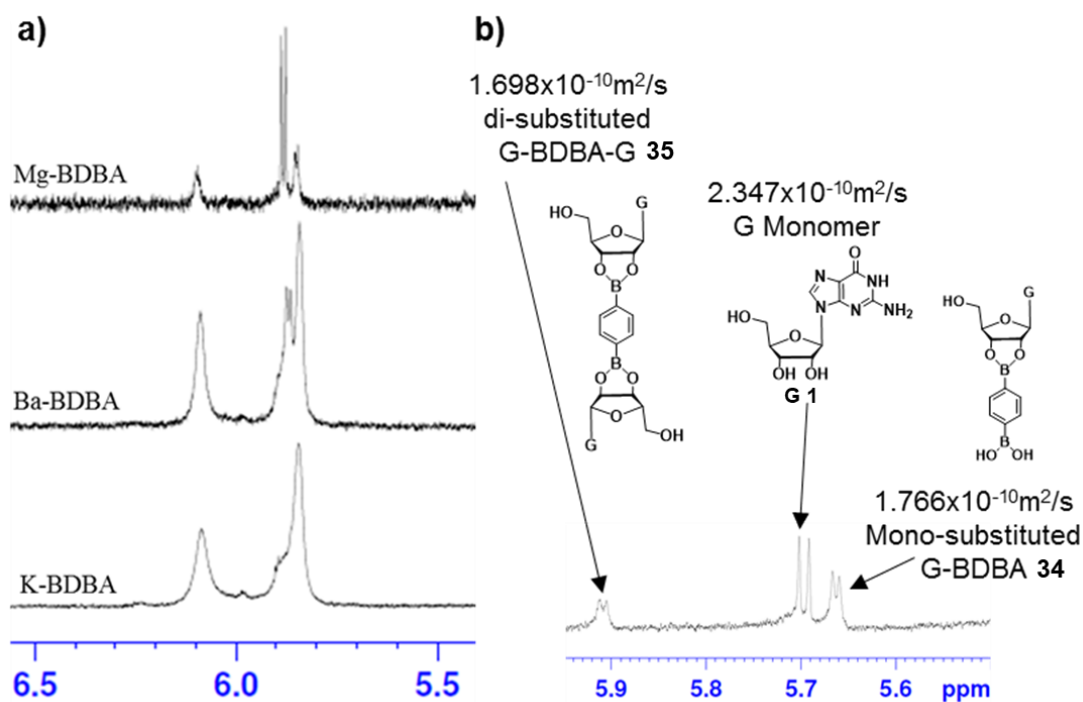
Figure 3.4: a) The H1′ region of the ^{1}H NMR spectra of BDBA-Mg (top), BDBA-Ba (middle), and BDBA-K (bottom) gels at 25 °C in D$_2$O show three peaks that correspond to different species of G **1** in solution. b) The diffusion coefficients of the three G **1** species (G-monomer, mono-substituted G-BDBA **34**, and di-substituted G-BDBA-G **35**) were determined for the H1′ peaks in a BDBA-Mg sample in D$_2$O at 5 °C.[16]

3.3.2 PXRD and CD Spectroscopy Show Hydrogels are G$_4$-Quartet Based

Powder x-ray diffraction (PXRD) obtained from a lyophilized sample of a BDBA-K gel showed a peak at $2\theta \sim 26.9°$ ($d = 3.3$Å), which is consistent with the π-π stacking distance between G4-quartet layers (**Figure 3.5**).[60,93]
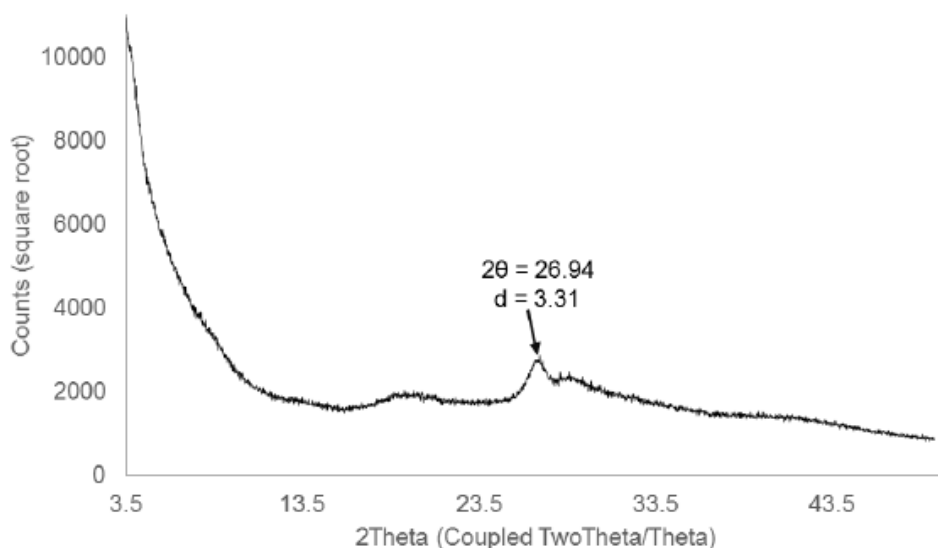
Figure 3.5: PXRD data of a lyophilized BDBA-K gel supporting the presence of stacked G$_4$-quartet layers in the sample.[16]

We used CD spectroscopy to further confirm the presence of stacked G$_4$-quartets, indicated by presence of bands in the 240-260 nm and/or 290-300 nm regions.[73] All three gels exhibited distinctive CD spectra indicative of different G$_4$-stacking interactions or different populations of *syn*/*anti*-conformers about the glycosidic bond of G **1**. The CD spectrum of BDBA-K showed an intense positive band at 300 nm with a broader negative band at 255 nm (**Figure 3.6a**). In BDBA-Ba, the oppositely signed negative–positive bands lower than 290 nm can be attributed to left-handed helical stacking of G$_4$-quartets (**Figure 3.6b**) indicating a different chiral

structure than that in BDBA-K. Finally, the spectrum of BDBA-Mg showed a small negative–positive band (240–260 nm), similar to BDBA-Ba, and a strong negative band at 290 nm, attributed to a unique G_4-orientation induced by Mg^{2+} (**Figure 3.6c**).
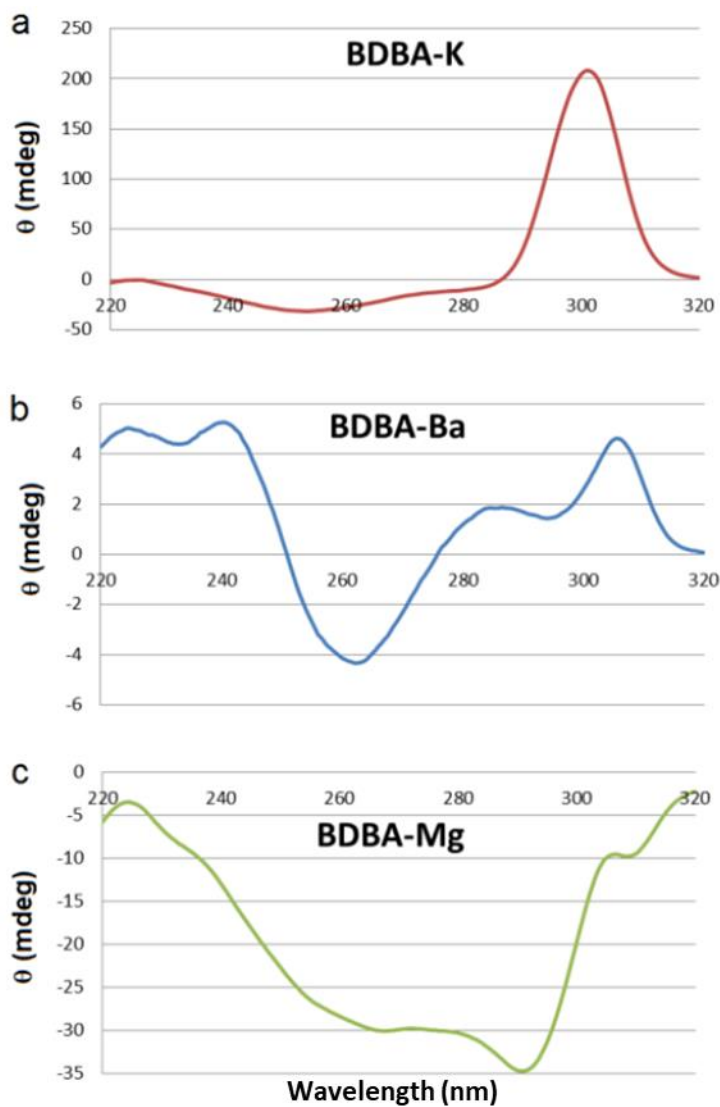
Figure 3.6: CD spectra for the BDBA-K, BDBA-Ba, and BDBA-Mg show peaks in the region characteristic of G_4-quartets.[16]

50

3.3.3 Hydrogels Have Solid-Like Rheology with Strength Dependent on Cation

Rheological studies of the three gels showed that all have solid-like rheology (**Figure 3.7**) with a storage modulus (G′) greater than the loss modulus (G″).[94] Both the BDBA-K and BDBA-Ba gels are stiffer than the BDBA-Mg gel, which contains a significantly lower concentration of G **1** than the other two gels. The important point is that, even at 5 mM G **1**, BDBA-Mg has rheological characteristics of a hydrogel, with a constant G′ value that is greater than G″ over the entire strain range of 0.1–100%.
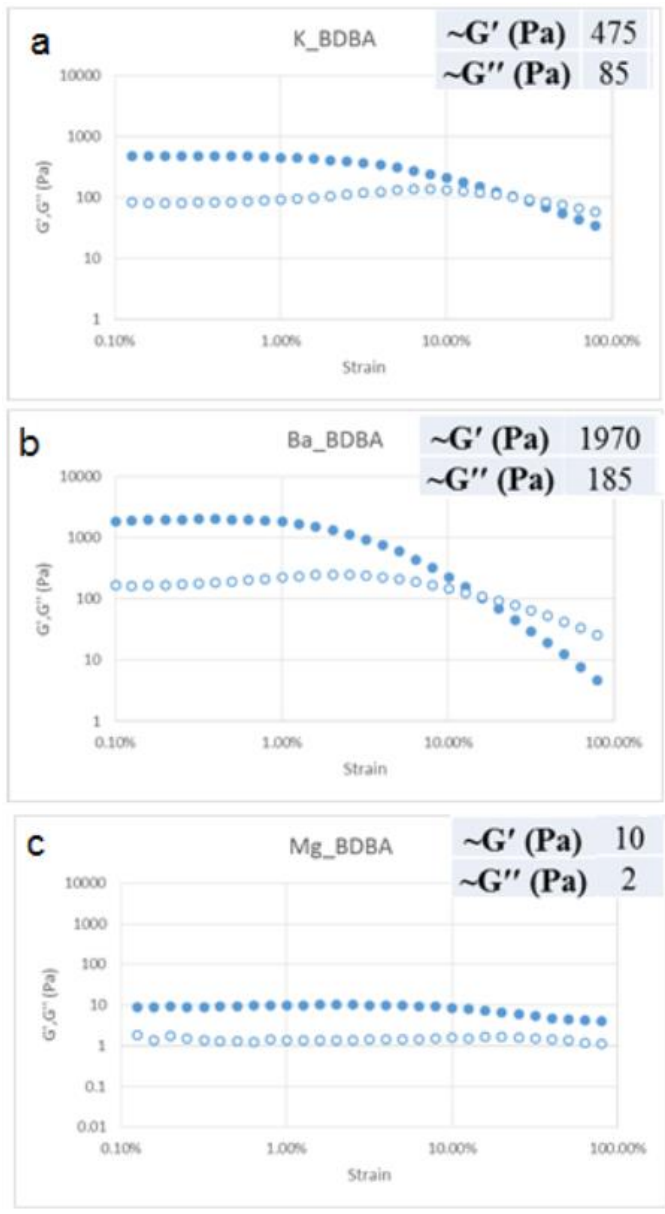
Figure 3.7: Rheological strain sweeps of the three gels show the storage modulus G′ (●) and the loss modulus G″ (○) in Pascals (Pa).[16]

3.3.4 Microscopy Shows Gels of Different Cations Have Unique Morphologies

Using atomic force microscopy (AFM) we found that each sample exhibits distinct morphologies on the microscale. BDBA-K has an organized wave-like structure with a unit size of ~1 mm (**Figure 3.8a**), while BDBA-Ba shows uniform fibrillar layers (**Figure 3.8b**). On the sub-mm scale, BDBA-K and BDBA-Ba hydrogels have similar structures (bottom **Figure 3.8a** and **b**). Importantly, the BDBA-Mg gel has a distinct morphology, with interconnected fibers up to several mm in length (**Figure 3.8c**). These AFM results, along with the tip-test, CD, and rheology data, highlight that Mg^{2+} serves as a bridging element between G_4-quartet structures formed by G-BDBA-G **35**. The width of the fibers suggests that 15–23 G-quartets, each having a diameter of ~3 nm, may self-assemble via Mg^{2+} external cross-linking, to form an aggregated fibrillar structure of 50–70 nm. It is important to note that although Ba^{2+} and Mg^{2+} are both divalent cations, the morphologies of their respective hydrogels are very different: the absence of the fibers for BDBA-Ba in the AFM is consistent with Ba^{2+} not forming bridges, but instead stabilizing the H-bonded G_4-quartets. A related cross-linking motif was reported for adenosine monophosphate hydrogels stabilized by selective synergetic interactions of Zn^{2+} with phosphate and adenine groups.[95]
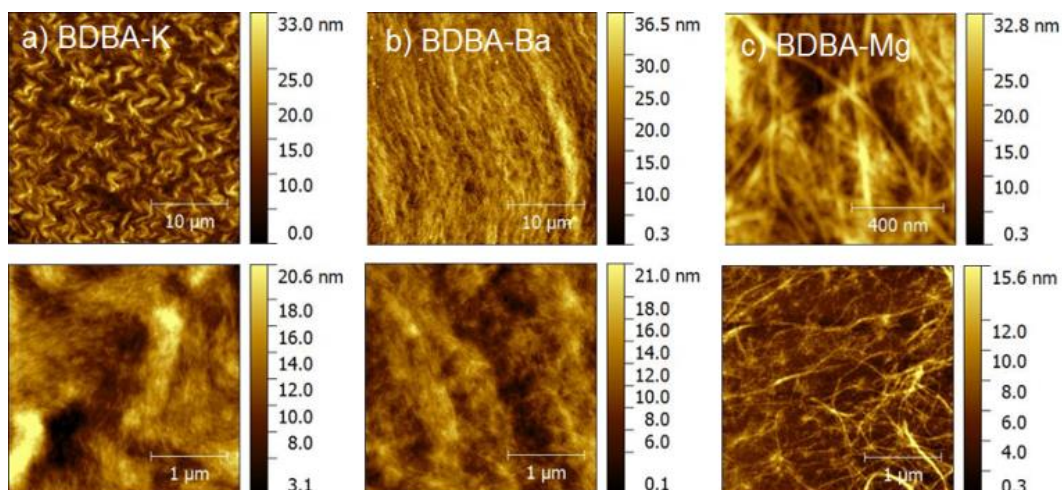
Figure 3.8: AFM images of a) BDBA-K, b) BDBA-Ba, and c) BDBA-Mg hydrogels.[16]

We also performed scanning electron microscopy (SEM) on a freeze-dried sample of a BDBA-K hydrogel, which showed a sponge-like microstructure with pore diameters between 5-8 μm (**Figure 3.9**).
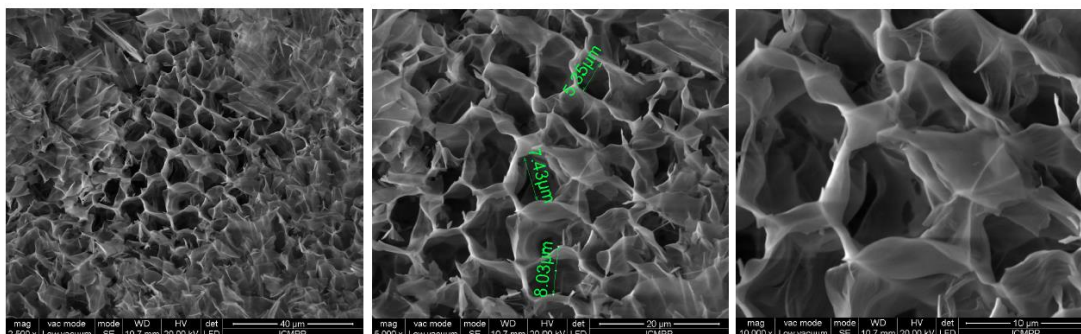
Figure 3.9: Representative SEM images of freeze-dried BDBA-K hydrogels.[16]

3.4 Hydrogels are Capable of Supporting Cell Growth

Having characterized the hydrogels we next tested their potential applicability in tissue engineering. We performed cell growth and viability tests on the NDF (Normal

Human Dermal Fibroblasts)[96] cell line using freshly-prepared BDBA-K (88 mM G **1**), BDBA-Ba (20 mM G **1**), and BDBA-Mg (18 mM G **1**) hydrogels. The high pH values of the initial hydrogels were adjusted to near neutral by washing with TAE buffer: BDBA-K (pH = 9.5 to pH = 7.6), BDBA-Ba (pH = 8.8 to pH = 7.5), and BDBA-Mg (pH = 9.5 to pH = 7.4). The BDBA-K gel was stable under both buffered and unbuffered conditions. The BDBA-Ba gel became cloudy after buffer treatment and no cell growth was observed. Although the buffer-treated BDBA-Mg gel initially supported cell growth it was unstable under these experimental conditions, and started to degrade after 24 h and it was almost all destroyed after 48 h (**Figure 3.10**).
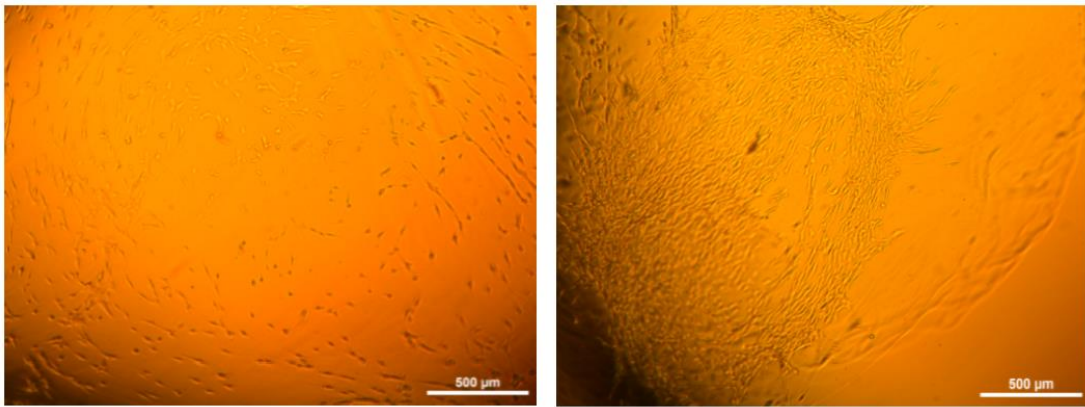
Figure 3.10: NHDF cells on BDBA-Mg hydrogels treated with 3xTAE + KCl (155 mM) visualized after 4 h (left) and 24 h (right).[16]

Based on these findings, the cell growth experiments on buffered BDBA-K, and unbuffered BDBA-Ba and BDBA-Mg gels were monitored, with images taken, at 0, 4 and 24 h of cell cultivation (**Figure 3.11**).
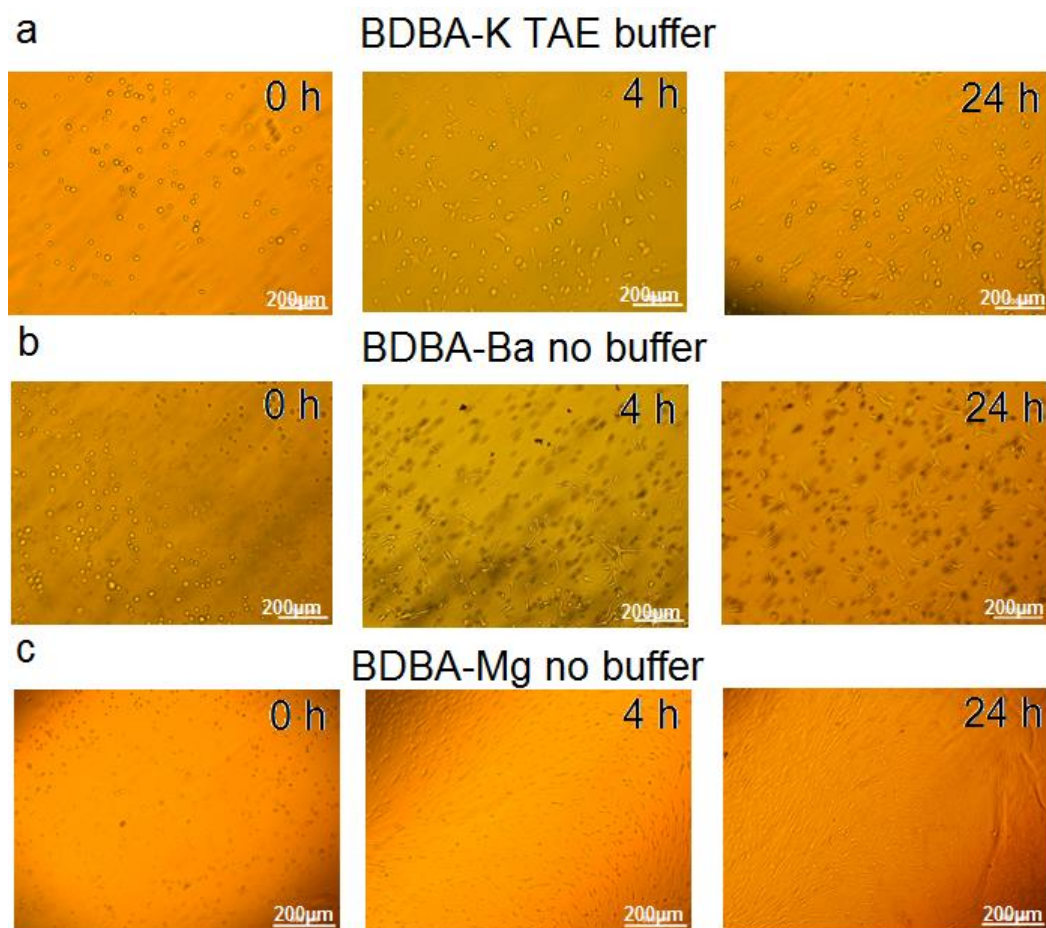
Figure 3.11: NHDF cells on a) BDBA-K gel washed w/ $3xTAE/Mg^{2+}$ buffer, b) BDBA-Ba gel (no buffer), and c) BDBA-Mg gel (no buffer); at different time points.[16]

As shown in **Figure 3.11a**, after 4 h, the cells had begun to attach to the BDBA-K surface, changing from a spherical to an ellipsoidal shape, with a clear improvement in cell density after 24 h. The most spectacular results were obtained with BDBA-Ba and BDBA-Mg hydrogels that were not treated with TAE buffer. As seen in **Figure 3.11b**, the cells adhered to the surface of the unbuffered BDBA-Ba hydrogel, forming a network of linked cells after 24 h. Similarly, untreated BDBA-Mg hydrogels showed

excellent properties as cell growth supports, with a dense network of connected cells, and the gel platform did not present any signs of degradation over 24 h (**Figure 3.11c**).

Cell viability on the hydrogels was evaluated using a colorimetric MTS cell proliferation assay and was calculated as a percentage relative to the viability of untreated cells supported by the culture medium.[97] Our experiments showed that the cell viability after 24 h was 42% for BDBA-K and 47% for BDBA-Ba, but was significantly greater at 73% for the less dense gel network resulting from the lower concentration of G **1** in the BDBA-Mg hydrogel (**Figure 3.12**). In our cytotoxicity experiments we have used the ISO 10993-5 standard, which recommends a quantitative evaluation of the cytotoxicity of a material after 24-72 h using a colorimetric method. The material tested is considered non-cytotoxic if the viable cells is greater than or equal to 70% of the untested control, as our results show for the BDBA-Mg hydrogel.[98]
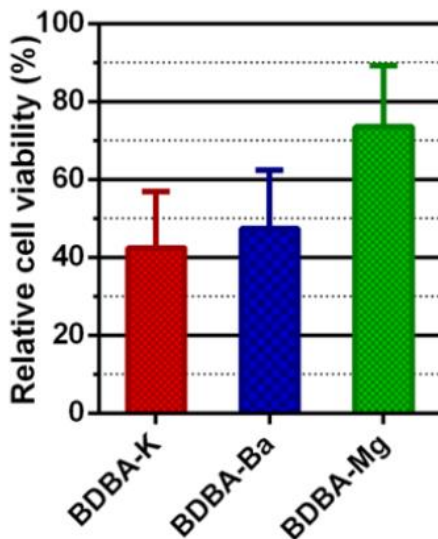
Figure 3.12: Cell viability by MTS assay on the three different hydrogels. The reference sample is considered 100% for cell viability on culture medium.[16]

3.5 Conclusions

We have designed and prepared G_4-quartet hydrogels readily made from the natural product G **1**, BDBA **4**, and various templating and bridging cations. These gels show interesting cation-dependent physical and functional properties. Tip tests, NMR, CD, and microscopy data show that the structure of the supramolecular hydrogels are governed by the identity of the cations used for internal stabilization of G-quartets (K^+ or Ba^{2+}) as well as by external cross-linking of anionic boronates by Mg^{2+}. The composition of each hydrogel determines the cgc of G **1**, with the Mg^{2+} crosslinked hydrogel requiring a cgc over 7 times lower than a non-externally crosslinked gel, such as BDBA-K. This decreased cgc makes these hydrogels perfect candidates for cell growth applications. Our initial findings using the NHDF cell line demonstrate that these G_4-quartet hydrogels can support significant cell growth on their surfaces.

3.6 Future Work

Future work on this system will include screening other formulations of the gel system (varying pH, ionic strength, and buffers) to find optimal conditions for growing cells on these easy to make and biocompatible G_4-quartet hydrogels.

In addition, we plan to test other boron-containing compounds to see how they affect gelation. Some possible options include, altering the position of the boron in benzene-diboronic acid, and altering the carbon linker size, such as with biphenyl-diboronic acids.

Chapter 4: 8-Aminoguanosine/Guanosine Binary Gels in Environmental Remediation – Selective Uptake of Anionic Dyes from Water

The majority of this chapter has been published in reference 17:

Plank, T.N.; Skala, L.P.; Davis, J.T. Supramolecular Hydrogels for Environmental Remediation: G_4-quartet Gels that Selectively Absorb Anionic Dyes from Water *Chem Commun.* **2016**, *53*, 6235-6238.

Some of the preliminary work for the experiments described in this chapter was performed by Luke P. Skala, who, at the time, was an undergraduate researcher in the Davis lab. ICP-MS data was collected by Dr. Richard Ash of the UMD Geology department. SEM images were obtained by Dr. Wen-An Chiou at the Maryland NanoCenter.

4.1 Summary

This chapter highlights how changing the salt with which guanosine (G **1**) based gels are formed can tailor gels for various properties. As previous research in our lab showed, the guanosine-borate (GB) gels made with G **1** and alkali metal borate salts are capable of absorbing and retaining cationic dyes from water, presumably due to electrostatic interactions with the anionic borate esters within the gel network.[12–14] We sought to find a system capable of forming gels with and without borate salts to give us the ability to selectively uptake either cationic or anionic dyes.

We discovered that binary gels made of 8-amingoguanosine (8AmG **5**) and guanosine (G **1**) are capable of forming stable, transparent gels with $KB(OH)_4$, as well as with nitrate or chloride salts. Using nitrate or chloride salts allowed to us to expand the scope of cations used in gelation to include the divalent Ba^{2+}, Sr^{2+}, and Pb^{2+} cations. We found that altering the salts with which the gels are made changes the ability of the hydrogel to absorb cationic (with $B(OH)_4^-$ salts) or anionic (with Cl^- or NO_3^- salts) dyes.

4.2 Introduction

Guanosine hydrogels, known since 1910,[5] are undergoing a resurgence because of their biocompatibility and many potential applications.[2,9–11,49,51,55] As described in more detail in the introduction to this thesis, we recently developed a hydrogel formed by guanosine (G **1**) and 0.5 eq of $MB(OH)_4$, where M is an alkali metal cation.[12–15] This guanosine-borate (GB) hydrogel is based on anionic GB-diesters that self-assemble into G_4-quartets. The gel's rheological properties are sensitive to the templating cation, with K^+ giving the strongest gels.[13,14] The GB hydrogel, with its anionic borates, selectively extracts cationic (vs. anionic) dyes from solution.[12,14]

We sought to develop a G_4-hydrogel to absorb anionic dyes, many of which are wastewater pollutants (**Figure 4.1**).[99,100] The GB gels do not bind anionic dyes well, likely due to electrostatic repulsion of the dye with the anionic borate esters. In order to uptake anionic dyes we needed to eliminate the borate esters, from the gel system. To develop a stable G_4-hydrogel without borate, which forms GB esters so as to better solubilize G **1** and allows for greater crosslinking of the gel fibers, we took a two-pronged approach. First, we sought to form G_4-M^{2+} hydrogels with divalent cations, reasoning that the higher charge density of M^{2+}, relative to M^+, should enhance electrostatic binding of anions. There are examples of lipophilic guanosines forming very stable G_4-quartets with divalent cations (Ba^{2+}, Sr^{2+} and Pb^{2+}) in organic solutions,[101,102] and G_4-DNA is known to bind divalent cations in water.[103,104] Surprisingly, at the time we discovered this hydrogel, there was just one reference, with no experimental detail, to a G_4-hydrogel containing divalent cations.[41] Second, we

searched for a binary system composed of two analogs that would form these G_4-M^{2+} hydrogels. Several binary systems are known to form stable G_4-K^+ hydrogels, and it is postulated that the binary mixtures add disorder that prevents crystallization of hydrophobic G **1**, thus promoting gelation.[9,10,49,51]
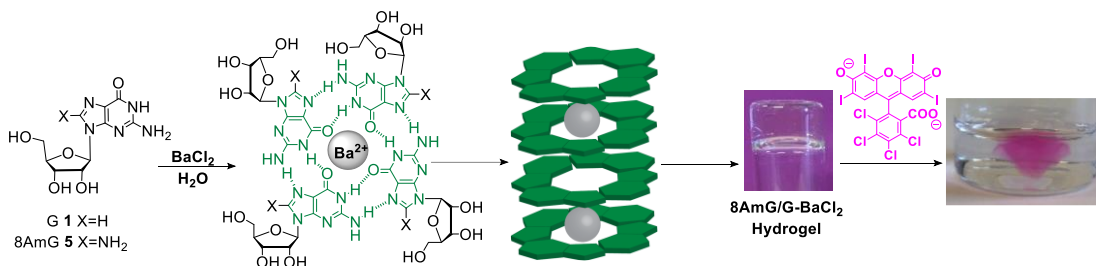
Figure 4..1: Binary 1:1 mixtures of G **1** and 8AmG **5** with alkali/alkaline earth salts (K^+ and Ba^{2+}) give G_4-quartet structures that lead to formation of stiff, stable, and transparent hydrogels. The 8AmG/G-BaCl$_2$ hydrogel can selectively extract anionic dyes from solution into the gel phase.[17]

In searching for binary G_4-hydrogels we focused on C8-substituted G derivatives, since that modification does not block G_4-quartet formation which is essential for hydrogelation. We chose to explore 8-aminoguanosine (8AmG **5**) as a gelation partner for G **1**, since 8AmG **5** forms G_4-quartets in DNA.[105] In addition, poly-8AmG's pK_a is 9.4,[106–108] suggesting that a significant amount of 8AmG **5** would be protonated in a G_4-hydrogel (**Figure 4.2**). Having a cationic gel network would further enhance electrostatic binding of anionic dyes by a G_4-M^{2+} gel.
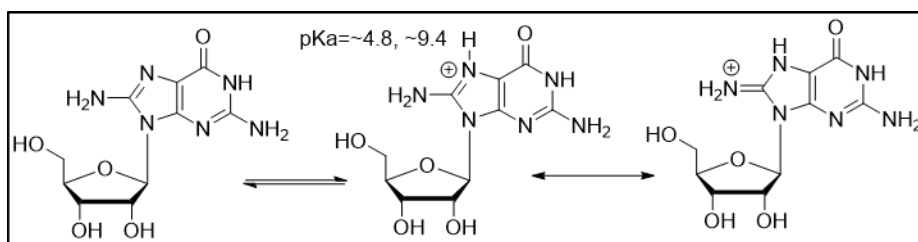
Figure 4.2: The potential protonation of the N7 position and subsequent resonance stabilization possible with 8AmG **5**.[17]

4.3 Binary Mixtures of 8AmG 5 and G 1 Form Stable Hydrogels

We found that 1:1 mixtures of G **1** and 8AmG **5** form strong, stable, and transparent G_4-hydrogels when treated with stoichiometric amounts of either K^+ or Ba^{2+}. These binary G_4-hydrogels show potential for use in environmental remediation,[109] as both the 8AmG/G-K^+ and 8AmG/G-Ba^{2+} hydrogels selectively bind anionic dyes, including naphthol blue black (NBB **36**), a diazo dye used in the textile industry and a major pollutant.[99] Most remarkably, we also show that the 8AmG/G-Ba^{2+} gel outcompetes the 8AmG/G-K^+ hydrogel for binding the anionic NBB **36**.

G **1** and 8AmG **5** alone do not form hydrogels with any alkali or alkaline earth salts that we tested. However, a 1:1 mixture of G **1** and 8AmG **2** form a transparent hydrogel in the presence of KNO_3 (**Figure 4.3a**). Using ^1H NMR spectroscopy we found that the solution phase of an 8AmG/G-K^+ sample contained an excess of G **1** (12 mM) relative to 8AmG **2** (7 mM), indicating a modest preference for 8AmG **5** (28 mM) to be incorporated into the gel over G **1** (23 mM). With 2 eq of KNO_3 (relative to nucleoside) this binary mixture had a critical gelation concentration (cgc) of ~18 mM.
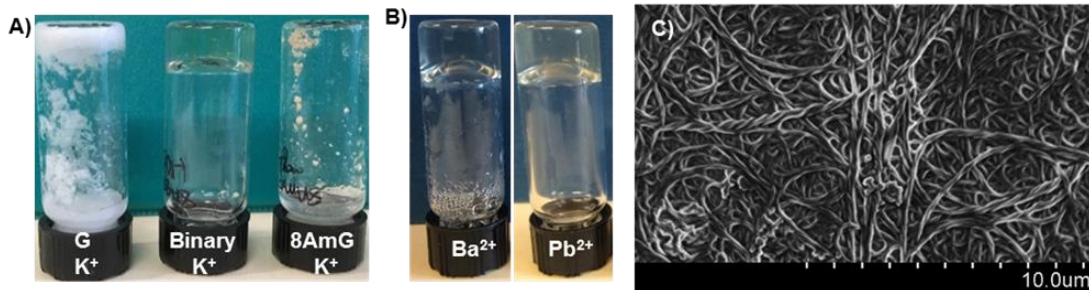
Figure 4.3: A) Mixtures of 2 wt% (70 mM) of G species with 2 eq of KNO_3 that were heated to 95 °C and cooled at 20 °C for 1 hr. Only the 1:1 binary mixture of G **1**/8AmG **5** forms a hydrogel. B) Binary 1:1 8AmG **5**/G **1** hydrogels formed with 2 eq of $Ba(NO_3)_2$ or $Pb(NO_3)_2$. C) An SEM image of an 8AmG **5**/G **1** gel (2wt%, 70 mM), made with 2 eq of $Pb(NO_3)_2$, shows a fibrous intertwined gel network.[17]

4.3.1 Hydrogels are G4-Quartet Based

Both circular dichroism (CD) spectroscopy and powder X-ray diffraction (PXRD) indicate this binary gel contains G_4-quartets (**Figure 4.4**). The dominant feature of the CD spectra was the exciton couplet centered near 260 nm, diagnostic of stacked G_4-quartets that are rotated with respect to one another, in either a classic G-quartet structure or in a helical structure.[110,111] PXRD data on a dried 8AmG/G-K^+ gel shows peaks corresponding to ~20 Å, a value that is close to the diameter of a G_4-quartet, and ~3.3 Å, which is the π-π stacking distance between G_4-quartets.[112]
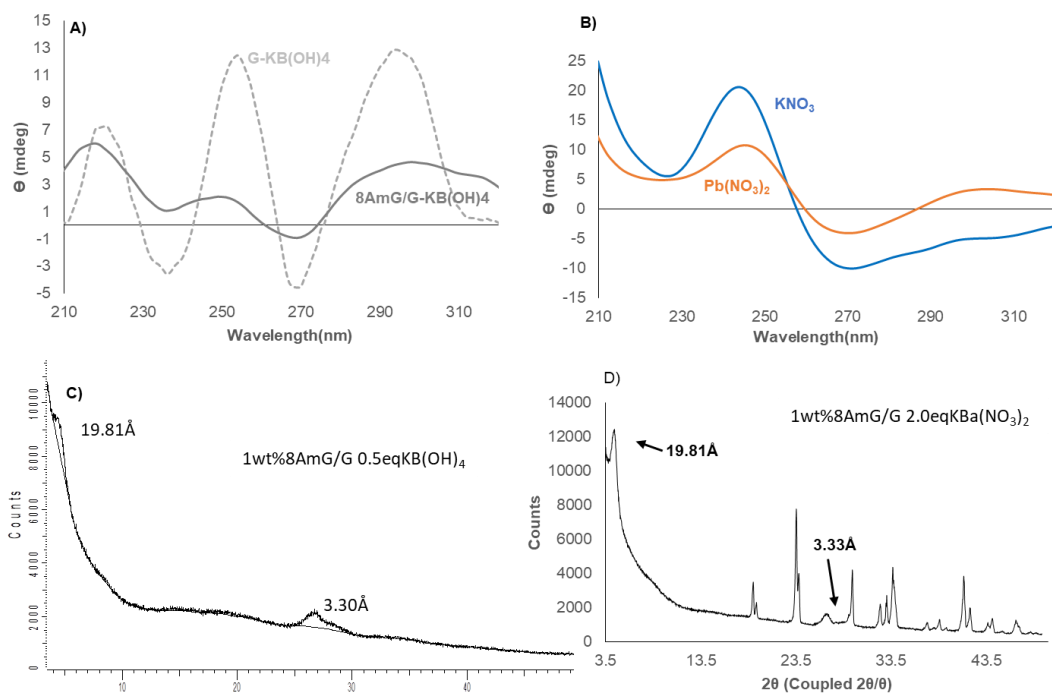
Figure 4.4 : CD Spectra (A and B) of the gels show signature peaks for G_4-assemblies. Representative PXRD data (C and D) show peaks corresponding to the diameter of a G_4-quartet (~20 Å) and the π-π stacking distance between layers (~3.3 Å).[17]

4.3.2 8AmG/G Hydrogels Form with Divalent Cations

In addition to forming transparent gels with K^+, we found that the 1:1 mixture of G **1** and 8AmG **5** (2 wt%, 70 mM) also formed clear hydrogels with 2 eq of Ba^{2+} (**Figure 4.3b**), Sr^{2+} or Pb^{2+}. This ability to form hydrogels with divalent cations seems unique to the 8AmG/G system, as other 1:1 binary mixtures known to gel with K^+, namely triacetylG **20**/G **1**,[10,51] 5′-GMP **19**/G **1**,[9] and 8-BrG **6**/G **1**,[11] did not form hydrogels when we mixed them with Ba^{2+} or Pb^{2+} (**Figure 4.5**). Only the 1:1 8AmG **5**/G **1** binary mixture led to transparent, self-standing gels when treated with $Ba(NO_3)_2$

or Pb(NO$_3$)$_2$. This is, to our knowledge, the first detailed report of a guanosine hydrogel containing divalent cations.
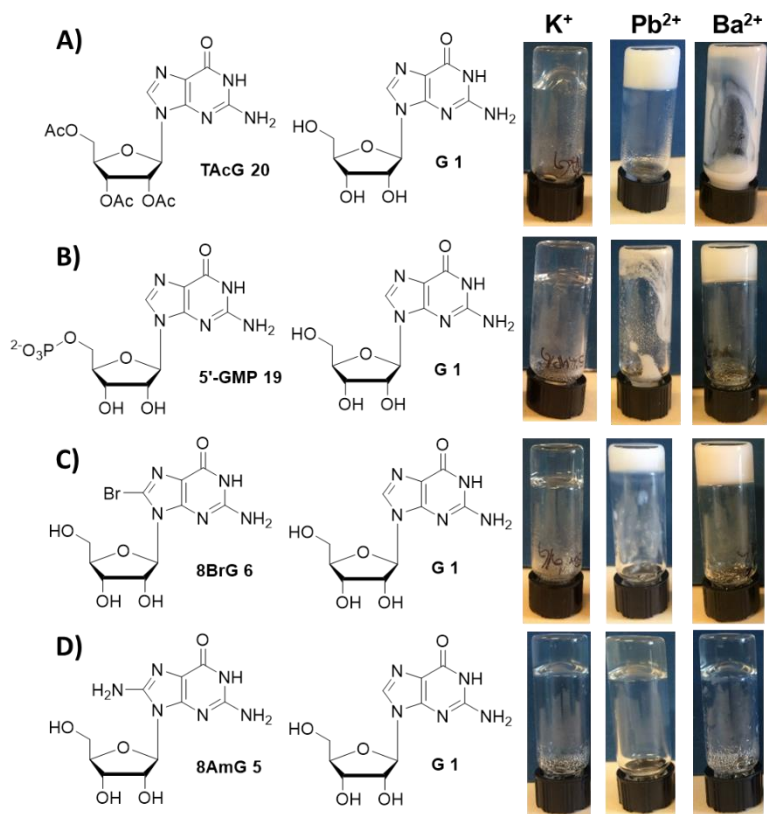
Figure 4.5: While the gels in A, B, and C have been previously reported to form gels with K$^+$ salts, they do not gel with Pb^{2+} or Ba^{2+}, only 8AmG (D) gels with all 3 cations.[17]

Scanning electron microscopy (SEM) of a 1:1 8AmG/G gel (with 2 eq of Pb(NO$_3$)$_2$) showed a dense fibrous network (**Figure 4.3c**). The entangled fibers, which are a few microns in diameter and hundreds of microns long, appear to be formed of bundles of strands (presumably G$_4$-nanowires) wrapping around one another in a helical fashion.

65

4.3.3 Less M^{2+} is Required for Gel Formation Compared to M^+

To investigate differences between the 1:1 8AmG/G gels containing K^+ and Ba^{2+} we first determined how many equivalents of the corresponding nitrate salts were needed to induce hydrogelation at 2 wt% of total nucleoside (70 mM for this system). The solution became viscous and eventually formed a cloudy, self-standing gel (**Figure 4.6**) with 0.25 eq of added KNO_3, a stoichiometry that corresponds to 1 K^+ cation per G_4-quartet. The same 1:1 8AmG/G mixture is completely transparent and begins to gel at just 0.125 eq of added $Ba(NO_3)_2$, which corresponds to 1 cation per G_8-octamer. Most notably all of the nucleoside is dissolved at just 0.125 eq of Ba^{2+} whereas with 0.125 eq of K^+ there is a large amount of solid precipitate (**Figure 4.6**). The 1:4 ratio for K^+ and 1:8 stoichiometry for Ba^{2+} is further evidence that G_4-quartets are the basis for hydrogelation of the binary 8AmG/G mixture, since X-ray crystal structures of G-quadruplexes made from lipophilic G nucleosides show K^+ cations bound between every G_4-quartet,[112] whereas divalent cations (Ba^{2+} or Pb^{2+}) are located between every other G_4-quartet in those same structures.[101,102]
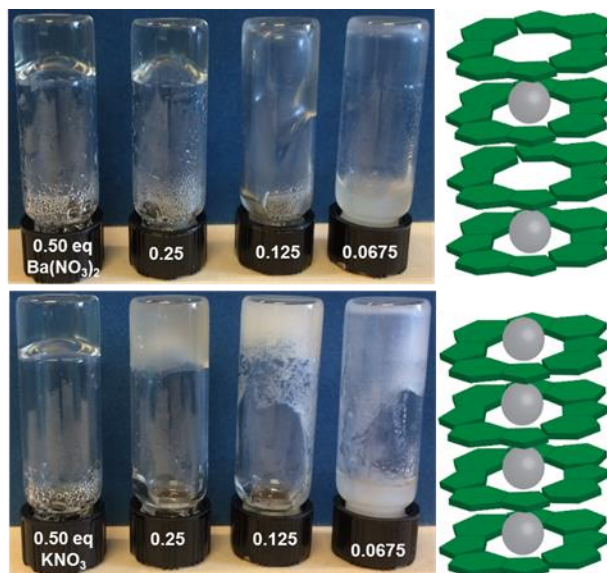
Figure 4.6: Top) A 1:1 binary mixture of G/8AmG begins to form transparent viscous solutions with 0.125 eq of Ba(NO3)$_2$, which is 1 Ba^{2+} per 8 nucleosides, as depicted schematically. Bottom) The same mixture begins to form a self-standing gel at 0.25 eq of added KNO$_3$, corresponding to 1 cation per 4 nucleosides.[17]

4.3.4 Gel Strength Varies Depending on Cation and Salt

Rheology also showed that the properties of the binary 8AmG/G gels differ as a function of the cation. Hydrogels exhibit solid-like rheology, where the storage modulus (G') of the material is larger than its loss modulus (G").[21] We compared the rheological properties of the 8AmG/G-K$^+$ and 8AmG/GBa^{2+} hydrogels. Dynamic frequency sweeps indicated that both the K$^+$ and Ba^{2+} hydrogels (2 wt% nucleoside, 2 eq cation) had an elastic response independent of frequency from 100 to 0.1 rad/s (**Figure 4.7**). Furthermore, the Ba^{2+} hydrogel, with a storage modulus (G') of ~5700 Pa, was stiffer than the K$^+$ hydrogel (G' ~3000 Pa), indicating that 8AmG/G hydrogels containing Ba^{2+} are stronger than those with K$^+$.
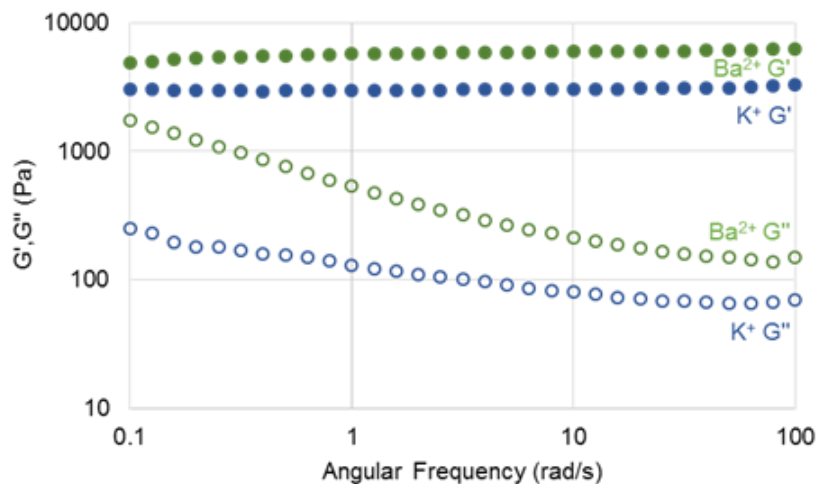
Figure 4.7: Frequency sweeps of 8AmG/G hydrogels (70 mM) with 2 eq of $Ba(NO_3)_2$ (green) or KNO_3 (blue). The 8AmG/G-$Ba(NO_3)_2$ gel has a G′ of ~5700 Pa compared to ~3000 Pa for the 8AmG/G-KNO_3 gel, indicating the divalent gel is stronger.[17]

Further rheology studies showed that increasing the amount of salt relative to G species in the hydrogels increased the stiffness (as measured by G′) of the gels. In general Ba^{2+} gels were the strongest, followed by K^+. The Pb^{2+} gels were much weaker, regardless of their salt content. (**Figure 4.8**).
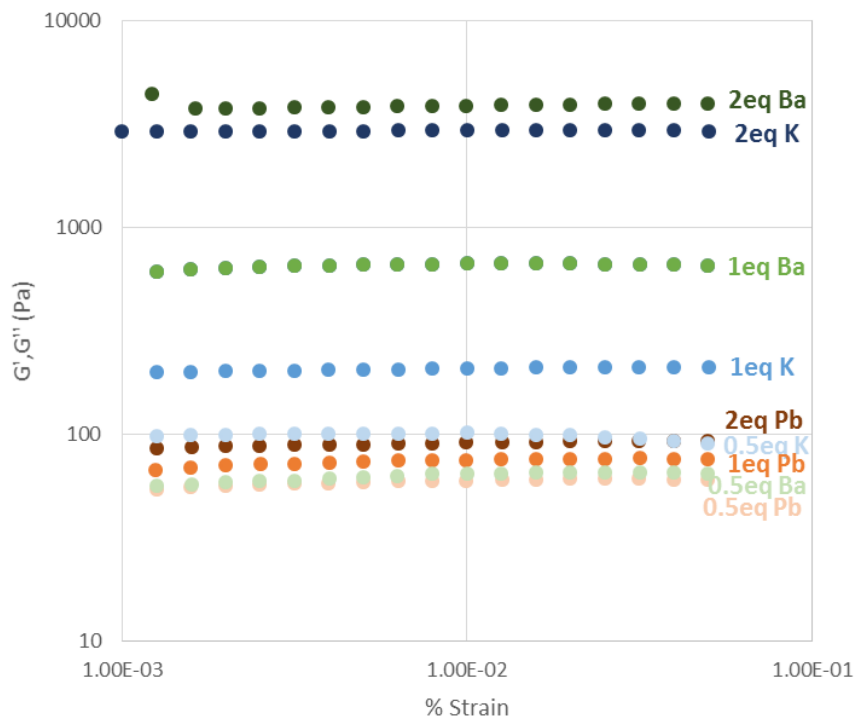
Figure 4.8: Strain sweeps of 2 wt% (70 mM) 8AmG/G gels with varying eqs of salt show that Ba^{2+} (green) gels are strongest, followed by K^+ (blue), and Pb^{2+} (orange) gels, which are much weaker. Adding more salt results in stronger hydrogels.[17]

4.4 Dye Uptake Based on Electrostatic Interactions

We previously established that GB hydrogels made from G **1** and $KB(OH)_4$ preferentially bind cationic (vs. anionic) dyes, presumably due to electrostatic interactions between the negatively charged borate esters and the cationic dyes.[12] Creating G_4-based hydrogels that could be readily altered to absorb cationic or anionic dyes by simply changing the salt used to make the gels, would provide an easy and versatile method for removal of pollutant dyes regardless of their charge. The binary

8AmG/G system is well suited for this task, as it is possible to make binary hydrogels with KB(OH)$_4$, and with chloride salts.

To study dye uptake by the binary 8AmG/G system we compared 3 aromatic compounds: naphthol blue black (NBB **36**), rose bengal (RB **21**), and safranin O (SO **37**). NBB **36**, an anionic diazo dye widely used in the textile industry, and a major wastewater pollutant, was specifically chosen to highlight the potential of this binary gel for environmental remediation.[99,100] RB **21**, an anionic dye, has previously been shown by the Dash group to bind to binary hydrogels made from G **1** and 8BrG **5**.[11] Finally, SO **36** is a cationic dye that we previously found binds to GB hydrogels made from G **1**.[14] Like the GB gels we find that the binary 8AmG/G gels are stable in salt water. This remarkable stability for a supramolecular hydrogel allows us to carry out dye uptake experiments with the binary 8AmG/G gels. Thus, we separately suspended a 0.5 mL cube of each type of binary 8AmG/G gel (i.e. ones made using 0.5 eq of KB(OH)$_4$ or 2.0 eq of either KCl or BaCl$_2$) in 3 mL of a solution of 155 mM KCl that had a 12.5 μM concentration of dye. The outside solution was monitored over time using UV-Vis spectroscopy, which allowed us to quantify how much dye had been absorbed from solution into the hydrogel network.

4.4.1 Quantitative Dye Uptake Studies

As expected from electrostatic considerations and analogy to the GB gel, the 8AmG/G-KB(OH)$_4$ gel absorbed significantly more cationic dye, SO **37** (61%) than either of the anionic dyes NBB **36** and RB **21** (22% and 4%, respectively) (**Figure 4.9**).
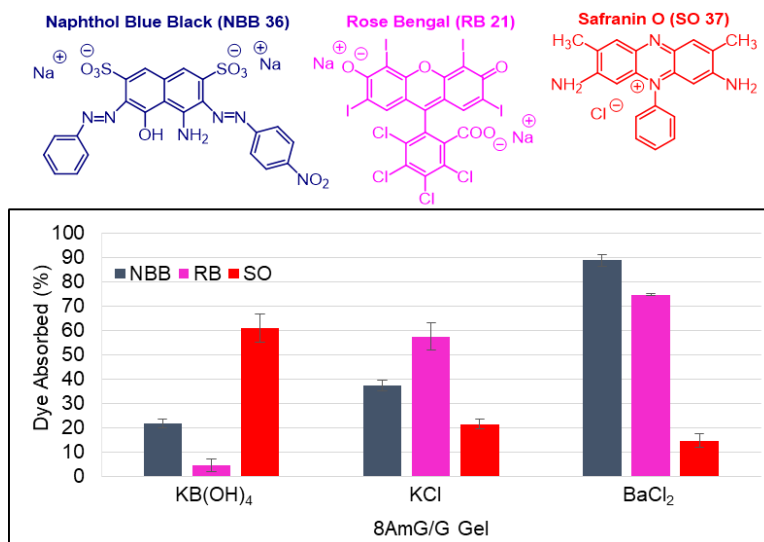
Figure 4.9: Top) the structures of the three dyes used. Bottom) This graph shows the percentage of the dyes each of the three 70 mM 8AmG/G gels absorbed after being suspended in a 155 mM KCl/12.5 μM dye solution for 24 hours.[17]

Although the 8AmG/G-KCl gel showed moderate to low uptake of each of the three dyes, these gels absorbed more of the anionic dyes (RB **21** - 58% and NBB **36** - 37%) than the cationic SO **37** (22%). Most importantly, the 8AmG/G-BaCl$_2$ gels showed both excellent efficiency and selectivity for the anionic dyes, NBB **36** and RB **21** (89% and 75%, respectively) as compared to extracting just 15% of SO **37**. Clearly the 8AmG/G-BaCl$_2$ gel, with its divalent cations is the best supramolecular hydrogel for uptake of the anionic dyes we tested.

In order to investigate how much anionic dye the gels would absorb, we soaked each of the gel cubes in a vial with 100 μM NBB **36** and monitored the uptake over one week (**Figure 4.10**). We found that after 3 days the dye uptake leveled off, with the 8AmG/G-BaCl$_2$ gel absorbing ~80% of the NBB **36**, the 8AmG/G-KCl gel absorbing ~55%, and the 8AmG/G-KB(OH)$_4$ gel absorbing just ~17% of the NBB **36**.

71
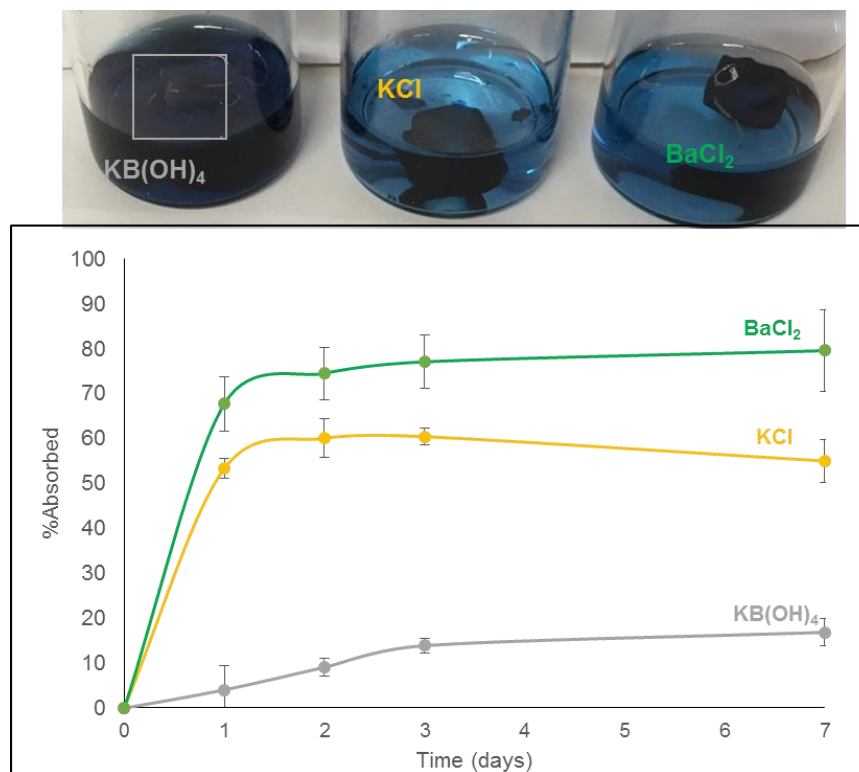
Figure 4.10 : Gels soaking in 100 μM NBB solution for 24 hours (top) absorb different amounts of NBB depending on the salt they are made with. $BaCl_2$ gels absorb ~80% of the dye after one week whereas $KB(OH)_4$ gels absorb less than 20%.[17]

4.4.2 Qualitative Dye Uptake Studies

To further probe the differences between the KCl and $BaCl_2$ gels we performed several qualitative dye competition experiments in which cubes of 2 different gels were suspended in a single vial containing 12.5 μM of NBB **36** dissolved in 155 mM KCl solution. When 8AmG/G-$BaCl_2$ and 8AmG/G-KCl gels were placed in the same vial the NBB **36** was clearly concentrated in the 8AmG/G-$BaCl_2$ gel after 24 hours (**Figure 4.11**). We attribute this difference in affinity to the stronger electrostatic interactions between the anionic dye and the gel that contains the divalent Ba^{2+} cation. That the

72

8AmG/G-BaCl$_2$ gel and 8AmG/G-KCl gel demonstrate different affinities for NBB, even when suspended in the same vial for 24 hours, indicates that the Ba^{2+} cation is kinetically stable within the G$_4$-assemblies that make up the gel fibers. It is impressive that the Ba^{2+} cations in the hydrogel would not exchange with the 155 mM K$^+$ that is in the outside solution. This may be due to preferential binding of the G$_4$-structures to Ba^{2+} over K$^+$ and may help explain why the Ba^{2+} gels are stronger than the K$^+$ gels.

Figure 4.11: Qualitative dye uptake experiments show 8AmG/G-KCl vs 8AmG/G-BaCl$_2$ gels after soaking in 12.5µM NBB 3 for 24 hours. While 8AmG/G-KCl gels will absorb NBB **36** from solution, 8AmG/G-the BaCl$_2$ gels absorbs the dye much faster.[17]

To further explore the qualitative differences between the 8AmG/G-BaCl$_2$ and 8AmG/G-KCl gels we prepared a cube of 8AmG/G-KCl gel with NBB **36** and placed it in a vial with 8AmG/G-BaCl$_2$ without dye. Over the course of two weeks the dye leached from the 8AmG/G-KCl gel into the 8AmG/G-BaCl$_2$ gel cube (**Figure 4.12**).
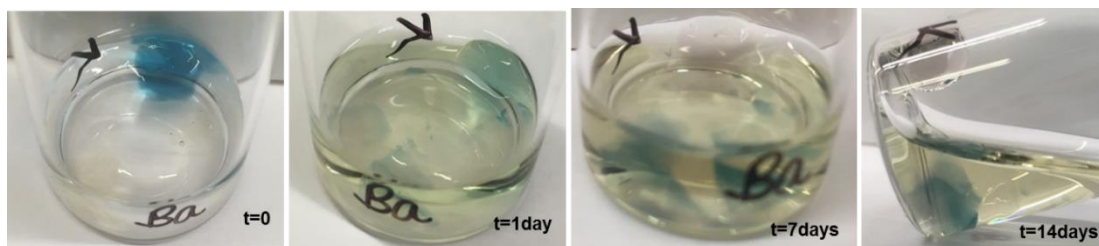
Figure 4.12: This qualitative dye experiment shows how a KCl gel loaded with 25 μM NBB **36** will release the dye into solution. The NBB **36** will then be absorbed by a BaCl$_2$ gel in the same vial over the course of 2 weeks.[17]

While the 8AmG/G-KCl gel clearly has a lower affinity for NBB **36** than 8AmG/G-BaCl$_2$, it will absorb the anionic dye more readily than the negatively charged 8AmG/G-KB(OH)$_4$ gel (**Figure 4.13**).
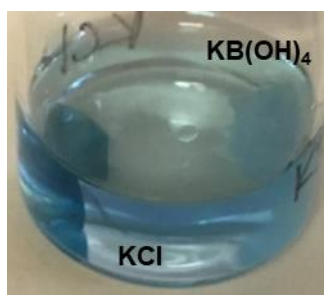
Figure 4.13: Qualitative dye uptake experiments show 8AmG/G-KCl vs 8AmG/G-KB(OH)$_4$ gels after soaking in 12.5 μM NBB **36** for 24 hours. The 8AmG/G-KCl gel absorbs the anionic NBB **36** much more than the 8AmG/G-KB(OH)$_4$ gel, likely due to the repulsion between the dye and the anionic borate esters.

4.5 Conclusions

We have shown that binary mixtures of 8AmG/G are able to form strong, stable, and transparent hydrogels in the presence of $KB(OH)_4$ or K^+, Ba^{2+}, Sr^{2+}, and Pb^{2+} nitrate or chloride salts. This is notable as they are the first well studied example of a **G 1** based hydrogel formed with divalent cations. These gels are capable of selectively removing both cationic and anionic dyes from aqueous solution. This charge selectively can be altered by changing the salt the gels are formed with.

4.6 Other Results – Uptake of Pb^{2+}

The ability to make G_4-hydrogels with divalent cations is reminiscent of previous work in our lab that showed G_4-quadruplexes could favor Pb^{2+} over K^+.[102] If this were true for our 8AmG/G hydrogels, we envisioned using K^+ gels to remove Pb^{2+} from waste water. We theorized that if Pb^{2+} binding to G_4-quartets was favored, we would be able to soak a K^+ gel in a Pb^{2+} solution and the K^+ would exchange for Pb^{2+}. To test this theory, we probed the ability of the binary gels to remove Pb^{2+} from water by soaking an 8AmG/G-KNO3 gel in a Pb^{2+} containing solution (**Figure 4.14**).
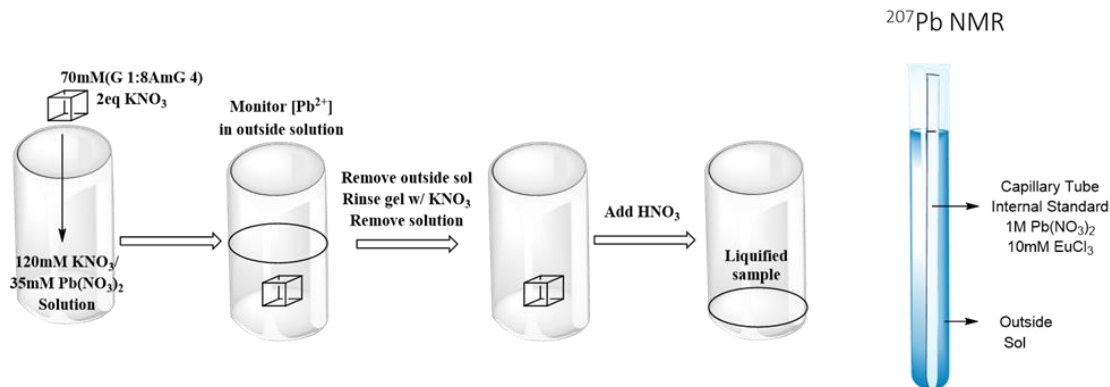
Figure 4.14: The experimental setup for Pb^{2+} uptake is shown above. A gel is suspended in $KNO_3/Pb(NO_3)_2$ solution. The outside solution is monitored over time by taking aliquots from the solution. ^{207}Pb NMR is performed with a Pb^{2+} internal standard contained within a capillary tube. After 3 days the outside solution is removed and the gel is rinsed with KNO_3. The gel is then dissolved with HNO_3 and the liquefied gel sample is analyzed with ^{207}Pb NMR following the same procedure.

We made a 3 mL solution that was 35 mM in $Pb(NO_3)_2$ and 120 mM in KNO_3 (previous research in our group showed that GB gels are stable in salt solutions of 155 mM K^+).[12] A 0.5 mL cube of an 8AmG/G gel with 2 eq of KNO_3 was then placed in the solution. The outside solution was monitored over time using ^{207}Pb NMR with a $Pb(NO_3)_2/EuCl_3$ internal standard enclosed within a capillary tube to monitor the concentration of Pb^{2+}. After 72 hours the Pb^{2+} in the outside solution could no longer be measured via NMR (**Figure 4.15**). We then disassembled the gel by adding 10 μL of concentrated HNO_3. After examining the liquefied gel via ^{207}Pb NMR, it was evident that the gel sample had absorbed Pb^{2+}.
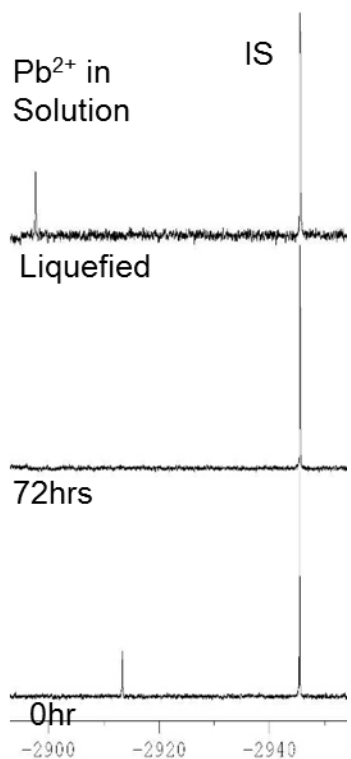
Figure 4.15: The ^{207}Pb NMR spectra show peaks from the outside solution and the Pb^{2+} internal standard contained within a capillary tube. After 72hrs the peak from the Pb^{2+} in solution has disappeared. After liquefying the gel sample with HNO$_3$, we can see the Pb^{2+} had been absorbed by the hydrogel cube.

Next, we turned to ICP-MS to quantify the amount of Pb^{2+} absorbed by the gel. Using the same experimental setup utilized for the NMR experiment (**Figure 4.14**), we found that ~3.1 mg of Pb^{2+} was absorbed after 72 hours (**Figure 4.16**). This corresponds to 304 mg of pollutant/gram of gelator, which is a moderate amount compared to other supramolecular hydrogels used for environmental remediation of Pb^{2+}.[109]
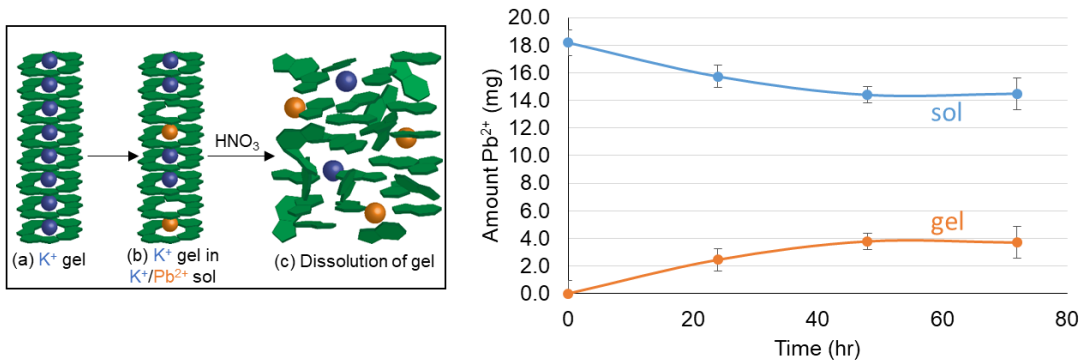
Figure 4.16: The illustration on the left shows (a) a depiction of the 8AmG/G hydrogel network made with K^+, (b) after soaking in K^+/Pb^{2+} solution some of the K^+ is replaced by Pb^{2+}, (c) the gel network dissociates with acid addition. Right) ICP-MS data shows that the amount of Pb^{2+} in solution decreases over time as it is absorbed by the gel.

4.7 Future Directions

While we have shown that the 8AmG/G hydrogels are capable of absorbing either anionic or cationic dyes from water based on the salt used to template their formation, the structure of the gel network is not entirely clear. CD and PXRD data shows G_4-assemblies, but further work using solid-state NMR could be useful in elucidating a more complete picture of the fiber networks in the different gels.

In addition, more complete studies of the uptake of toxic metal cations (Pb^{2+} and others) by the hydrogels could be done. This would include finding the maximum uptake capacity for gels made with different cations and different amounts of salt, as well as different concentrations of nucleoside.

Chapter 5: Utilizing Binary Mixtures of 8-Substituted Guanosine Derivatives with Guanosine for Room Temperature Hydrogelation

5.1 Summary

Work in this chapter highlights how templating the formation of G_4-quartets can promote hydrogelation at room temperature. Continuing experiments on 8-substituted G-derivatives we found that 8-bromoguanosine (8BrG **6**) in binary mixtures with G **1**, will form hydrogels in the presence of $KB(OH)_4$ without heat.

Further investigation into this unusual property lead us to discover that other 8-substituted derivatives, 8-iodoguanosine (8IG **7**) and 8-morpholinoguanosine (8morphG **8**) also form room temperature binary gels with G **1** and $KB(OH)_4$. All of these derivatives have a high preference for the *syn* conformation over the *anti* conformation about the glycosidic bond. This preference for the syn conformation can template G_4-quartet formation, which promotes gelation since G_4-quartets are the basis of the hydrogel network. We studied the differences in physical properties between hydrogels formed at room temperature versus those made via the traditional heating method. The role of the solubility of the G-derivative is also discussed.

5.2 Introduction

The use of supramolecular hydrogels for a variety of applications has seen a dramatic increase in recent years.[8,31,113] Of particular interest for our group are guanosine based hydrogels.[2,3] As discussed in the introduction and **Chapters 2-4** of this thesis, we have previously reported on guanosine-borate (GB) based hydrogels in which G **1** (or a G-derivative) is heated with an aqueous solution of $KB(OH)_4$ and forms

79

a self-standing hydrogel upon cooling.[12–17] These gels have been applied to many fields of chemistry from drug delivery and cell growth to sensing and environmental remediation.[15,17,53,55,57,86] However, the ability to form gels at room temperature (RT) would potentially enable the GB hydrogels to be used for more applications that have yet to be explored with these systems.

This expanded scope of applications would include the encapsulation of enzymes or temperature sensitive drugs that would be destroyed in the heating process traditionally required for G-based hydrogels. This encapsulation could help improve the stability of reactive enzymes and drugs.[114,115] In addition, gels that form at room temperature can be used for environmental remediation by gelling *in situ* upon contact with a gelating trigger. There are several examples of gels used to gel oil or petrol with implications for environmental remediation.[116,117]

While there have been several reports of room temperature organo-gelators,[118,119] as well as peptides,[38,120] and a few other systems that form gels at room temperature,[121] to the best of our knowledge there have not been any reports of G **1** or its analogs capable of forming gels at room temperature. Guanosine derivatives have the advantages of being commercially available at low costs and/or being relatively easy to synthesize. In addition guanosine based hydrogels have already shown promise in both drug encapsulation and delivery,[15,55,56] and environmental remediation.[17]

5.3 Binary Hydrogel Formation with 8-Bromoguanosine and Guanosine

We found that when mixed with 0.5 eq of $B(OH)_3$ and 0.5 eq of KOH, binary mixtures of 8BrG **6** and G **1** (64 mM, 2 wt % total nucleoside) form hydrogels within

minutes. These gels are initially opaque, but become transparent within ~20 minutes. These RT hydrogels are distinct from their heated counterparts (gels made by heating the mixtures to ~95°C until clear that undergo gelation upon cooling) as shown in **Figure 5.1**. With no heating 100% G **1** does not form a gel, but adding as little as 1% of BrG **6** results in a self-standing hydrogel. Hydrogels with 40% - 90% BrG **6** form stable, transparent hydrogels at RT. Interestingly heated gels with 70% BrG **6** or more are white, and heated mixtures with more than 90% BrG **6** do not gel.
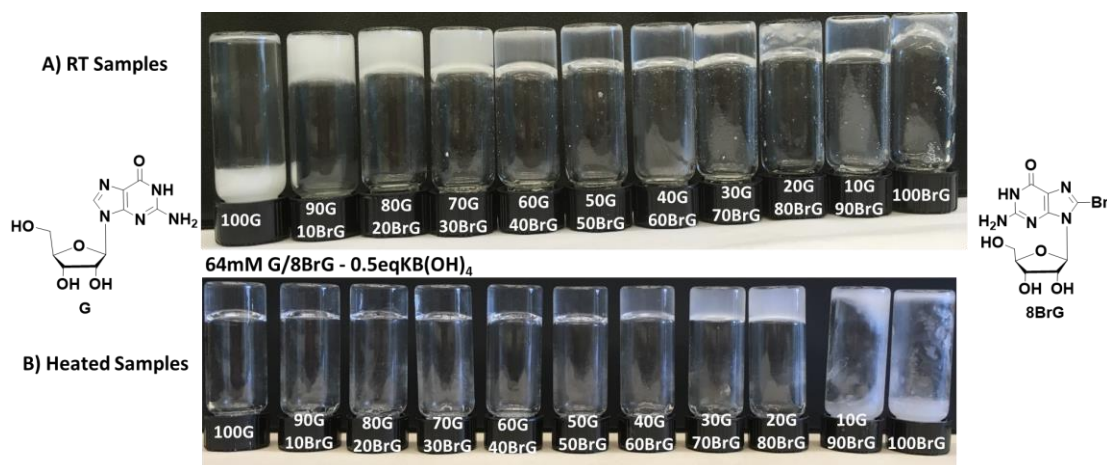
Figure 5.1: Images of 64 mM, 2 wt% BrG **6**/G **1** hydrogels with 0.5 eq of KB(OH)4 with different ratios of G **1**:8BrG **6**. A) Shows room temperature samples after 1 hour. B) Shows heated samples after 1 hour.

To further investigate the differences between the heated gel samples and the unique room temperature gels we performed a series of experiments including, CD spectroscopy, PXRD, ^{1}H NMR, and stability studies.

5.3.1 Hydrogels are G$_4$-Quartet Based and Contain Borate Esters

First, the ^{1}H NMR spectra of both heated and RT gels showed evidence of borate ester species for both 8BrG **6** and G **1** in the H1′ region. In addition, the solution phase of both gels looks nearly identical, with some small differences in the ratios of the species in the solution. Further experiments are needed to determine if there are differences in the concentration of nucleoside in the gel phase versus the sol phase for the RT and heated gels.
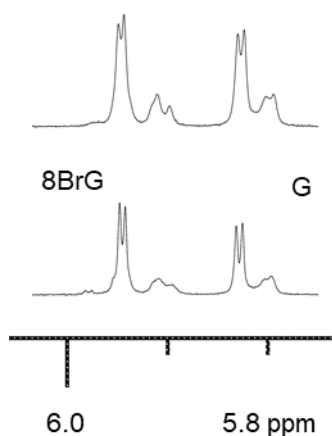
Figure 5.2: The H1′ region of the ^{1}H NMR spectra of 1:1 8BrG **6**:G **1** (64 mM, 2 wt%, 0.5 eq of KB(OH)$_4$) in D$_2$O top) RT gel, bottom) heated gel.

CD spectroscopy shows that both of the gel systems are G$_4$-quartet based. Both the RT and heated samples (1:1 BrG **6**:G **1**, 64 mM, 2 wt% nucleoside, 0.5 eq of KB(OH)$_4$) showed the characteristic peaks and troughs between 200 – 320 nm arising from G$_4$-quartet assemblies.[110] Both gave the same pattern in the CD spectra, however the signal from the RT gel had a higher amplitude than its heated counterpart (**Figure 5.2**). This could mean that there are more G$_4$-quartets in the RT sample.
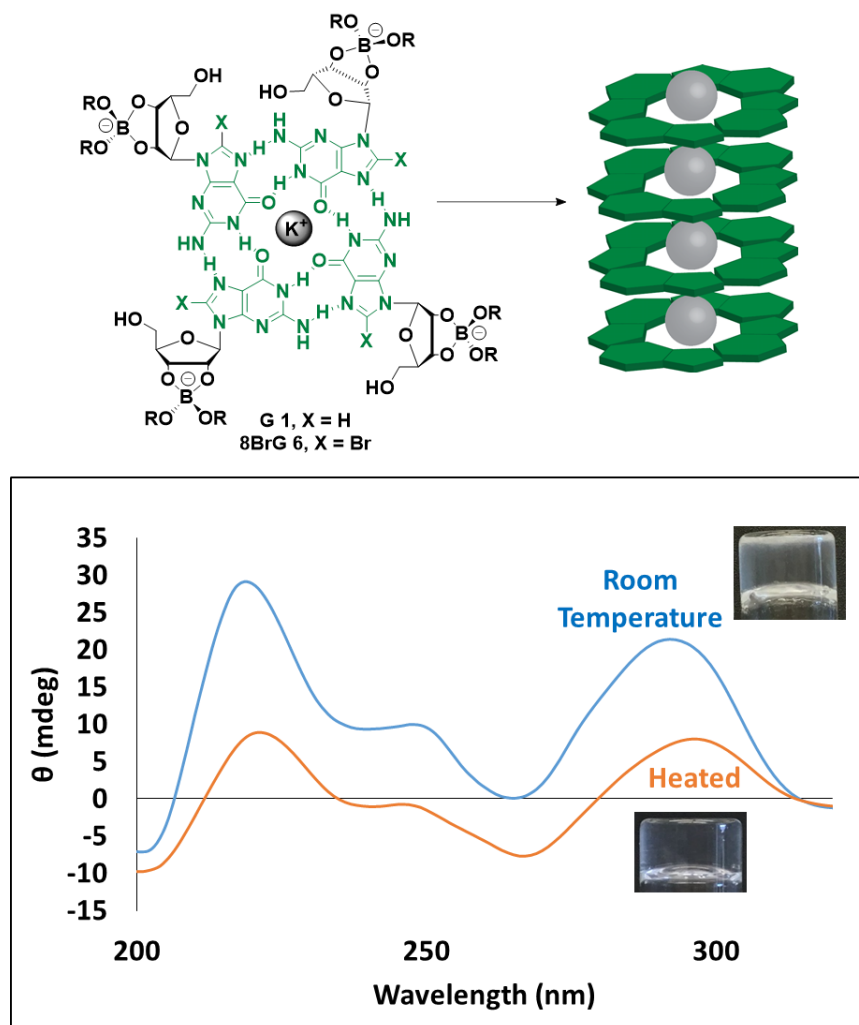
Figure 5.3: Top) G_4-quartets composed of 8BrG **6** and G **1** self-assemble into G_4-fibers to form a hydrogel. Bottom) The CD spectra of RT and heated gels (1:1 8BrG **6**:G **1** - 64 mM, 2 wt%, 0.5 eq of $KB(OH)_4$) shows evidence for G_4-quartets.

PXRD data (Figure 5.4) for both RT and heated 8BrG **6**/G**1** hydrogels showed evidence for G_4-quartets. The data show peaks corresponding to distances of ~3.3 Å and ~21.9 Å, which are the distances between layers in a G_4-quartet, and the diameter of G_4-quartet, respectively.
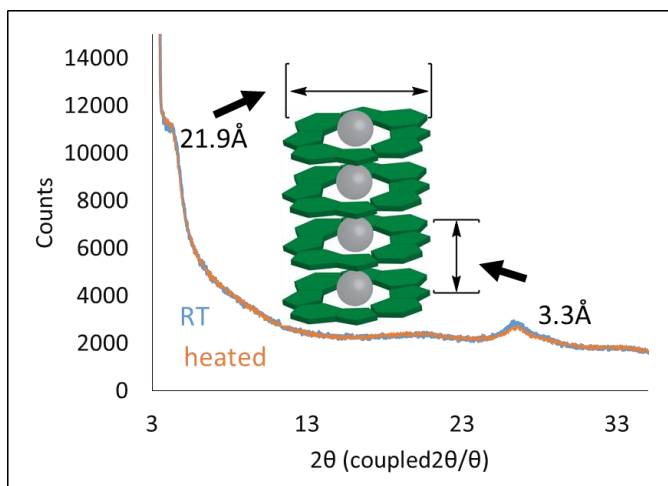
Figure 5.4: PXRD data for lyophilized hydrogels made from 8BrG/G show evidence of G$_4$-quartets in both heated and RT gel samples.

After determining that the structural basis for both the RT and heated gel networks were GB-esters and G$_4$-quartets we next sought to explore the stabilities of both of these systems to see if there were any differences.

5.3.2 Both the RT and Heated Hydrogels are Stable and Robust

Using rheological strain sweeps we quantified the strength differences between A) RT and B) heated gels made of either 50% BrG **6**/50% G **1**, 100% BrG **6**, or 100% G **1** (64 mM, 2 wt% with 0.5 eq of KB(OH)$_4$, tests were run after gels sat at RT overnight). As shown in the **Figure 5.5**, the binary mixture is critical in forming stable gels at RT as the 50/50 mix with a G′ ~3100Pa, is nearly 300 times stronger than either G **1** or BrG **6** alone. For the heated gels the binary mixture is the strongest, closely followed by the G **1** hydrogel. The BrG **6** gel is very weak.
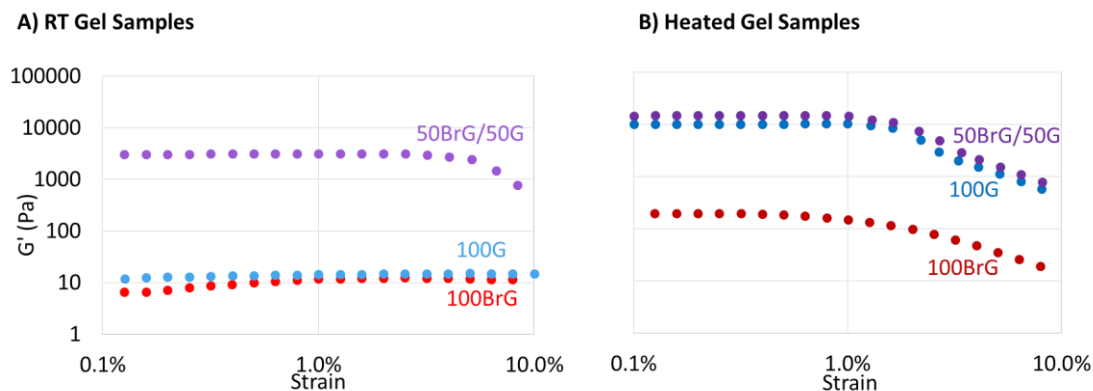
Figure 5.5: Rheological strain sweeps of BrG/G hydrogels and G hydrogels - A) RT samples and B) heated samples.

Since previous work in our lab showed that G **1**, KB(OH)$_4$ gels were stable in water with 155 mM K$^+$,[12–14,17] we tested both heated and RT gels to see how much nucleoside leached from the gel network. This experiment allows to see if there is a difference in the stability of the gel networks in water for the two gels. In three separate vials we placed 0.5 mL gel cubes (for 8BrG **6**/G **1** binary gels - 64 mM, 2 wt%, 0.5 eq of KB(OH)$_4$, for G **1** gel – 72 mM, 2 wt%, 0.5eq KB(OH)$_4$). We found that there was no appreciable difference between the RT and heated binary gels or the heated G **1** gel used as a control, with all samples releasing less than 3 % of the nucleoside from their gel network (**Figure 5.6**). This indicates that the RT and heated gels are equally stable.
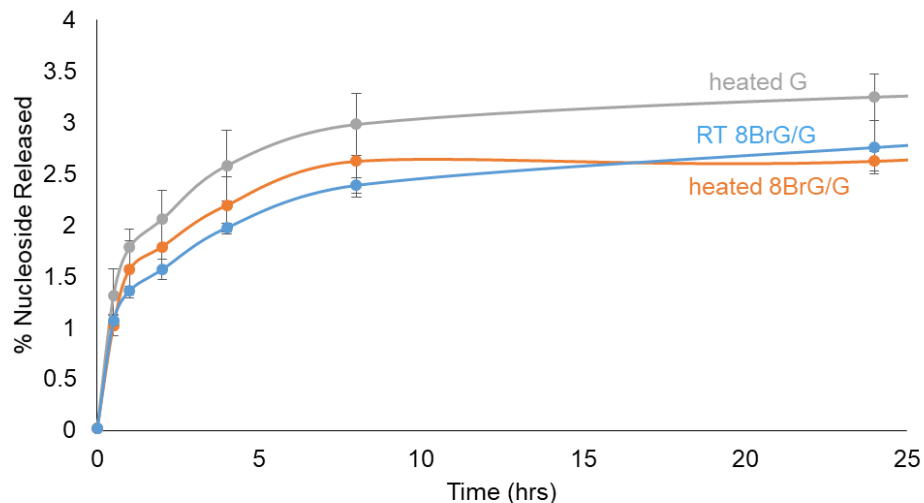
Figure 5.6: The graph shows the release of nucleoside from the hydrogel networks of a heated G **1** gel (gray), a heated 8BrG **6**/G **1** gel (orange), and a RT 8BrG **6**/G **1** gel (blue) into 3 mL of water with 155 mM of KB(OH)$_4$.

Having examined some of the physical properties of the RT and heated gel systems we sought to explore why 8BrG **6** has the unique ability to form room temperature gels with G **1**.

5.4 Room Temperature Gelation and Correlation with the *Syn/Anti* Glycosidic Bond Preference and Gelator Solubility

We hypothesize that this unique room temperature gelating ability arises due to the preference of 8BrG **6** for the *syn* conformation about the glycosidic bond. While G **1** favors the *anti* conformation over the *syn* (60% to 40%), 8BrG **6** is reported to exist mostly in the syn conformation (90%).[68,122] Both *syn* and *anti* conformations allow for the formation of G$_4$-quartets. However, in the *anti* conformation the N2 and N3 positions (pink in **Figure 5.7**) can form intermolecular H-bonds to form G-ribbons, in

the *syn* conformation these positions are blocked by the sugar. This blocking could allow for faster formation of G₄-quartets (the building blocks of the hydrogels) and thus catalyze gelation at RT.
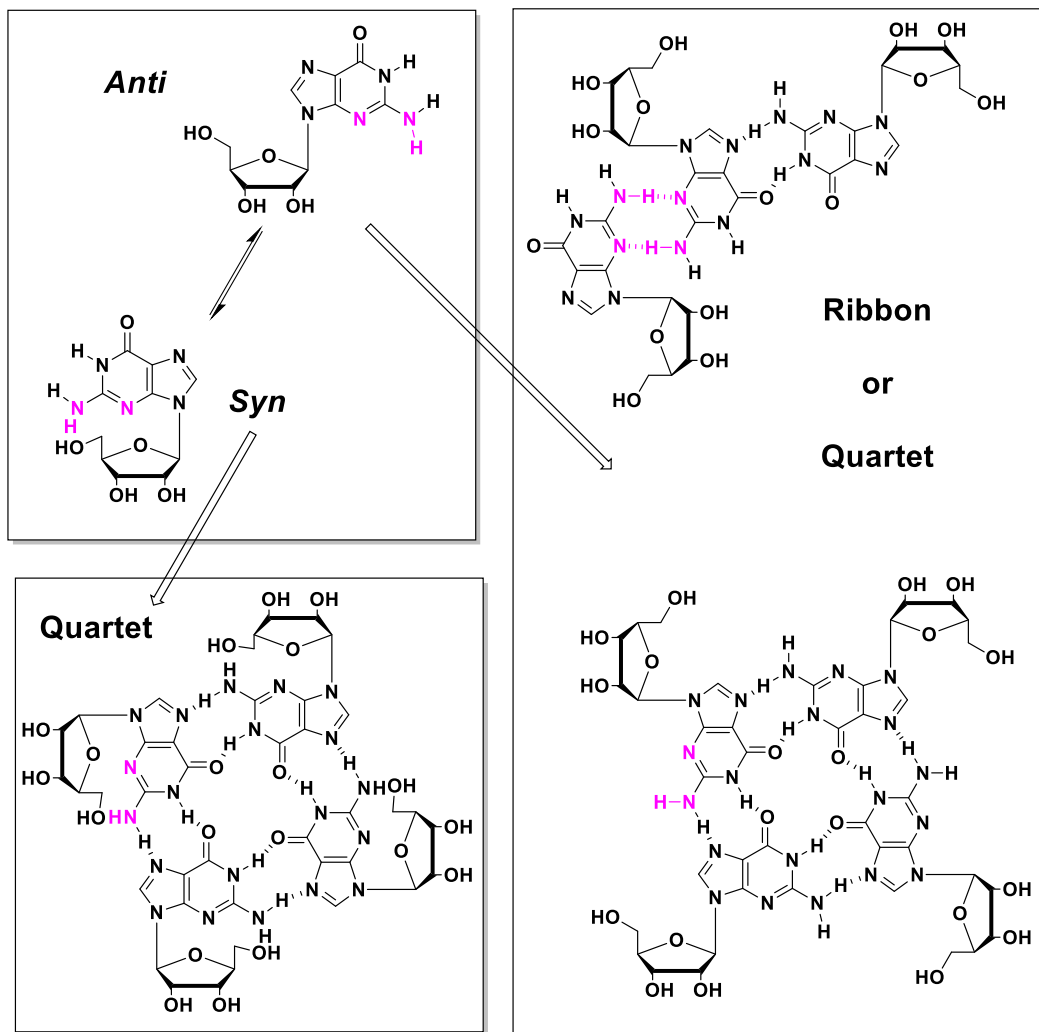
Figure 5.7: There is an equilibrium between the *syn* and *anti* conformations of the nucleobase and ribose about the glycosidic bond of G **1**. These conformation lead to different possible assemblies of the G-units

5.4.1 *Syn/Anti* Glycosidic Bond Conformation and RT Gelation

Based on this hypothesis we synthesized binary hydrogels (1:1 G-derivative:G **1**, 2 wt% nucleoside, 0.5eq KB(OH)$_4$) from various G-derivatives with different *syn/anti* ratios (the *syn/anti* ratios were determined based on literature precedent and/or the ^{1}H NMR shifts).[49,68] Preliminary results on these derivatives show that of those tested only 8BrG **6**, 8-iodoguanosine (8IG **7**), and 8-morpholinoguanosine (8morphG **8**) formed mostly transparent hydrogels with G **1** after 2 hrs at RT. Interestingly, while both 8BrG **6** and 8IG **7** begin to form gels within 1 minute of mixing, 8morphG **8** takes significantly longer, at least 2 hours, to form a gel. 5′-GMP **19** did not gel with G **1**. Both 8AmG **5** and 5′-IG **2** formed white gels with G **1** that had undissolved solid (the 5′-IG **2** gel was also very weak). 8BrG **6** and 8IG **7** both have ~90% preference for the *syn* conformation whereas 5′-GMP **19** and 8AmG **5** are only ~30% and 40% *syn*, respectively.[6] While 5′IG **2** has a slight preference for the *syn* conformation (~65%) it is very hydrophobic, which could be preventing gelation at RT.
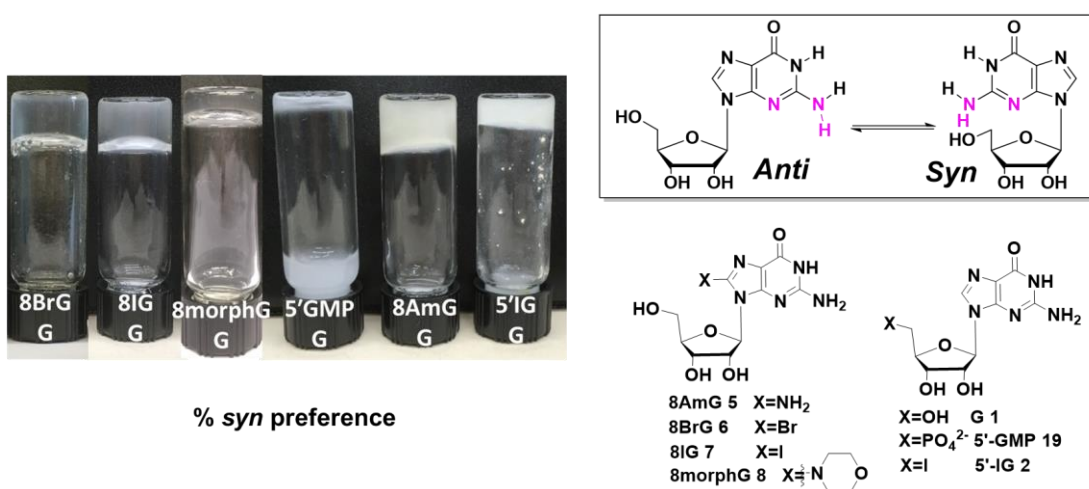
Figure 5.8: The image shows binary hydrogels made of G **1** and various other G-derivatives (2 wt% nucleoside, 0.5 eq of KB(OH)$_4$.

5.4.2 Gelator Solubility and RT Gelation

We next determined the solubilities for G **1** and the three 8-substituted G-derivatives that form transparent, binary hydrogels at room temperature. We determined that G **1** has a solubility of 1.90 ± 0.08 mM, 8BrG **6** is slightly more soluble at 2.81 ± 0.28 mM, and 8IG **8** is less soluble at 0.83 ± 0.08 mM. Interestingly 8morphG **8** is significantly more soluble than any of the other derivatives tested, with a solubility of 11.82 ± 0.51 mM. Gelation requires a balance between hydrophobicity and hydrophilicity. If a molecule is soluble in water it will simply dissolve rather than forming a gel, on the other hand if a compound is too insoluble it cannot form a gel network. The increased solubility of 8morphG **8** may help explain the longer time period required to form a gel. As 8morphG is quite soluble in comparison to its hydrophobic counterparts (G **1**, 8BrG **6**, and 8IG **7**) it is conceivable that the gel network takes longer to form since there is no hydrophobic effect to push gelation.

Based on the results from these preliminary studies we decided to pursue further experiments with 8morphG **8** (while 8IG **7** also formed gels they were less transparent, likely due to the lower solubility of the compound).

5.5 Differences Between Room Temperature Hydrogels from 8-Morpholinoguanosine/Guanosine and 8-Bromoguanosine/Guanosine

Rheological comparisons of binary hydrogels made from 8morphG **8**/G **1** and 8BrG **6**/G **1** (2 wt% nucleoside, 0.5 eq of $KB(OH)_4$) show (**Figure 5.9**) that binary gels with 8morphG **8**/G **1** are weaker (G′ ~800 Pa) than those of 8BrG **6**/G **1** (G′ ~3100 Pa).
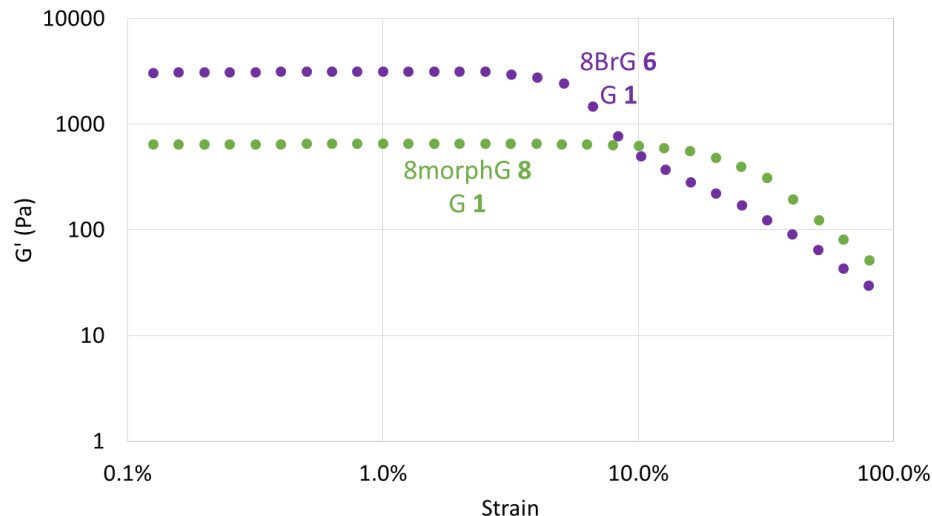
Figure 5.9: Strain Sweeps show the G′ values for RT gels made from 2 wt% 8BrG/G (purple) and 8morphG/G (green).

While the rheological studies clearly show that the 8BrG **6**/G **1** system is stronger than the 8morphG **8**/G **1** system, having the ability to tailor the strength of gels formed at room temperature could be advantageous. For example, the 8BrG **6**/G **1** system may be too stiff for potential applications as a bioink or for injections. In addition, literature on 8-substituted G-derivatives indicates that 8-amine substituted guanosine's are more robust than 8-BrG **6** when it comes to degradation of the monomer such as in glycosidic bond cleavage.[123]

5.6 Conclusions

We have shown that 8-substituted guanosine derivatives with a high preference for the *syn* conformation about the glycosidic bond can template the formation of G$_4$-quartets. In addition to the conformational preference, solubility also seemingly plays a role in both the speed of gelation and the transparency of the resulting hydrogels.

90

5.7 Future Directions

While our initial findings are promising, there is still much to learn in the area of room temperature guanosine-derivative hydrogels. Questions remain about the structural differences between heated and room temperature hydrogels. While both systems seem to be based on GB-ester formation and G_4-quartets, the actual composition of the gel network remains unknown. Solid state NMR would be useful in elucidating the structure of the gel network, as well as examining the proporties of each nucleoside in the gel state vs the sol state. It is also evident that the room temperature gels, especially those made with 8morphG **8** and G **1**, change over time. More studies could be done to study the time dependency on the physical properties of the materials including rheology, CD, and NMR spectroscopy.

In addition to further characterization, applications for these hydrogel systems can be explored. As mentioned in the introduction to this chapter these RT gels may be useful in immobilization of enzymes. Simple experiments in which an enzyme loaded gel cube is suspended in an aqueous solution containing 155 mM K^+ (to stabilize the hydrogel) and an enzyme substrate, could be used to test the activity and reusability of the enzyme versus a control with free enzyme.

As previous research in our group has shown, GB hydrogels can incorporate drugs via either G_4-quartet H-bonding (for guanine analog drugs), or through borate-ester linkages (with diol containing drugs).[13,15] The RT hydrogels could be utilized to store and deliver unstable drugs containing either guanine units and/or 1,2- or 1,3-diols.

Lastly, these systems could be used in environmental remediation to form gel *in situ* with pollutants. For example, since we have shown that Pb^{2+} can form hydrogels with G-derivatives (see **Chapter 4.6**), adding a room temperature gelator to an aqueous solution of Pb^{2+} could trigger gel formation. This would trap Pb^{2+} in the hydrogel network, thus removing it from the solution.

Chapter 6: Future Work

In the past five years our group has made several contributions to the field of supramolecular guanosine hydrogels. In addition to the future directions discussed at the end of Chapters 2-5, there is potential to alter the gel network by adding additional covalent crosslinking to the supramolecular hydrogel. One method for this would be to form a hydrogel and then add a cross-linker to the preexisting fibrous network in a second step (**Figure 6.1**). Presumably these added connections between fibers in the hydrogel network would strengthen the gel.
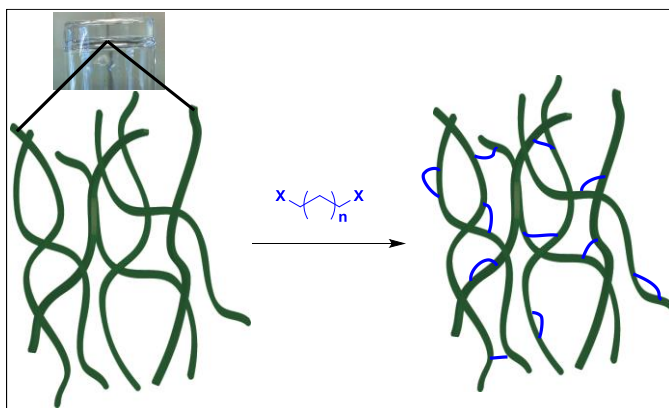
Figure 6.1: A potential method to add covalent cross-linking to the supramolecular hydrogel network.

Some examples of potential gel systems are shown in **Figure 6.2**. Modifying the 5′-position with a reactive group and adding a double ended cross-linker would allow for a variety of different covalently-linked gel networks. The length of the cross-linking chain length could also be tuned.
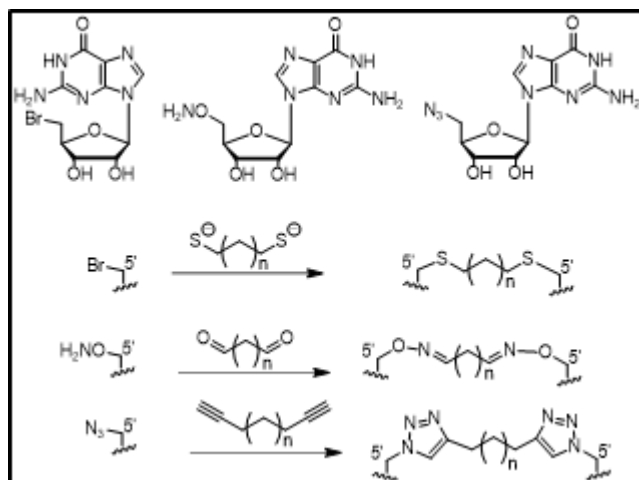
Figure 6.2: Some potential G-derivatives and their corresponding linkers are shown.

As evidenced by the work presented in this thesis the role of supramolecular hydrogels, including those made of G **1** and its derivatives, is an interesting and rapidly growing area of chemistry. While a number of novel applications for these materials has been presented there are numerous potential applications that have yet to be explored.

Chapter 7: Supporting Information

7.1 General Experimental for Chapters 2-5

General Experimental: NMR spectra were recorded on Bruker DRX-400, Bruker DRX-500, or Bruker AVIII-600 spectrometers. Chemical shifts are reported in ppm relative to the residual solvent peak. Deuterated solvents were purchased from Cambridge Isotope Labs. Mass spectrometry experiments were performed on a JEOL AccuTOF-CS Spectrometer. CD Spectroscopy was performed on a Jasco J-810 spectropolarimeter. Rheological data was collected with an AR2000 stress-controlled rheometer from TA instruments, New Castle DE. SEM images were obtained on a Hitachi SU-70 High Resolution Analytical SEM. ICP-MS data was obtained on a Single Collector Element 2 ICP-MS. UV-Vis spectra were obtained on Varian Cary 100 spectrometer. PXRD experiments were performed with a Bruker D8 Advance Bragg-Brentano Diffractometer. Chemicals and solvents were purchased from Acros, Sigma-Aldrich, Alfa Aesar, Fisher, and Santa Cruz Biotechnology and used without further purification.

7.2 Supporting Information for Chapter 2

General Gel Preparation Procedure: The desired amount of 5′-IG **2** was weighed into a vial, and the appropriate amounts of $KB(OH)_4$ stock solution and water were added. The vial was physically shaken and sonicated for ~1 minute. The mixture was placed in a water bath and heated to the desired temperature (90 °C unless otherwise noted) at a rate of ~5 °C/min. The vial was then removed from the bath and was allowed to cool

at room temperature (20 °C). Unless otherwise noted gels were formed at a 5′-IG **2** concentration of 50 mM and a 1:2 ratio of 5′-IG **2**:KB(OH)$_4$. G **1** gels were formed at a 1:0.5 ratio of G **1** to KB(OH)$_4$.

2D NMR – HSQC and COSY procedures: 50 mM 5′-IG **2** gels were formed following the general 5′-IG **2** gel procedure. Two samples were made; one in 90% H$_2$O:10% D$_2$O and one in D2O. NMR experiments were run at 25 °C (32 scans, 1.5 second delay). Upon examination of the HSQC it was evident there were two 5′ signals. One, corresponding to 5′-IG **2** at low ppm values (yellow box), and a second with two separate H's (green box), which we would assign as 5′-*c*G **3** using the COSY spectrum. Since experiments were performed on gels NMR signals correspond to the borate esters of 5′-IG **2** and 5′-*c*G **3**. Note that 5′-*c*G **3** is a known compound, and our spectra match literature values with slight differences due to different solvents (d-6 DMSO in the literature) and borate esters.[65]

Mass Spectrometry Procedure: 50 mM 5′-IG **2** gels were formed following the general 5′-IG **2** gel procedure. The gel was then diluted with water and sonicated until the system was no longer a gel and could be injected into the JEOL AccuTOF-CS Spectrometer.

Rheology Procedure: 72 mM 5′-IG **2** and G **1** gels were prepared following the general gel procedures. Experiments were performed on an AR2000 stress-controlled rheometer from TA instruments at 20 °C with a 20 mm diameter parallel plate geometry. The gels were allowed to equilibrate on the plate for 10 minutes. Frequency sweeps were performed at 1% strain.

Circular Dichroism Spectroscopy Procedure: 50 mM 5′-IG **2** or G **1** gels were prepared according to the general gel procedure. The gels were allowed to sit for 1-2 hours before the experiments. Spectra were collected at room temperature in a Hellma 106-QS quartz cell with an optical path length of 0.01 mm. Experiments were performed at 25 °C with a scanning speed of 200 nm/min, response time of 2 sec, and a bandwidth of 1 nm. Each experiment was repeated at least 3 times, and the signals were averaged.

^{1}H NMR – Quantification of cyclization and drug release procedures: 50 mM 5′-IG **2** gels were formed following the general 5′-IG **2** gel procedure in 90% H_2O:10% D_2O. For the drug incorporation experiments the solid drug was added to the vial along with the solid 5′-IG **2** in order to afford a final drug concentration of 5mM. When the vials were removed from the heat 0.5 mL of the gel was pipetted into an NMR tube, with deuterated DMSO inside of a capillary tube sealed with parafilm as an internal standard. The gels were allowed to sit for 1 hour before initial experiments were run. Experiments were run at 25 °C with solvent suppression (32 scans) and repeated on at least 3 gel samples. Room temperature samples were allowed to sit at 20 °C; heated samples were submerged in an oil bath at 37 °C for the time indicated. After the scans were run on the samples left sitting for 72 hours, 10 μL of HCl was added to the NMR tube to completely break up any aggregates and determine the total G-derivative or drug concentration. The integration of the DMSO peak was set to 1.00 and the H1′ peaks of the G-derivatives or drugs were used. Experiments were performed 3 times,

and data is reported as the average of the experiments. Error bars represent the standard deviation between the 3 trials. The amount of G-derivative or the amount of drug in solution was determined according to the following equation:

$$\% \ drug \ in \ solution = \frac{[target \ at \ desired \ time]}{[target \ after \ HCl \ addition]}$$
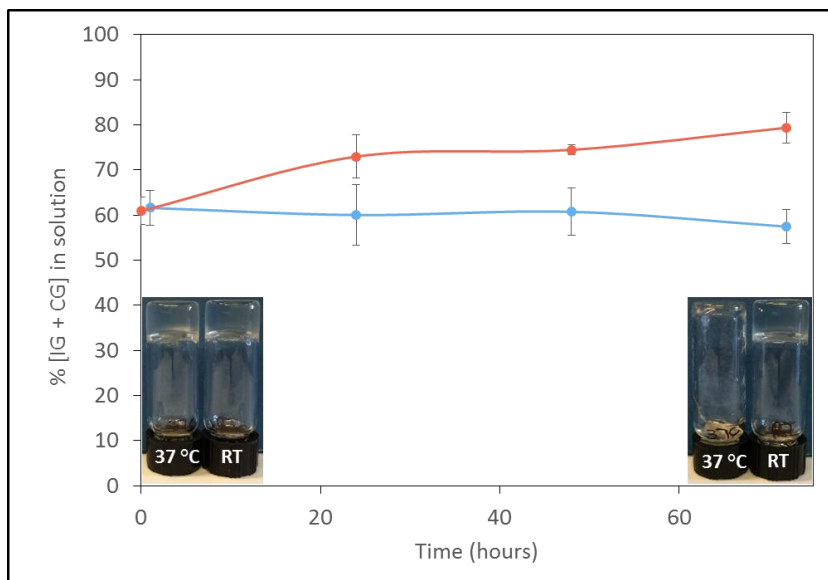
Figure 7.1: Gels allowed to sit at RT (blue) and 37 °C (orange) were monitored over time. After 72 hours at 37 °C the amount of G species in solution increased and the system was no longer a gel.

Synthesis of 5'-deoxy-5'-iodoguanosine (5'-IG 2):[63] Guanosine hydrate (2.5 g, 8.33 mmol), triphenylphosphine (7.2 g, 27.5 mmol), and imidazole (3.75 g, 55.2 mmol) were placed in a clean, dry, 250 mL 2-neck round bottom flask with a stir bar and flushed with N_2. N-methyl-2-pyrrolidinone (33.3 mL) was added and the mixture was allowed to stir for 3 minutes. Iodine (6.70 g, 26.3 mmol) was added in 2 batches over the course of 5 minutes. The solution was allowed to stir for 2-3 hours. When ^{1}H NMR of a small aliquot showed complete reaction methylene chloride (333 mL) and

water (100 mL) were added. Product was collected via vacuum filtration to afford an off-white powder (up to 2.39 g, 73% yield). ^{1}H NMR (d-6 DMSO) δ: 10.65 (s br, 1H, NH), 7.93 (s, 1H, H8), 6.49 (s br, 2H, NH$_2$), 5.71 (d, 1H, J = 6.4 Hz, H1′), 5.55 (d, 1H, J = 6 Hz, OH), 5.39 (d, 1H, J = 4.8 Hz, OH), 4.652-4.608 (m, 1H, H2′), 4.079-4.046 (m, 1H, H3′), 3.952-3.912 (m, 1H, H4′), 3.584-3.399 (m, 2H, H5′). ^{13}C NMR (d-6 DMSO) δ: 156.55 (C6), 153.54 (C2), 151.24 (C4), 135.64 (C8), 116.70 (C5), 86.65 (C1′), 83.53 (C4′), 73.02 (C2′), 72.68 (C3′), 7.80 (C5′). NMR data matches literature values.[63]
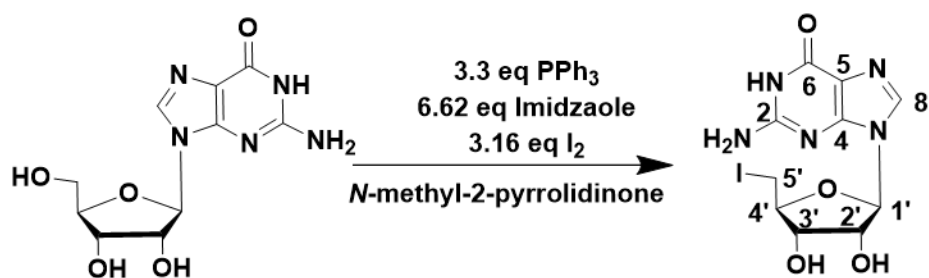
Figure 7.2: The synthesis of 5'-IG **2** from G **1**.
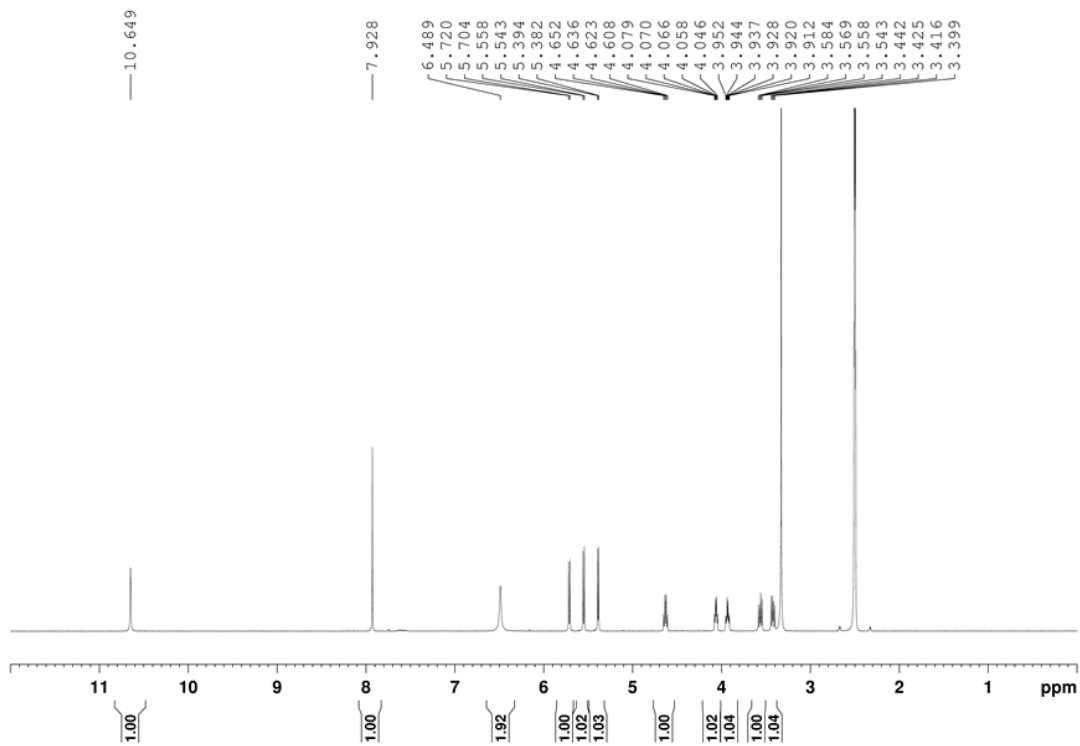
Figure 7.3: ^{1}H NMR spectrum of 5'-IG **2**.
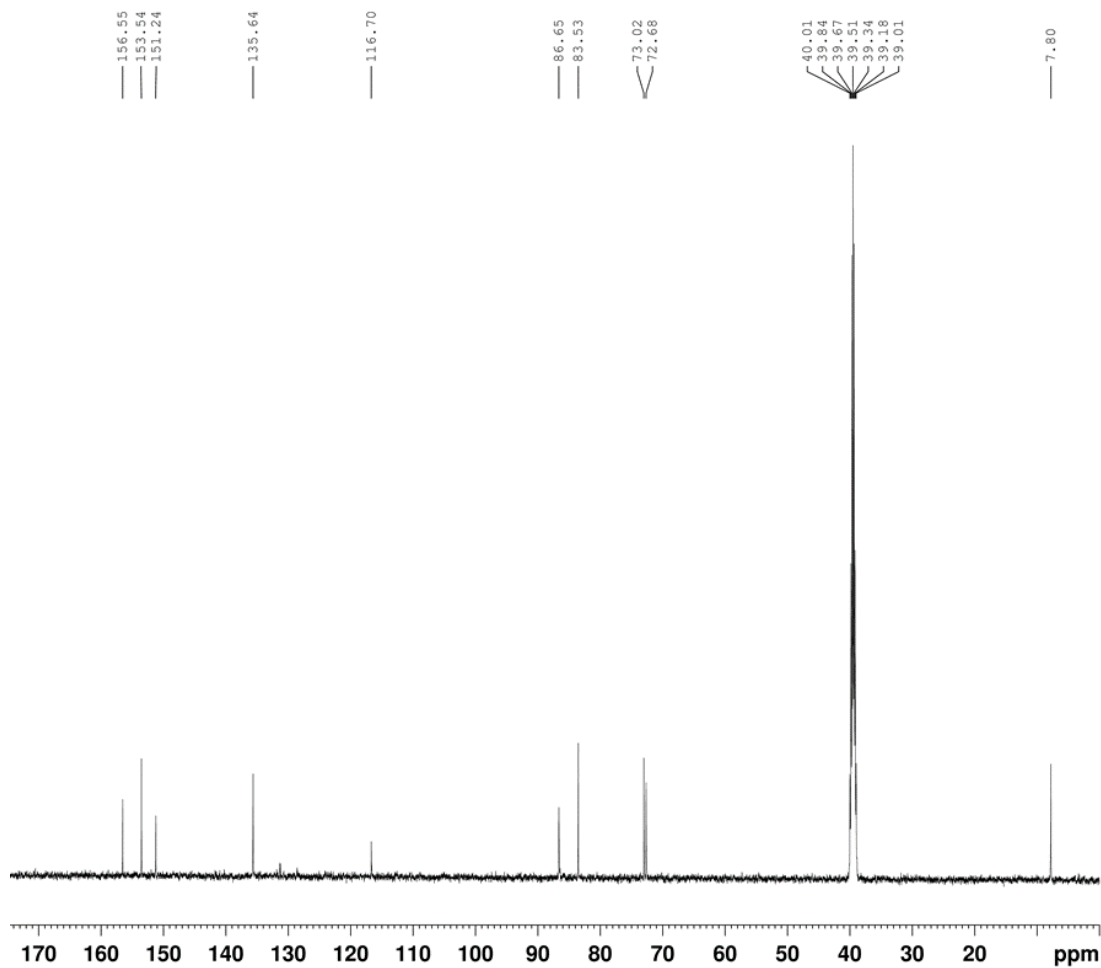
Figure 7.4: ^{13}C NMR spectrum of 5'-IG **2**.

7.3 Supporting Information for Chapter 3

Hydrogel Synthesis Protocols:

Synthesis protocol BDBA-K: In a glass vial 0.05g, 0.2 mmol (1 eq) of guanosine is mixed with 0.0146 g, 0.1 mmol (0.5 eq) of benzene-1,4-diboronic acid (BDBA). Distilled water (1.9 mL) is added, and the mixture is sonnicated for a few minutes, until all the components are dispersed. The suspension is then heated in an oil bath preheated

to 120°C until the solution becomes transparent. To avoid pressure in the vial upon heating a syringe needle in the plastic cap of the vial is used. Then, 100 μL, 0.01 g, 0.2 mmol KOH (1eq, stock solution of KOH: 0.66 g in 6.6 mL distilled water) is added and the mixture is heated and stirred for a few more minutes, and then left to cool down at room temperature. After cooling a transparent and strong gel is formed.

Synthesis protocol BDBA-Ba: In a vial, an amount of 0.05g, 0.2 mmol (1 eq) of guanosine is mixed with 0.0146g, 0.1 mmol (0.5 eq) of benzene-1,4-diboronic acid (BDBA). Distilled water (6.58 mL) is added, and the mixture is sonnicated for a few minutes, until all the components are dispersed. The suspension is then heated on an oil bath preheated to 120°C until the solution becomes transparent. To avoid pressure in the vial upon heating a needle in the cap of the vial is used. Then, 1.42 mL containing 0.015g, 0.1 mmol Ba(OH)$_2$*H$_2$O (0.5eq, stock solution of Ba(OH)$_2$*H$_2$O: 0.31g in 30 mL distilled water) is added and the mixture is heated and stirred for a few more minutes, and then left to cool down at room temperature. After cooling a transparent and strong gel is formed. Note that, at smaller amount of water used, the gel is cloudy.

Synthesis protocol BDBA-Mg: In a vial, an amount of 0.05g, 0.2 mmol (1 eq) of guanosine is mixed with 0.0146g, 0.1 mmol (0.5 eq) of benzene-1,4-diboronic acid (BDBA). Distilled water (1.9 mL) is added, and the mixture is sonicated for a few minutes, until all the components are dispersed. The suspension is then heated on an oil bath preheated to 120°C until the solution becomes transparent. To avoid pressure in the vial upon heating a needle in the cap of the vial is used. Then, 100 μL containing 0.01 g, 0.2 mmol, KOH (1 eq) is added and the mixture is heated and stirred for a few

more minutes, and then left to cool down at room temperature. After cooling, the gel is diluted with 38 ml distilled water in a NUNC tube (50 mL). The mixture is then sonnicated for few seconds to remove the air bubbles and then 4 mL of Mg^{2+} solution containing 0.041 g of $MgCl_2*6H_2O$ or 0.059 g 0.2 mmol (1 eq) of $Mg(NO_3)_2*6H_2O$ is added (stock solution: 0.59g in 40mL). We used initially chloride and then nitrate in the presence of TAE buffer to avoid $MgCl_2$/TAE pH change effects.

Comparison of water retention between BDBA-K, BDBA-Ba and BDBA-Mg hydrogels: We have observed the differences in the behavior of hydrogels containing K^+, Ba^{2+} and Mg^{2+} ions as jellifying triggers. In order to get a primary insight into the differences of hydrogel properties, we have performed water retention experiments. Two similar hydrogels were prepared using the standard protocol described above: hydrogel BDBA-K stabilized with K^+ and hydrogel BDBA-Ba stabilized with Ba^{2+}. Next, 2 mL of water to each sample was added and the reactions heated until melted. Then, the samples were cooled down and turned upside-down to check the self-sustainability. The gel BDBA-K is self-sustainable at maximum 3 mL of overall water content, collapsing at the volume of 4 mL. Hydrogel BDBA-Ba is self-sustainable at volumes up to 14 mL. To check the influence of Mg^{2+} to the formation of hydrogel, we used the collapsed BDBA-K gel and step wise added water solution containing Mg^{2+} (12 mM). We have observed an astonishing effect of Mg^{2+} ions over the self-sustainability of the gel, the same amount of organic matrix was sustaining up to 44 mL of water.

¹H NMR Procedure*:* Gels were formed in D₂O according to the afore mentioned procedures. In the case of the BDBA-K and BDBA-Ba gels, immediately following the final heating, 0.5mL of the hot solution was pipetted into a hot NMR tube. For the BDBA-Mg gel after addition of the $Mg(NO_3)_2$ 0.5mL of the mixture was pipetted into an NMR tube. Samples were allowed to sit overnight prior to running NMR experiments. Experiments were performed on a Bruker AVIII-600 at 25 °C and the solvent peak was used to calibrate the shifts.

Diffusion-Ordered Spectroscopy (DOSY) NMR Procedure: A Mg-BDBA gel was formed in D₂O according to the previously established procedure. After adding the $Mg(NO_3)_2$ 0.5 mL of the mixture was pipetted into an NMR tube and the gel was allowed to sit overnight. Diffusion experiments were performed on a Bruker AVIII-600 at 5 °C to maximize the separation of the H1′ signals with 18 points of 256 scans, a delay of 5 seconds, a gradient pulse length of 2300 μseconds and a delta value of 0.10 seconds. The spectral width and offset were set at 8ppm and 5.5 ppm respectively. The diffusion coefficients for each peak were calculated using their integration and the fitting function in the Bruker software.

Procedure for Powder X-ray diffraction*:* A G-BDBA-K⁺ gel was prepared according the established procedure. The sample was allowed to sit at 20 °C overnight and was then frozen and dried on a lyophilizer to form a white powder. Diffraction measurements were performed using a Cu radiation source at 20 °C on a Bruker D8 Advance Bragg-Brentano Diffractometer with a LynxEye detector.

Rheology: Gels were made as described in the procedures above and allowed to sit at room temperature overnight before experiments were performed. Experiments were run on an AR2000 stress-controlled rheometer from TA Instruments in New Castle, DE at 20 °C with a 20mm diameter parallel plate geometry. The gels were loaded onto the rheometer and allowed to equilibrate on the plate for 10 minutes before running the experiment. Frequency sweeps were performed at 0.2% strain.

AFM Atomic Force Microscopy: The Ntegra Spectra Atomic Force Microscope (NT-MDT, Russia) operated in tapping mode under ambient conditions was used to image gels structures. Silicon cantilever tips (NSG 10, NT-MDT) with gold reflecting coating, a resonance frequency of 140–390 kHz, a force constant of 3.1–37.6 N m^{-1} and a tip curvature radius of 10 nm were used. Sample preparation: a 10 mL aliquot of the gel solution was deposited on freshly cleaved mica substrates and dried in air at room temperature prior to imaging.

Cell growth experiments: 100 µl of freshly prepared hot solutions of BDBA-K, BDBA-Ba and BDBA-Mg, prepared as previously describe in Section 1, were dispensed in each well with a pipette, and left to cool down and form hydrogels. Subsequently, 100 µl of Tris-acetate-EDTA –TAE buffer was added to adjust the hydrogels at the physiological pH. In parallel, several wells containing all three hydrogels were left without TAE buffer treatment. After 2 hours of incubation, the buffer was removed, and DMEM culture medium supplemented with 10% fetal bovine serum (FBS) and 1% Penicillin-Streptomycin-Amphotericin B mixture (10K/10K/25 µg) was added (100 µl/well). One hour later, the cell suspension was added to each

well (1×10^4 NHDF cells/well in a total volume of 100 µl/well). In the MEM culture medium the concentration of possible competitive ions is rather small (0.2 g/L Ca^{2+} and 0.1 g/L Mg^{2+}) but with a very high concentration of Na^+ (6.8 g/L) and, under these conditions we do not expect major ion exchange processes as previously observed with Na^+, 300-500 mM by Davis et al. *J. Am. Chem. Soc*. 2014, 136, 12596−12599)

Cytotoxicity assay: The reported results represent the average of three individual MTS tests, where at least 6 replicates were performed for each type of hydrogel. Aliquots of 20, 90, 100 µl of hydrogel samples containing 0.5 mg guanosine were distributed in 96 well plates and incubated with 100 µl DMEM culture medium for one hour in order to better adjust the hydrogels for cell culture. The BDBA-K hydrogel samples were previously treated for 2 hours with 3xTAEMg^{2+} buffer solution, in order to adjust the pH value. NHDF cells were seeded at a density of 5×10^3 cells/well, in 96 well plates, on top of the hydrogel samples. After 20 hours 20 µL of CellTiter 96® Aqueous One Solution reagent were added to each well, and the plates were incubated for another 4 hours before reading the result. Absorbance at 490 nm was recorded with a plate reader (EnSight, PerkinElmer).

7.4 Supporting Information for Chapter 4

General Gel Procedure: The desired amounts of equimolar mixtures of 8AmG **5** and G **1** were weighted into a vial then the appropriate amounts of salt solution and water were added and the mixtures were sonicated for ~1 minute (in the case of the $KB(OH)_4$ gels KOH and water were added, then the mixture was sonicated, and $B(OH)_3$ was added and the mixture was sonicated again). The mixture was placed in a water bath at

room temperature (20 °C) and heated to 95-100 °C at a rate of ~5 °C/min until the solution was clear. The vial was then removed from the bath and was allowed to cool to room temperature (20 °C). $KB(OH)_4$ gels were made with 0.5 eq of salt, all other gels were made with various salt eqs as noted throughout the paper.

NMR Procedure: Gels were formed following the general gel procedure (0.5mL, 1wt%, 35mM 8AmG/G with 0.5eq salt) in D_2O. After heating the hot gel solutions were pipetted into hot NMR tubes. A capillary tube with d6-DMSO was sealed with parafilm and placed inside the NMR tube as an internal standard. ^1H NMR spectra were recorded on a Bruker AVIII-600 spectrometer. The DMSO peak was set to 2.5 and integrated to 1.00. The H1′ peaks for G and 8AmG were then integrated in comparison the DMSO peak. After the experiment the internal standard was removed and 10μL of DCl was added to the NMR tube to destroy the gel network. The capillary tube was re-inserted and new ^1H NMR spectra were obtained. The DMSO peak was again integrated to 1.00 and the H1′ peaks for G and 8AmG were integrated in comparison to the DMSO peak. The amounts of 8AmG and G in the gel and the sol were then calculated.

	KB(OH)4	KCl		KNO3		BaCl2		Ba(NO3)2		Pb(NO3)2	
	8AmG/G	8AmG	G	8AmG	G	8AmG	G	8AmG	G	8AmG	G
Gel (mM)	57	28	23	28	24	30	26	30	27	32	24
Sol (mM)	13	7	12	7	11	5	9	5	8	3	11
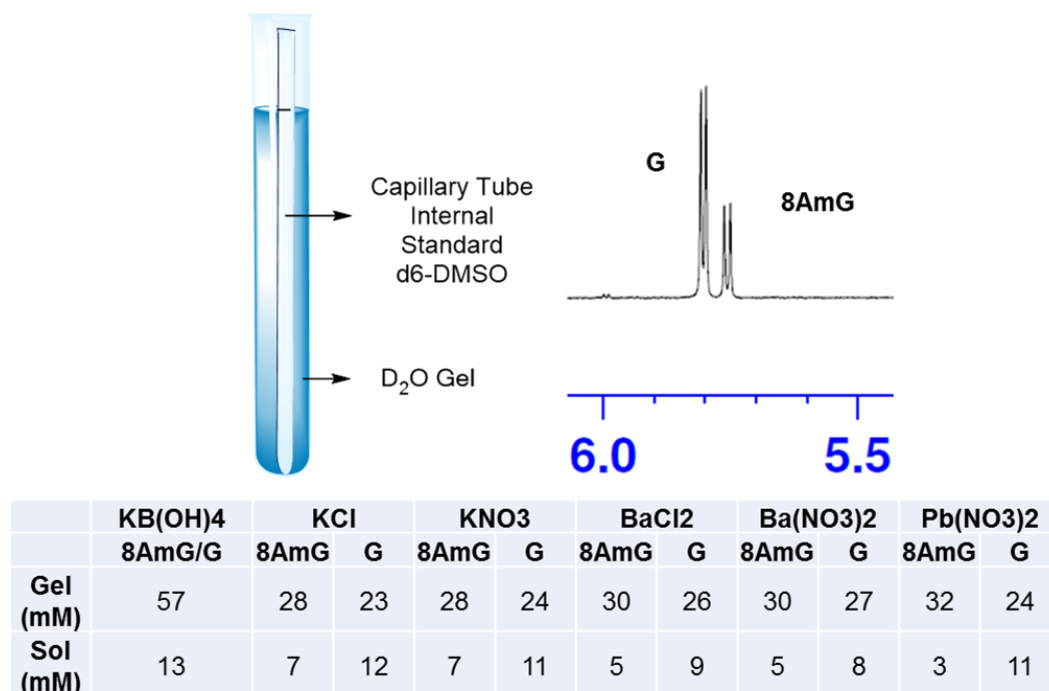
Figure 7.5: Experimental setup for the gel network quantification, a D_2O gel is made and placed in an NMR tube with a capillary tube of d6-DMSO (top left). ^{1}H NMR spectra are taken and the H1′ region (top right) is used to quantify the amounts of G species in the gel and sol network. The error associated with NMR is ±10%.

^{207}Pb NMR Procedure: Samples (0.5mL) where taken from the Pb^{2+} solution and placed in an NMR tube. Then a capillary tube containing 1 M $Pb(NO_3)_2$ and 1mM $EuCl_3$ was sealed with parafilm and placed inside of the NMR tube. ^{207}Pb was run on the sample with a Bruker DRX-500
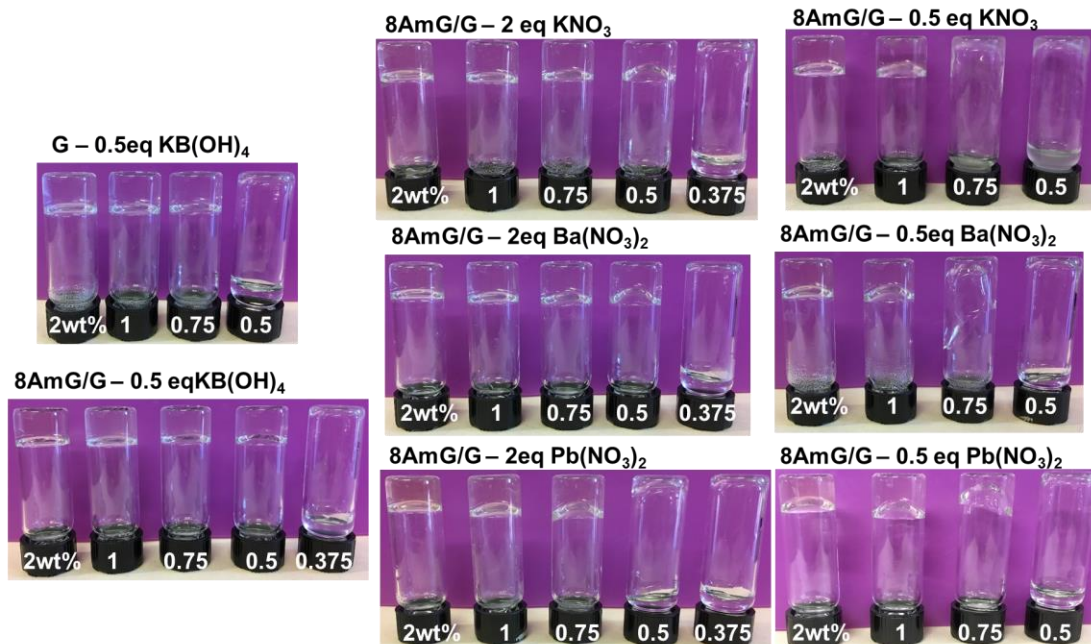
Figure 7.6: The critical gelation concentration (CGC) for several 8AmG/G systems is calculated by forming gels of varying concentrations of nucleoside.

CD Procedure: Gels were prepared following the general gel procedure. $KB(OH)_4$ gels were prepared at 2wt% with 0.5 eq of salt. KNO_3 and $Pb(NO_3)_2$ gels were prepared at 1wt% with 0.5 eq salt. The gels were allowed to sit for 2 hours prior to the experiments. The CD spectra were recorded at 25 °C in a Hellma 106-QS quartz cell with a path length of 0.01 mm. Experiments were run on a Jasco J-810 spectropolarimeter with a scanning speed of 200 nm/min, response time of 2 sec, and a bandwidth of 1 nm. Each experiment was repeated at least 3 times, and the signals averaged.

PXRD Procedure: Gels were prepared according the general gel procedure (1 wt%, 35 mM 8AmG/G with 0.5 eq salt). After sitting at 20 °C overnight the gels were lyophilized to form white powders. Powder X-ray diffraction measurements were

109

performed with a Cu radiation source at 20 °C using a Bruker D8 Advance Bragg-Brentano Diffractometer equipped with a LynxEye detector.
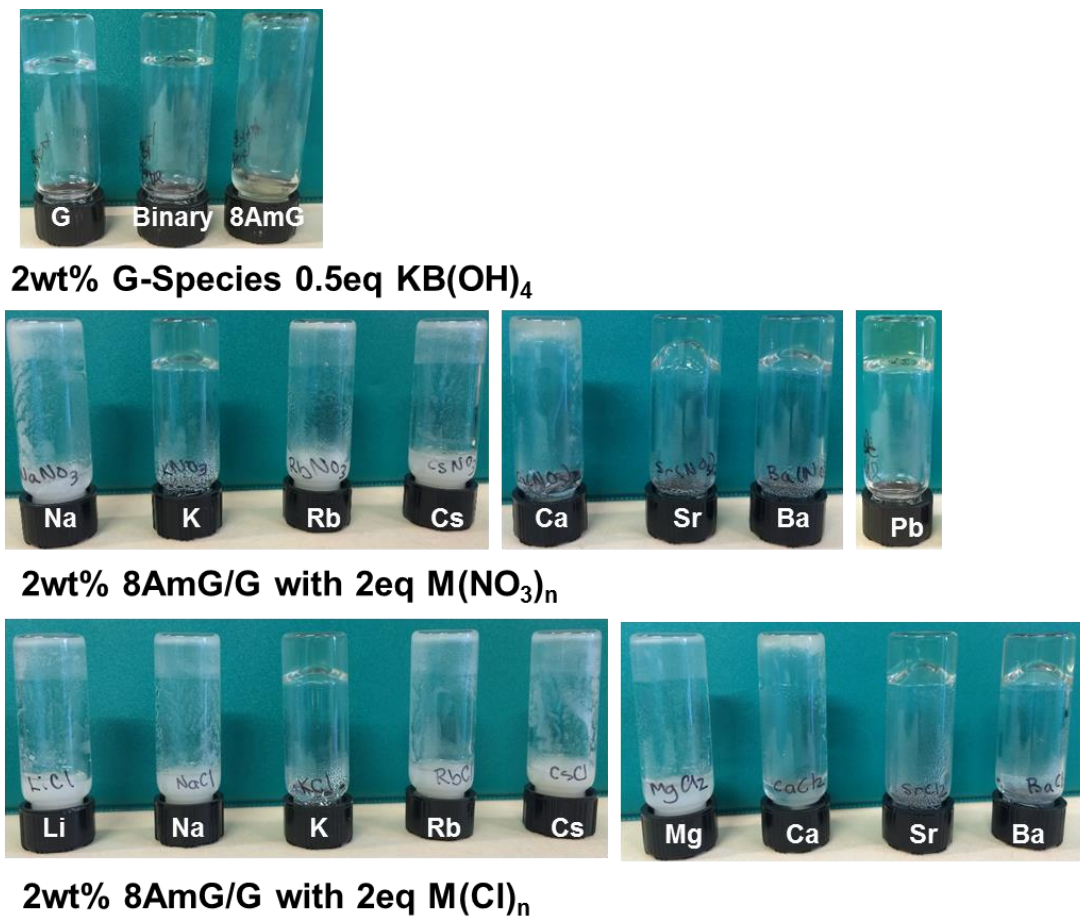
Figure 7.7: We attempted to form gels with all of the salts shown following the general gel procedure. Gels were only able to form with K^+, Sr^{2+}, Ba^{2+}, and Pb^{2+} salts.

SEM Procedure: A 2 wt% (70 mM) binary 8AmG/G hydrogel was prepared according to the general gel procedure. A small portion of the gel was scooped up with a small spatula and placed on an AL stub with a small dimple. A 0.3 μL aliquot of 3% ionic liquid (HILEM 1000 for Hitachi EM) was pipetted onto the gel sample and set in the air for 10 minutes prior to SEM examination.

Rheology Procedure: Gels were made following the general gel procedure (2 wt%, 70 mM 8AmG/G with various salt concentrations). Gels were allowed to cool overnight before rheology was performed. Experiments were performed on an AR2000 stress-controlled rheometer from TA instruments in New Castle, DE at 20 °C with a 20mm diameter parallel plate geometry. The gels were allowed to equilibrate on the plate for 10 minutes. Frequency sweeps were performed at 0.5% strain.

Dye Release Procedure: Gels were prepared following the general gel procedure (2 wt%, 70 mM 8AmG/G, 0.5 eq of $KB(OH)_4$ or 2 eq of KCl or 2 eq of $BaCl_2$) with the following alterations. After heating to ~95 °C both MB and RB were added (25 μM each) and the vials were shaken to distribute the dyes. The vials were returned to the heat bath for ~2 mins. After the 2 min heating 0.5 mL of the hot dyed gel solution was pipetted into a parafilm lined cube mold. After cooling for 1 hour at room temperature the gel cubes were suspended in 3 mL of 155 mM KCl solutions. The systems were monitored visually for dye release.
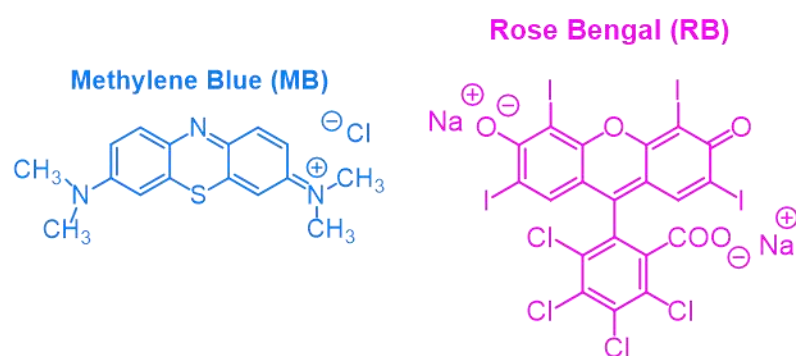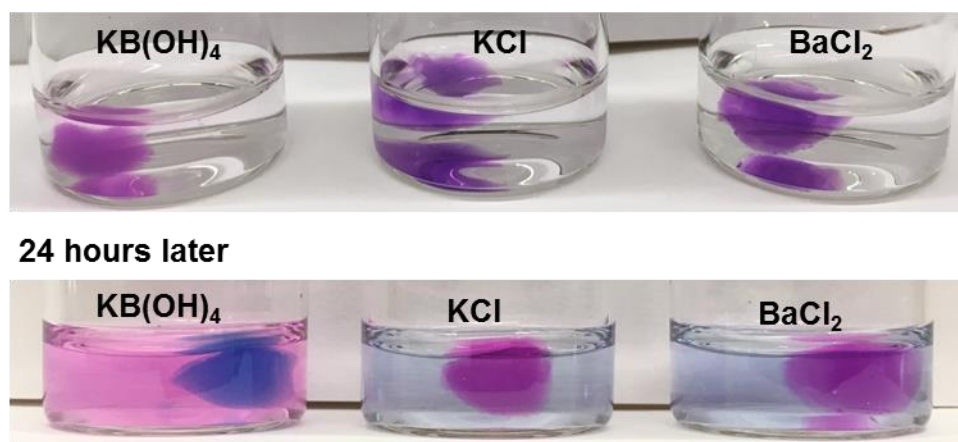
Figure 7.8: Gels loaded with MB and RB (25 μM each) suspended in 155 mM KCl buffer will release different dyes based on their charge.

Dye Uptake Procedure: Gels were prepared according to the general gel procedure (2 wt%, 70 mM, 8AmG/G with 0.5 eq of KB(OH)$_4$ or 2 eq of KCl or 2 eq of BaCl$_2$). After heating 0.5 mL aliquots of the hot gel solution were pipetted into parafilm lined cube molds and allowed to cool at RT for 1 hr. The cubes were then suspended in 3 mL of 155 mM KCl with 12.5 μM dye. The outside solution was monitored over time via UV-Vis spectroscopy.
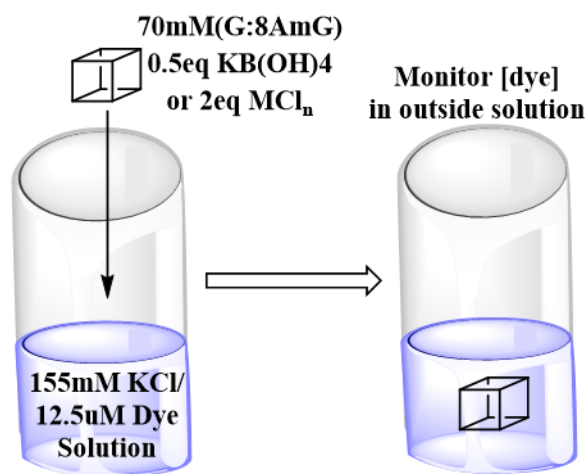
Figure 7.9: Illustration of the dye uptake experiments.
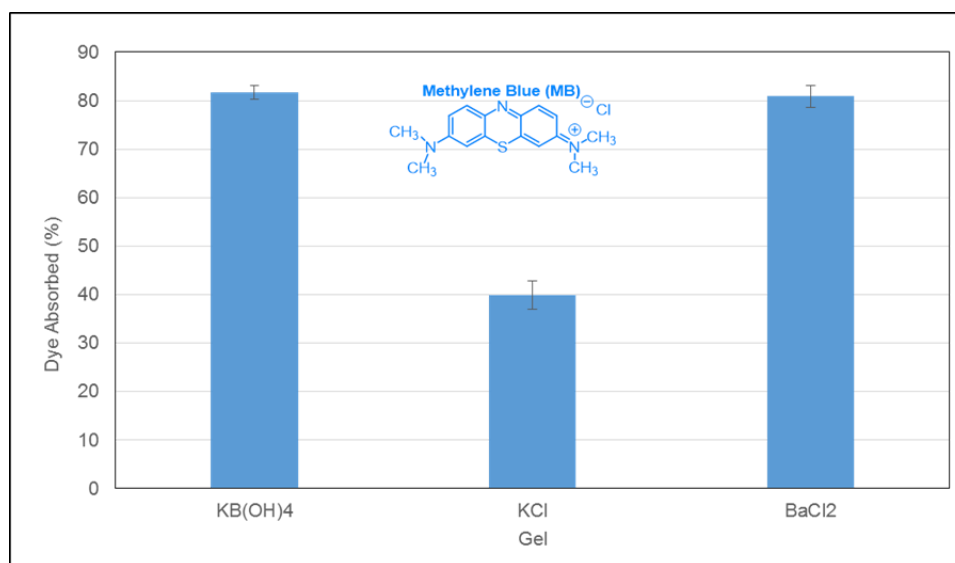
Figure 7.10: Gels were suspended in a 155 mM KCl solution with 12.5 μM MB dye and the amount of dye in the outside solution was monitored using UV-Vis. The graph shows the amount of MB absorbed by the gel after 24 hours.

NBB Max Procedure: Gels were prepared according to the general gel procedure (2 wt%, 70 mM, 8AmG/G with 0. 5eq of KB(OH)$_4$ or 2 eq of KCl or 2 eq of BaCl$_2$). After heating 0.5 mL aliquots of the hot gel solution were pipetted into parafilm lined cube molds and allowed to cool at RT for 1 hr. The cubes were then suspended in 3 mL of 155 mM KCl with 100 µM NBB. The outside solution was monitored over time via UV-Vis spectroscopy.

Qualitative Dye Procedure: Gels were prepared following the general gel procedure (2 wt%, 70 mM 8AmG/G with 0.5 eq of KB(OH)$_4$ or 2 eq of KCl or 2 eq of BaCl$_2$). The hot gel solution was pipetted into parafilm lined cube molds in 0.5 mL increments. The gel cubs were allowed to cool for 1hr before being suspended in 3 mL of 155 mM KCl.

7.5 Supporting information for Chapter 5

General Gel Procedure: The desired amounts of equimolar mixtures of the 8-substituted guanosine and G were weighted into a vial and then 0.5 eq of aqueous B(OH)$_3$ and any necessary H$_2$O was added. The mixture was sonicated for ~30 seconds and 0.5 eq of aqueous KOH was added. The mixtures was sonicated for ~1 minute. *For room temperature gels*: At this point the gels were allowed to sit at room temperature to form gels. *For heated gels:* The mixture was placed in a water bath at room temperature (20 °C) and heated to 95-100 °C at a rate of ~5 °C/min until the solution was clear. The vial was then removed from the bath and was allowed to cool to room temperature (20 °C).

NMR Procedure: Gels were formed following the general gel procedure (0.5 mL, 1 wt%, 8-substittued G/G with 0.5 eq $KB(OH)_4$) in D_2O. *For RT Gels*: The nucleoside/$B(OH)_3$ mixture was placed in an NMR tube after sonication and aqueous KOH was added directly to the NMR tube followed by sonication. Gels formed directly in the tube. *For heated gels*: After heating the hot gel solutions were pipetted into hot NMR tubes.

CD Procedure: Gels were prepared following the general gel procedure. The gels were allowed to sit for overnight prior to the experiments. The CD spectra were recorded at 25 °C in a Hellma 106-QS quartz cell with an optical path length of 0.01 mm. Experiments were run on a Jasco J-810 spectropolarimeter with a scanning speed of 200 nm/min, response time of 2 sec, and a bandwidth of 1nm. Each experiment was repeated at least 3 times, and the signals were averaged.

PXRD Procedure: Gels were prepared according the general gel procedure. After sitting at 20 °C overnight the gels were lyophilized to white powders. PXRD measurements were performed with a Cu radiation source at 20 °C using a Bruker D8 Advance Bragg-Brentano Diffractometer equipped with a LynxEye detector.

Rheology Procedure: Gels were made following the general gel procedure (2wt%, nucleoside, 0.5 eq of $KB(OH)_4$). Gels were allowed to cool overnight before rheology was performed. Experiments were performed on an AR2000 stress-controlled rheometer from TA instruments in New Castle, DE at 20 °C with a 20mm diameter parallel plate geometry. The gels were allowed to equilibrate on the plate for 10 minutes. Frequency sweeps were performed at 0.5% strain.

Gel Cube Stability Procedure: Gels were made following the general gel procedure (2wt% nucleoside, 0.5 eq of KB(OH)$_4$). *RT gels* were made in a parafilm lined mold. *Heated gels* were pipetted into a parafilm lined mold while hot. After sitting in the mold overnight the gels were placed in 3 mL of 155 mM KCl solution. Aliquots were taken from the outside solution and diluted as necessary to monitor the nucleoside concentration via UV-vis spectroscopy.

Synthesis of 8-mopholinoguanosine (8morphG 8):[124] Guanosine (0.5 g, 1.38 mmol), was placed in a clean, dry, 50 mL 2-neck round bottom flask with a stir bar and a condenser and flushed with N$_2$. After ~15 min, 15 mL of morpholine was added and the mixture was allowed to stir in an oil bath at ~129 °C overnight. After 17 hours the flask was removed from the heat and rotovapped to remove the solvent. The resulting brown oil was dissolved in water and recrystallized to form a white powder. (60% yield). ^{1}H NMR (d-6 DMSO) δ: 10.660 (s br, 1H, NH), 6.284 (s br, 2H, NH$_2$), 5.588 (d, 1H, *J* = 6.6 Hz, H1′), 5.371 (d, 1H, *J* = 6 Hz, OH), 5.063-5.055 (m, 2H, 2-OH), 4.986-4.956 (m, 1H, H2′), 4.111-4.106 (m, 1H, H3′), 3.827-3.821 (m, 1H, H4′), 3.723-3.500 (m, 6H, H5′ and morph. ring) 3.147-2.971 (m, 4H, morph ring).
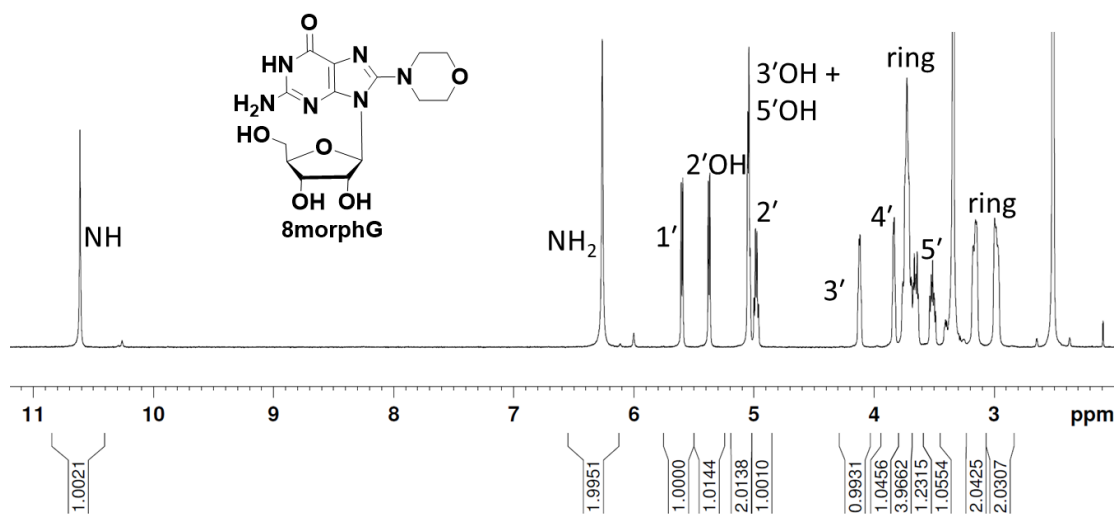
Figure 7.11: ^{1}H NMR spectra of 8morphG **8**.

BIBLIOGRAPHY

(1)   Webber, M. J.; Appel, E. A.; Meijer, E. W.; Langer, R. Supramolecular Biomaterials. *Nat. Mater.* **2016**, *15*, 13–26.

(2)   Peters, G. M.; Davis, J. T. Supramolecular Gels Made from Nucleobase, Nucleoside and Nucleotide Analogs. *Chem. Soc. Rev.* **2016**, *45*, 3188–3206.

(3)   Bhattacharyya, T.; Saha, P.; Dash, J. Guanosine-Derived Supramolecular Hydrogels : Recent Developments and Future Opportunities. *ACS Omega* **2018**, *3*, 2230–2241.

(4)   Davis, J. T. G-Quartets 40 Years Later: From 5′-GMP to Molecular Biology and Supramolecular Chemistry. *Angew. Chemie - Int. Ed.* **2004**, *43* (6), 668–698.

(5)   Bang, I. Examination of Guanilyic Acid. *Biochem. Z.* **1910**, *26*, 293–310.

(6)   Buerkle, L. E.; Rowan, S. J. Supramolecular Gels Formed from Multi-Component Low Molecular Weight Species. *Chem. Soc. Rev.* **2012**, *41* (18), 6089.

(7)   Du, X.; Zhou, J.; Xu, B. Supramolecular Hydrogels Made of Basic Biological Building Blocks. *Chem. - An Asian J.* **2014**, *9* (6), 1446–1472.

(8)   Du, X.; Zhou, J.; Shi, J.; Xu, B. Supramolecular Hydrogelators and Hydrogels: From Soft Matter to Molecular Biomaterials. *Chem. Rev.* **2015**, *115*, 13165–13307.

(9)   Yu, E.; Nakamura, D.; DeBoyace, K.; Neisius, A. W.; McGown, L. B. Tunable Thermoassociation of Binary Guanosine Gels. *J. Phys. Chem. B* **2008**, *112* (4), 1130–1134.

(10)   Buerkle, L. E.; Li, Z.; Jamieson, A. M.; Rowan, S. J. Tailoring the Properties of Guanosine-Based Supramolecular Hydrogels. *Langmuir* **2009**, *25* (15), 8833–8840.

(11)   Das, R. N.; Kumar, Y. P.; Pagoti, S.; Patil, A. J.; Dash, J. Diffusion and Birefringence of Bioactive Dyes in a Supramolecular Guanosine Hydrogel. *Chem. - A Eur. J.* **2012**, *18*, 6008–6014.

(12)   Peters, G. M.; Skala, L. P.; Plank, T. N.; Hyman, B. J.; Reddy, M. G. N.; Marsh, A.; Brown, S. P.; Davis, J. T. A $G_4 \cdot K^+$ Hydrogel Stabilized by an Anion. *J. Am. Chem. Soc.* **2014**, *136*, 12596–12599.

(13)   Peters, G. M.; Skala, L. P.; Plank, T. N.; Oh, H.; Reddy, M. G. N.; Marsh, A.;
         Brown, S. P.; Raghavan, S. R.; Davis, J. T. G4-Quartet•M$^+$ Borate Hydrogels.
         J. Am. Chem. Soc. **2015**, *137*, 5819–5827.

(14)   Peters, G. M.; Skala, L. P.; Davis, J. T. A Molecular Chaperone for G4-Quartet
         Hydrogels. *J. Am. Chem. Soc.* **2016**, *138* (1), 134–139.

(15)   Plank, T. N.; Davis, J. T. A G$_4$ ·K$^+$ Hydrogel That Self-Destructs. *Chem.
         Commun.* **2016**, *52* (28), 5037–5040.

(16)   Rotaru, A.; Pricope, G.; Plank, T. N.; Clima, L.; Ursu, E. L.; Pinteala, M.;
         Davis, J. T.; Barboiu, M. G-Quartet Hydrogels for Effective Cell Growth
         Applications. *Chem. Commun.* **2017**, *53*, 12668–12671.

(17)   Plank, T. N.; Skala, L. P.; Davis, J. T. Supramolecular Hydrogels for
         Environmental Remediation : G$_4$ -Quartet Gels That Selectively Absorb
         Anionic Dyes from Water. *Chem. Commun.* **2017**, *53*, 6235–6238.

(18)   *Molecular Gels: Materials with Self-Assembled Fibrillar Networks*; Weiss, R.
         G., Terech, P., Eds.; Springer: Dordrecht, The Netherlands, 2006.

(19)   Lloyd, D. J. *Colloid Chemistry*; The Chemical Catalog Company Inc.: New
         York, 1926.

(20)   Estroff, L. A; Hamilton, A. D. Water Gelation by Small Organic Molecules
         Water Gelation by Small Organic Molecules. *Chem. Rev.* **2004**, *104* (3), 1201–
         1218.

(21)   Yu, G.; Yan, X.; Han, C.; Huang, F. Characterization of Supramolecular Gels.
         Chem. Soc. Rev. **2013**, *42* (16), 6697–6722.

(22)   Caran, K. L.; Lee, D.-C.; Weiss, Richard, G. Small Molecule Gels. In *Soft
         Fibrillar Materials: Fabrication and Applications*; Liu, X. Y., Li, J.-L., Eds.;
         Wiley-VCH: Weinheim, Germany, 2013; pp 1–75.

(23)   Yang, X.; Zhang, G.; Zhang, D. Stimuli Responsive Gels Based on Low
         Molecular Weight Gelators. *J. Mater. Chem.* **2012**, *22* (1), 38–50.

(24)   Segarra-Maset, M. D.; Nebot, V. J.; Miravet, J. F.; Escuder, B. Control of
         Molecular Gelation by Chemical Stimuli. *Chem. Soc. Rev.* **2013**, *42* (17),
         7086–7098.

(25)   *Boron: Sensing, Synthesis and Supramolecular Self-Assembly*; Li, M., Fossey,
         J. S., James, T. D., Eds.; The Royal Society of Chemistry: Cambridge, 2015.

(26) Duin, M. Van; J.A., P.; Kieboom, A. P. G.; Van Bekkum, H. Studies on Borates Esters 1: The pH Dependence of the Stability of Esters of Boric Acid and Borate in Aqueous Medium as Studied by 11B NMR. *Tetrahedron* **1984**, *40* (2901–2911).

(27) Casassa, E. Z.; Sarquis, A. M.; Van Dyke, C. H. The Gelation of Polyvinyl Alcohol with Borax: A Novel Class Participation Experiment Involving the Preparation and Properties of "Slime." *J. Chem. Ed.* **1986**, *63* (57–60).

(28) Wu, X.; Li, Z.; Chen, X.-X.; Fossey, J. S.; James, T. D.; Jiang, Y.-B. Selective Sensing of Saccharides Using Simple Boronic Acid and Their Aggregates. *Chem. Soc. Rev.* **2013**, *42*, 8032–8048.

(29) Sun, X.; James, T. D. Glucose Sensing in Supramolecular Chemistry. *Chem. Rev.* **2015**, *115*, 8001–8037.

(30) Nishiyabu, R.; Kubo, Y.; James, T. D.; Fossey, J. S. Boronic Acid Building Blocks: Tools for Self Assembly. *Chem. Commun.* **2011**, *47*, 1124–1150.

(31) Guan, Y.; Zhang, Y. Boronic Acid Containing Hydrogels: Synthesis and Their Applications. *Chem. Soc. Rev.* **2013**, *42*, 8106–8121.

(32) Kubo, Y.; Nishiyabu, R.; James, T. D. Hierarchical Supramolecules and Organization Using Boronic Acid Building Blocks. *Chem. Commun.* **2015**, *51*, 2005–2020.

(33) Sarkar, K.; Dastidar, P. Supramolecular Hydrogel Derived from a C3-Symmetric Boronic Acid Derivative for Stimuli-Responsive Release of Insulin and Doxorubicin. *Langmuir* **2018**, *34*, 685–692.

(34) Ikeda, M.; Fukuda, K.; Tanida, T.; Yoshii, T.; Hamachi, I. A Supramolecular Hydrogel Containing Boronic Acid-Appended Receptor for Fluorocolorimetric Sensing of Polyols with a Paper Platform. *Chem. Commun.* **2012**, *48* (21), 2716.

(35) Ikeda, M.; Tanida, T.; Yoshii, T.; Hamachi, I. Rational Molecular Design of Stimulus-Responsive Supramolecular Hydrogels Based on Dipeptides. *Adv. Mater.* **2011**, *23*, 2819–2822.

(36) Ikeda, M.; Tanida, T.; Yoshii, T.; Kurotani, K.; Onogi, S.; Urayama, K.; Hamachi, I. Installing Logic-Gate Responses to a Variety of Biological Substances in Supramolecular Hydrogel-Enzyme Hybrids. *Nat. Chem.* **2014**, *6* (6), 511–518.

(37)   Yoshii, T.; Onogi, S.; Shigemitsu, H.; Hamachi, I. Chemically Reactive Supramolecular Hydrogel Coupled with a Signal Amplification System for Enhanced Analyte Sensitivity. *J. Am. Chem. Soc.* **2015**, *137* (9), 3360–3365.

(38)   Grigoriou, S.; Johnson, E. K.; Chen, L.; Adams, D. J.; James, T. D.; Cameron, P. J. Dipeptide Hydrogel Formation Triggered by Boronic Acid–Sugar Recognition. *Soft Matter* **2012**, *8* (25), 6788–6791.

(39)   Jones, B. H.; Martinez, A. M.; Wheeler, J. S.; McKenzie, B. B.; Miller, L. L.; Wheeler, D. R.; Spoerke, E. D. A Multi-Stimuli Responsive, Self-Assembling, Boronic Acid Dipeptide. *Chem Commun* **2015**, *51*, 14532–14535.

(40)   Gellert, M.; Lipsett, M. N.; Davies, D. R. Helix Formation By Guanylic Acid. *Proc. Natl. Acad. Sci. U. S. A.* **1962**, *48* (12), 2013–2018.

(41)   Chantot, J.-F.; Guschlbauer, W. Physicochemical Properties of Nucleosides 3. Gel Formation by 8-Bromoguanosine. *FEBS Lett.* **1969**, *4* (3), 173–176.

(42)   Chantot, J.-F.; Sarocchi, M.-T.; Guschlbauer, W. Physico-Chemical Properties of Nucleosides. 4.- Gel Formation by Guanosine and Its Analogues. *Biochimie* **1971**, *53*, 347–354.

(43)   Chantot, J. F.; Haertle, T.; Guschlbauer, W. Nucleoside Conformations. XIII. Circular Dichroïsm of Guanosine Gels and the Conformation of GpG and Poly (G). *Biochimie* **1974**, *56* (4), 501–507.

(44)   Sreenivasachary, N.; Lehn, J.-M. Gelation-Driven Component Selection in the Generation of Constitutional Dynamic Hydrogels Based on Guanine-Quartet Formation. *Proc. Natl. Acad. Sci.* **2005**, *102*, 5938–5943.

(45)   Lehn, J.-M. From Supramolecular Chemistry Towards Constitutional Dynamic Chemistry and Adaptive Chemistry. *Chem. Soc. Rev.* **2007**, *36*, 151–160.

(46)   Sreenivasachary, N.; Lehn, J. M. Structural Selection in G-Quartet-Based Hydrogels and Controlled Release of Bioactive Molecules. *Chem. - An Asian J.* **2008**, *3* (1), 134–139.

(47)   Dash, J.; Patil, A. J.; Das, R. N.; Dowdall, F. L.; Mann, S. Supramolecular Hydrogels Derived from Silver Ion-Mediated Self-Assembly of 5'-Guanosine Monophosphate. *Soft Matter* **2011**, *7*, 8120–8126.

(48)   Ghosh, A.; Parasar, B.; Bhattacharyya, T.; Dash, J. Chiral Carbon Dots Derived From Guanosine 5'-Monophosphate Form Supramolecular Hydrogels. *Chem. Commun.* **2016**, *52* (11159–11162).

(49)   Buerkle, L. E.; von Recum, H. A.; Rowan, S. J. Toward Potential
        Supramolecular Tissue Engineering Scaffolds Based on Guanosine
        Derivatives. *Chem. Sci.* **2012**, *3* (2), 564–572.

(50)   Carducci, F.; Yoneda, J. S.; Itri, R.; Mariani, P. On the Structural Stability of
        Guanosine-Based Surpramolecular Hydrogels. *Soft Matter* **2018**, *Accepted M*,
        DOI: 10.1039/C8SM00299A.

(51)   Li, Z.; Buerkle, L. E.; Orseno, M. R.; Streletzky, K. A.; Seifert, S.; Jamieson,
        A. M.; Rowan, S. J. Structure and Gelation Mechanism of Tunable Guanosine-
        Based Supramolecular Hydrogels. *Langmuir* **2010**, *26* (12), 10093–10101.

(52)   Adhikari, B.; Shah, A.; Kraatz, H.-B. Self-Assembly of Guanosine and Deoxy-
        Guanosine into Hydrogels: Monovalent Cation Guided Modulation of
        Gelation, Morphology and Self-Healing Properties. *J. Mater. Chem. B* **2014**, *2*
        (30), 4802.

(53)   Bhattacharyya, T.; Kumar, Y. P.; Dash, J. Supramolecular Hydrogel Inspired
        from DNA Structures Mimics Peroxidase Activity. *ACS Biomater. Sci. Eng.*
        2017, *3* (10), 2358–2365.

(54)   Zhong, R.; Xiao, M.; Zhu, C.; Shen, X.; Tang, Q.; Zhang, W.; Wang, L.; Song,
        S.; Qu, X.; Pei, H.; et al. Logic Catalytic Interconversion of G-Molecular
        Hydrogel. *ACS Appl. Mater. Interfaces* **2018**, *10* (5), 4512–4518.

(55)   Venkatesh, V.; Mishra, N. K.; Romero-Canelón, I.; Vernooij, R. R.; Shi, H.;
        Coverdale, J. P. C.; Habtemariam, A.; Verma, S.; Sadler, P. J. Supramolecular
        Photoactivatable Anticancer Hydrogels. *J. Am. Chem. Soc.* **2017**,
        DOI:10.1021/jacs.7b00186.

(56)   Li, Y.; Liu, Y.; Ma, R.; Xu, Y.; Zhang, Y.; Li, B.; An, Y.; Shi, L. A G-
        Quadruplex Hydrogel via Multicomponent Self-Assembly: Formation and
        Zero-Order Controlled Release. *ACS Appl. Mater. Interfaces* **2017**, *9* (15),
        13056–13067.

(57)   Biswas, A.; Malferrari, S.; Kalaskar, D. M.; Das, A. K. Arylboronate Esters
        Mediated Self-Healable and Biocompatible Dynamic G-Quadruplex Hydrogels
        as Promising 3D-Bioinks. *Chem. Commun.* **2018**, *54* (14), 1778–1781.

(58)   Cornwell, D. J.; Smith, D. K. Expanding the Scope of Gels – Combining
        Polymers with Low-Molecular-Weight Gelators to Yield Modified Self-
        Assembling Smart Materials with High-Tech Applications. *Mater. Horiz.*
        2015, *2*, 279–293.

(59)   Steed, J. W. Supramolecular Gel Chemistry: Developments over the Last Decade. *Chem. Commun.* **2011**, *47*, 1379–1383.

(60)   Arnal-Hérault, C.; Pasc, A.; Michau, M.; Cot, D.; Petit, E.; Barboiu, M. Functional G-Quartet Macroscopic Membrane Films. *Angew. Chemie - Int. Ed.* **2007**, *46*, 8409–8413.

(61)   Kwan, I. C. M.; Delley, R. J.; Hodgson, D. R. W.; Wu, G. Single Atom Modification Leads to Enhanced Nucleotide Self-Assembly: The Role of Cation Bridging. *Chem. Commun.* **2011**, *47* (13), 3882–3884.

(62)   Wong, A.; Ida, R.; Spindler, L.; Wu, G. Disodium Guanosine 5'-monophosphate Self-Associates into Nanoscale Cylinders at pH 8: A Combined Diffusion NMR Spectroscopy and Dynamic Light Scattering Study. *J. Am. Chem. Soc.* **2005**, *127* (19), 6990–6998.

(63)   McGee, D. P. C.; Martin, J. C. Acyclic Nucleoside Analogues: Methods for the Preparation of 2',3'-secoguanosine, 5'-deoxy-2',3'-secoguanosine, and (R,S)-9-[1-(2-Hydroxyethoxy)-2-Hydroxyethyl]guanine. *Can. J. Chem.* **1986**, *64*, 1885–1889.

(64)   Holmes, R. E.; Robins, R. K. December, 1963 Purine Nucleosides. *Purine Nucleosides* **1963**, *1557* (5), 3483–3486.

(65)   Li, H.; Miller, M. J. Syntheses of and Purine Nucleosides: Building Blocks for Novel Antisense Oligonucleosides with Hydroxamate Linkages. *J. Org. Chem.* **1999**, *64* (14), 9289–9293.

(66)   Mieczkowski, A.; Roy, V.; Agrofoglio, L. A. Preparation of Cyclonucleosides. *Chem. Rev.* **2010**, *110* (4), 1828–1856.

(67)   Saenger, W. Physical Properties of Nucleotides : Charge Densitites, pK Values, Spectra, and Tautomerism. In *Principles of Nucleic Acid Structure*; Springer New York, 1984; p 108.

(68)   Stolarski, R.; Dudycz, L.; Shugar, D. NMR Studies in the Syn-Anti Dynamic Equilibrium in Purine Nucleosides and Nucleotides. *Eur. J. Biochem.* **1980**, *108* (1), 111–121.

(69)   Wada, T.; Minamimoto, N.; Inaki, Y.; Inoue, Y. Conformational and Orientational Switching of Uridine Derivatives by Borates. *Chem. Lett.* **1998**, 1025–1026.

(70) Wada, T.; Minamimoto, N.; Satoh, H.; Inoue, Y. Recognition Control of the Nucleic Acid Model through Conformational Switching of Nucleobase Induced by Borate Ester Formation of Cis-2',3'-diol. *Nucleic Acids Res.* **1999**, *42*, 145–146.

(71) Wada, T.; Minamimoto, N.; Inaki, Y.; Inoue, Y. Peptide Ribonucleic Acids (PRNA). 2 . A Novel Strategy for Active Control of DNA Recognition through Borate Ester Formation. *J. Am. Chem. Soc.* **2000**, *122*, 6900–6910.

(72) Wada, T.; Sato, H.; Inoue, Y. External Reversible Control of Recognition Behavior of Alpha-Peptide Ribonucleic Acid (α-PRNA) through Anti-Syn Orientational Switching of the Nucleobase Induced by Borate Esterification of the Cis-2′,3′-Diol. *Pept. Sci.* **2004**, *76* (1), 15–20.

(73) Masiero, S.; Trotta, R.; Pieraccini, S.; De Tito, S.; Perone, R.; Randazzo, A.; Spada, G. P. A Non-Empirical Chromophoric Interpretation of CD Spectra of DNA G-Quadruplex Structures. *Org. Biomol. Chem.* **2010**, *8* (12), 2683.

(74) Panda, M.; Walmsley, J. A. Circular Dichroism Study of Supramolecular Assemblies of Guanosine 5′-Monophosphate. *J. Phys. Chem. B* **2011**, *115* (19), 6377–6383.

(75) Yu, X.; Chen, L.; Zhang, M.; Yi, T. Low-Molecular-Mass Gels Responding to Ultrasound and Mechanical Stress: Towards Self-Healing Materials. *Chem. Soc. Rev.* **2014**, *43* (15), 5346.

(76) James, S. H.; Prichard, M. N. Current and Future Therapies for Herpes Simplex Virus Infections: Mechanism of Action and Drug Resistance. *Curr. Opin. Virol.* **2014**, *8*, 54–61.

(77) Elion, G. B. Mechanism of Action and Selectivity of Acyclovir. *Am. J. Med.* **1982**, *73* (1A), 7–13.

(78) Matthews, T.; Boehme, R. Antiviral Activity and Mechanism of Action of Ganciclovir. *Rev. Infect. Dis.* **1988**, *10* (3), S490-4.

(79) Hummer, G.; Garde, S.; García, A. E.; Pratt, L. R. New Perspectives on Hydrophobic Effects. *Chem. Phys.* **2000**, *258*, 349–370.

(80) Oakenfull, D.; Fenwick, D. E. Hydrophobic Interaction in Deuterium Oxide. *Aust. J. Chem.* **1975**, *28*, 715–720.

(81) Wilf, J.; Ben-Naim, A. Intramolecular Hydrophobic Interaction in Light and Heavy Water. *J. Chem. Phys.* **1979**, *70* (6), 3079–3081.

(82)   Graziano, G. On the Solvent Isotope Effect in Hydrophobic Hydration. *J. Phys. Chem.* **2000**, *104*, 9249–9254.

(83)   Constitutional Dynamic Chemistry. In *Topics in Current Chemistry*; Barboiu, M., Ed.; Springer Verlag: Berlin, 2012; p 322.

(84)   Barboiu, M. Dynamic Interactive Systems: Dynamic Selection in Hybrid Organic-Inorganic Constitutional Networks. *Chem. Commun.* **2010**, *46*, 7466–7476.

(85)   Dash, J.; Saha, P. Functional Architectures Derived from Guanine Quartets. *Org. Biomol. Chem* **2016**, *14*, 2157–2163.

(86)   Shigemitsu, H.; Hamachi, I. Design Strategies of Stimuli-Responsivec Supramolecular Hydrogels Relying on Structural Analyses and Cell-Mimicking Approaches. *Acc. Chem. Res.* **2017**, *50*, 740–750.

(87)   Wang, H.; Feng, Z.; Xu, B. Bioinspired Assembly of Small Molecules in Cell Mileu. *Chem. Soc. Rev.* **2017**, *46*, 2421–2436.

(88)   Mihai, S.; Cazacu, A.; Arnal-Herault, C.; Nasr, G.; Meffre-Anca; van der Lee, A.; Barboiu, M. Supramolecular Self-Organization in Constitutional Hybrid Materials. *New J. Chem* **2009**, *33*, 2335–2343.

(89)   Mihai, S.; Le Duc, Y.; Cot, D.; Barboiu, M. Sol-Gel Selection of Hybrid G-Quadruplex Architectures from Dynamic Supramolecular Guanosine Libraries. *J. Mater. Chem.* **2010**, *20*, 9443–9448.

(90)   Belda, R.; Garcia-Espana, E.; Morris, G. A.; Steed, J. W.; Aguilar, J. A. Guanosine-5'-Monophosphate Polyamine Hybrid Hydrogels: Enhanced Gel Strength Probed by Z-Spectroscopy. *Chem. Eur. J.* **2017**, *23*, 7755–7760.

(91)   Cohen, Y.; Avram, L.; Frish, L. Diffusion NMR Spectroscopy in Supramolecular and Combinatorial Chemistry: An Old Parameter—New Insights. *Angew. Chemie - Int. Ed.* **2005**, *44*, 520–554.

(92)   Kaucher, M. S.; Lam, Y.-F.; Pieraccini, S.; Gottarelli, G.; Davis, J. T. Using Diffusion NMR to Characterize Guanosine Self-Association: Insights into Structure and Mechanism. *Chem. Eur. J.* **2004**, *11*, 164–173.

(93)   Arnal-Herault, C.; Banu, A.; Barboiu, M.; Michau, M.; van der Lee, A. Amplification and Transcription of the Dynamic Supramolecular Chirality of the Guanine Quadruplex. *Angew. Chemie - Int. Ed.* **2007**, *46*, 4268–4272.

(94) Dawn, A.; Kumari, H. Low Molecular Weight Supramolecular Gels Under Shear: Rheology as the Tool for Elucidating Structure-Function Correlation. *Chem. - A Eur. J.* **2018**, *24*, 762–776.

(95) Liang, H.; Zhang, Z.; Yuan, Q.; Liu, J. Self-Healing Metal-Coordinated Hydrogels Using Nucleotide Ligands. *Chem. Commun.* **2015**, *51*, 15196–15199.

(96) Venugopal, J. R.; Zhang, Y.; Ramakrishna, S. In Vitro Culture of Human Dermal Fibroblasts on Electrospun Polycaprolactone Collagen Nanofibrous Membrane. *Artif. Organs* **2006**, *30*, 440–446.

(97) Stockert, J. C.; Blazquez-Castro, A.; Canete, M.; Horobin, R. W.; A., V. MTT Assay for Cell Viability: Intracellular Localization of the Formazan Product Is in Lipid Droplets. *Acta Histochem* **2012**, *114*, 785–796.

(98) *International Organization for Standardization: Biological Evaluation of Medical Devices - Part 5: Tests for Invitro Cytotoxicity*, [ISO 10993.; Geneva, Switzerland, 2009.

(99) *Advanced Nanomaterials for Wastewater Remediation*; Kumar, R., Chattopadhyaya, M. C., Eds.; CRC Press, Taylor & Francis Group: Boca Raton, 2017.

(100) Ferkous, H.; Hamdaoui, O.; Merouani, S. Sonochemical Degradation of Naphthol Blue Black in Water: Effect of Operating Parameters. *Ultrason. Sonochem.* **2015**, *26*, 40–47.

(101) Shi, X.; Fettinger, J. C.; Davis, J. T. Ion-Pair Recognition by Nucleoside Self-Assembly: Guanosine Hexadecamers Bind Cations and Anions. *Angew. Chemie - Int. Ed.* **2001**, *40* (15), 2827–2831.

(102) Kotch, F. W.; Fettinger, J. C.; Davis, J. T. A Lead-Filled G-Quadruplex: Insight into the G-Quartet's Selectivity for Pb(2+) over K(+). *Org Lett* **2000**, *2* (21), 3277–3280.

(103) Zhang, D.; Huang, T.; Lukeman, P. S.; Paukstelis, P. J. Crystal Structure of a DNA/Ba2+ G-Quadruplex Containing a Water-Mediated C-Tetrad. *Nucleic Acids Res.* **2014**, *42* (21), 13422–13429.

(104) Deng, J.; Xiong, Y.; Sundaralingam, M. X-Ray Analysis of an RNA Tetraplex (UGGGGU)(4) with Divalent Sr(2+) Ions at Subatomic Resolution (0.61 A). *Proc. Natl. Acad. Sci. U. S. A.* **2001**, *98* (24), 13665–13670.

(105) Gros, J.; Aviñó, A.; Lopez de la Osa, J.; González, C.; Lacroix, L.; Pérez, A.; Orozco, M.; Eritja, R.; Mergny, J.-L. 8-Amino Guanine Accelerates Tetramolecular G-Quadruplex Formation. *Chem. Commun.* **2008**, No. 25, 2926–2928.

(106) Hattori, M.; Frazier, J.; Miles, H. T. Ordered Forms of 5'-8-Aminoguanylic Acid. *Biopolymers* **1975**, *14* (10), 2095–2106.

(107) Hattori, M.; Frazier, J.; Miles, H. T. Poly(8-Aminoguanylic Acid): Formation of Ordered Self-Structures and Interaction with Poly(cytidylic Acid). *Biochemistry* **1979**, *14* (23), 5033–5045.

(108) Engelhart, A. E.; Morton, T. H.; Hud, N. V. Evidence of Strong Hydrogen Bonding by 8-Aminoguanine. *Chem. Commun. (Camb).* **2009**, *7345* (6), 647–649.

(109) Okesola, B. O.; Smith, D. K. Applying Low-Molecular Weight Supramolecular Gelators in an Environmental Setting – Self-Assembled Gels as Smart Materials for Pollutant Removal. *Chem. Soc. Rev.* **2016**, *45*, 4226–4251.

(110) Gottarelli, G.; Masiero, S.; Spada, G. P. The Use of CD Spectroscopy for the Study of the Self-Assembly of Guanine Derivatives. *Enantiomer* **1998**, *3*, 429–438.

(111) Wu, G.; Kwan, I. C. M. Helical Structure of Disodium 5'-guanosine Monophosphate Self-Assembly in Neutral Solution. *J. Am. Chem. Soc.* **2009**, *131* (9), 3180–3182.

(112) Sutyak, K.; Zavalij, P. Y.; Robinson, M.; Davis, J. Controlling Molecularity and Stability of Hydrogen Bonded G-Quadruplexes by Modulating the Structure's Periphery. *Chem. Commun.* **2016**, *52*, 11112–11115.

(113) Babu, S. S.; Praveen, V. K.; Ajayaghosh, A. Functional π-Gelators and Their Applications. *Chem. Rev.* **2014**, *114* (4), 1973–2129.

(114) Wang, Q.; Yang, Z.; Wang, L.; Ma, M.; Xu, B. Molecular Hydrogel-Immobilized Enzymes Exhibit Superactivity and High Stability in Organic Solvents. *Chem. Commun.* **2007**, No. 10, 1032–1034.

(115) Wang, J.; Miao, X.; Fengzhao, Q.; Ren, C.; Yang, Z.; Wang, L. Using a Mild Hydrogelation Process to Confer Stable Hybrid Hydrogels for Enzyme Immobilization. *RSC Adv.* **2013**, *3* (37), 16739–16746.

(116) Trivedi, D. R.; Dastidar, P. Instant Gelation of Various Organic Fluids Including Petrol at Room Temperature by a New Class of Supramolecular Gelators. *Chem. Mater.* **2006**, *18* (6), 1470–1478.

(117) Kesava Raju, C. S.; Pramanik, B.; Ravishankar, R.; Chalapathi Rao, P. V.; Sriganesh, G. Xylitol Based Phase Selective Organogelators for Potential Oil Spillage Recovery. *RSC Adv.* **2017**, *7* (59), 37175–37180.

(118) Suzuki, M.; Nakajima, Y.; Yumoto, M.; Kimura, M.; Shirai, H.; Hanabusa, K. In Situ Organogelation at Room Temperature: Direct Synthesis of Gelators in Organic Solvents. *Org. Biomol. Chem.* **2004**, *2*, 1155–1159.

(119) George, M.; Weiss, R. G. Chemically Reversible Organogels: Aliphatic Amines as "Latent" Gelators with Carbon Dioxide. *Langmuir* **2002**, No. 24, 7124–7135.

(120) Wang, H.; Feng, Z.; Lu, A.; Jiang, Y.; Wu, H.; Xu, B. Instant Hydrogelation Inspired by Inflammasomes. *Angew. Chemie - Int. Ed.* **2017**, *56* (26), 7579–7583.

(121) Sahoo, P.; Kumar, D. K.; Raghavan, S. R.; Dastidar, P. Supramolecular Synthons in Designing Low Molecular Mass Gelling Agents: L -Amino Acid Methyl Ester Cinnamate Salts and Their Anti-Solvent-Induced Instant Gelation. *Chem. - An Asian J.* **2011**, *6* (4), 1038–1047.

(122) Stolarski, R.; Hagberg, C. E.; Shugar, D. Studies on the Dynamic Syn-Anti Equilibrium in Purine Nucleosides and Nucleotides with the Aid of 1H and 13C NMR Spectroscopy. *Eur. J. Biochem.* **1984**, *138* (1), 187–192.

(123) Jordan, F.; Niv, H. Glycosyl Conformational and Inductive Effects on the Acid Catalyzed Hydrolysis of Purince Nucleosides. *Nucleic Acids Res.* **1977**, *4* (3), 697–709.

(124) Läppchen, T.; Pinas, V. A.; Hartog, A. F.; Koomen, G. J.; Schaffner-Barbero, C.; Andreu, J. M.; Trambaiolo, D.; Löwe, J.; Juhem, A.; Popov, A. V.; et al. Probing FtsZ and Tubulin with C8-Substituted GTP Analogs Reveals Differences in Their Nucleotide Binding Sites. *Chem. Biol.* **2008**, *15* (2), 189–199.